Myocardial Perfusion Imaging

(Revised Edition)

A Technologist's Guide

Editors

Ryder, Helen (Dublin)

Testanera, Giorgio (Rozzano, Milan)

Veloso Jerónimo, Vanessa (Almada)

Vidovič, Borut (Munich)

Contributors

Abreu, Carla (London)

Acampa, Wanda (Naples)

Assante, Roberta (Naples)

Ballinger, James (London)

Fragoso Costa, Pedro (Oldenburg)

Figueredo, Sergio (Lisbon)

Geão, Ana (Lisbon)

Ghilardi, Adriana (Bergamo)

Holbrook, Scott (Gray)

Koziorowski, Jacek (Linköping)

Lezaic, Luka (Ljubljana)

Mann, April (South Hadley)

Medolago, Giuseppe (Bergamo)

Pereira, Edgar (Almada)

Santos, Andrea (Alverca do Ribatejo)

Vara, Anil (Brighton)

Zampella, Emilia (Naples)

Contents

**(*) Articles were written with the kind support
of and in cooperation with:**

S|N|M|M|I SOCIETY OF
NUCLEAR MEDICINE
AND MOLECULAR IMAGING

TECHNOLOGIST SECTION

EANM

Foreword

The EANM Technologist Committee was created more than 20 years ago. From the outset it worked not only to improve the professional expertise of nuclear medicine technologists (NMTs) in Europe but also to assist in raising the quality of Nuclear Medicine clinical practice. Over the past two decades, it has developed continuously to become an important group within the EANM.

With the above-mentioned goals of the Committee in mind, in early 2004 the idea of providing a series of books on imaging for technologists was conceived. By September 2004, thanks to the hard work of the EANM Technologist Sub-committee on Education, it was possible to publish the first Technologist's Guide, dedicated to myocardial perfusion scintigraphy. The success of this first guide led the Technologist Committee to propose a new book every year, starting a series of guides that is still ongoing.

The technological advancements in Nuclear Medicine and Molecular Imaging of the past decade have necessitated an upgrading of this pioneering series, and the EANM Technologist Committee accordingly decided to expand it to encompass recent developments in scanner technology, radiopharmaceuticals and stress tests.

Myocardial perfusion imaging (MPI) has a leading role in cardiological diagnostic protocols due to its great efficiency in detecting ventricular perfusion defects with an almost non-invasive procedure. MPI is, however, a challenging methodology for technologists, who may cover various roles in the procedural workflow and need to cooperate with different professionals including nurses, physicians, cardiologists and radiopharmacists.

The current book is specifically aimed at radiographers and technologists working or intending to work in a Nuclear Medicine department performing MPI; it will also have value for other healthcare professionals working or willing to work in this challenging environment. As you will see, some chapters from the previous edition of the guide have been revised and updated by the authors while new chapters and new contributors have been added to extend and further improve the quality of the book.

I would like to thank all those who have contributed to the realisation of this project, whether as authors or reviewers, without whom the book would not have been possible. I also wish to thank SNMMITS (Society of Nuclear Medicine and Molecular Imaging Technologist Section) and EANM Cardiovascular Committee for their help and high-quality contributions.

Special thanks are due to Helen Ryder, Vanessa Veloso Jerónimo and Borut Vidovič for their incredible enthusiasm and competence in dealing with the editorial duties and organisational work. Finally, I remain extremely grateful to the EANM Board, the EANM Executive Office, the Technologist Committee and all the other EANM committees involved in the project.

Giorgio Testanera
Chair, EANM Technologist Committee

Introduction

Borut Vidovič

Cardiovascular diseases are the leading cause of morbidity and mortality in the developed world, and their frequency is also increasing in less developed countries [1]. Reliable and rapid diagnosis is important to reduce the number of deaths and allow introduction of appropriate therapy at a very early stage of the disease.

Given that the last EANM Technologist's Guide entitled Myocardial Perfusion Imaging was released way back in 2004, it is certainly time for this new book. During the intervening period, Nuclear Medicine Cardiology has made great progress, with the development of new radiopharmaceuticals for myocardial perfusion imaging and the introduction of new imaging equipment with new post-processing programs.

This book provides the reader with information on the current state of the art in myocardial imaging in Nuclear Medicine. It opens by introducing all the myocardial imaging methods, including those beyond Nuclear Medicine. The common clinical indications for myocardial perfusion scintigraphy are then discussed, followed by guidance on patient preparation and the different types of stress protocol and presentation of the main advantages and disadvantages of the multidisciplinary approach and advanced practice. Advances in radiopharmaceuticals for myocardial perfusion imaging are then introduced. The following three chapters are more technically oriented, enabling the reader to learn about the different SPECT, SPECT/CT, D-SPECT and PET/CT protocols and the imaging equipment, with image processing and software. The final chapter elucidates the causes and effects of potential artefacts and pitfalls in myocardial perfusion imaging.

I would like to thank all the authors who have taken the time to write the chapters and all of my fellow editors who have helped to create this book. I hope all professionals who work in the area of Nuclear Medicine Cardiology or are interested in this topic will enjoy reading and using the book.

Reference

1. http://epp.eurostat.ec.europa.eu/cache/ITY_OFFPUB/KS-30-08-357/EN/KS-30-08-357-EN.PDF, accessed July 2014

Chapter 1

State of the Art in Myocardial Imaging

Wanda Acampa, Emilia Zampella and Roberta Assante

Introduction

The prevalence of coronary artery disease (CAD) is rising, and non-invasive myocardial imaging is increasingly being used to:

- Detect obstructive CAD and define the number, location and significance of coronary stenoses

- Guide medical therapy and monitor the treatment effect after revascularisation procedures

- Risk stratify patients and provide prognostic information

- Assess myocardial viability

Nuclear myocardial perfusion imaging procedures, such as myocardial perfusion single-photon emission computed tomography (MPS) and positron emission tomography (PET), have emerged not only as diagnostic techniques but also as robust prognostic tools able to provide data about myocardial perfusion, ventricular function and viability by means of a single test.

Several other imaging modalities are available for evaluation of the presence and severity of CAD, including echocardiography, cardiac computed tomography and cardiac magnetic resonance imaging (CMR). The most appropriate imaging modality should be chosen according to the clinical question, patient characteristics, strengths, limitations, risks, costs and availability.

Myocardial perfusion single-photon emission computed tomography

Myocardial perfusion imaging is the stress imaging procedure that is most widely used in the management of patients with coronary artery disease (CAD) [1]. Gated MPS provides important information on the extent and severity of myocardial perfusion abnormalities, including myocardial ischaemia, left ventricular (LV) cavity size and function, and mechanical dyssynchrony. Moreover, it can deliver miscellaneous prognostic imaging data regarding, for example, transient ischaemic dilation (TID), lung uptake, right ventricular uptake, post-stress left ventricular ejection fraction (LVEF) and sphericity index. One of the reasons for use of MPS in the management of patients with suspected or known CAD is that it can be performed in any patient, even in those with a poor "acoustic window", implanted metal objects, cardiac dysrhythmias or renal dysfunction. With the introduction of pharmacological stressor agents, MPS can now be safely performed in most patients who would not be candidates for exercise stress, thereby adding flexibility in testing strategy and affording greater availability of the test to virtually all patients. The concern of radiation exposure, although a real one, has been proactively addressed through scientific innovation and appropriate changes in MPS guidelines. The introduction of new-generation gamma cameras, which allow acquisition of high-quality images using smaller doses of radiotracers, has

the potential to decrease patient radiation exposure. Low-dose protocols have been shown to yield high-quality images while limiting radiation exposure to as little as 1–2 mSv [2]. The last three decades have also witnessed changes in radionuclide use (less dual-isotope imaging) and imaging sequences (more stress/rest imaging with the option of stress only) and improvements in processing software that incorporate iterative reconstruction techniques.

New-generation cardiac scanners: cadmium-zinc-telluride detectors

In new-generation dedicated cardiac ultra-fast-acquisition scanners, eight detectors surrounding the patient simultaneously image the heart. These new designs vary in respect of the number and type of scanning or stationary detectors and whether NaI, CsI or cadmium-zinc-telluride (CZT) solid-state detectors are used. They all have in common the potential for a five- to tenfold increase in count sensitivity at no loss of, or even a gain in, resolution, resulting in the potential for acquisition of a scan within 2 min or less if the patient is injected with a standard dose.
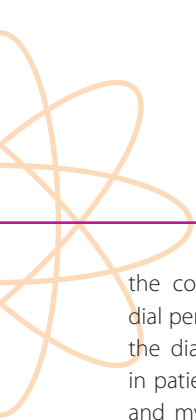
The introduction of modern dedicated gamma cameras allows some limitations of Anger SPECT, such as the lengthy acquisition time and radiation exposure, to be overcome. Traditional Anger SPECT uses collimators to direct photons towards a scintillation crystal, and a photomultiplier tube converts and am-

plifies the light signal into an electrical signal. This requires a large number of photons to be incident at the detectors. Novel semiconductor CZT SPECT uses detectors that directly convert photon energy into an electrical signal, eliminating the photomultiplier tube and resulting in better energy resolution and a much more compact detector. This new geometric design and the new detector material, combined with novel reconstruction algorithms, have led to improved diagnostic performance of CZT SPECT, with reduction of acquisition times and radiation dose (4.2 mSv vs 11.8 mSv) [3] without any significant sacrifice in accuracy. Low-dose protocols have been shown to yield high-quality images and several studies have not only revealed a good concordance with results provided by a conventional Anger camera but also demonstrated that the physical characteristics of CZT cameras, such as their enhanced count sensitivity, have the potential to improve on and therefore modify the results from Anger SPECT.

SPECT/CT cameras

Hybrid systems combining SPECT and computed tomography (CT) acquisition are available. SPECT/CT devices can perform CT acquisitions for attenuation correction of SPECT data and to estimate the coronary calcium score. For clinical applications, these devices permit 3D fusion display of SPECT and CT images, thereby allowing accurate assignment of a stenotic coronary vessel to

the corresponding stress-induced myocardial perfusion defect [4]. SPECT/CT increases the diagnostic accuracy of SPECT imaging in patients with suspected and known CAD and myocardial perfusion defects at SPECT imaging. Moreover, in patients with normal perfusion at SPECT and suspected three-vessel disease, SPECT/CT can provide useful information on risk stratification [4].

Diagnostic and prognostic value of MPS

In clinical practice, MPS is used to establish a diagnosis of CAD and to provide accurate risk stratification. Diagnostic accuracy of the method is influenced by several variables, such as pre-test likelihood of disease. Accuracy in the identification of CAD has been demonstrated to be highest in patients with intermediate pre-test CAD likelihood. Similarly, when performed for the purpose of prognostic evaluation in patients with suspected or known CAD, MPS offers the greatest benefit in those at intermediate risk [5]. On the basis of MPS, a large majority of intermediate-risk patients may be shifted to lower-risk cohorts (when the test result is negative) or higher-risk cohorts (in the setting of a moderately to severely abnormal perfusion scan). Published reports note that, on average, 53% of patients have normal or low-risk myocardial perfusion imaging results. Accordingly, it is expected that approximately half of intermediate-risk patients will be at low risk after testing, with an expected annual mortality of approximately 0.6% [6].

The prognostic power of MPS has been extensively evaluated, and several studies have demonstrated that it adds incremental prognostic value to the information obtained from patient clinical variables, stress test and angiographic findings. SPECT has a high negative predictive value and patients with normal MPS have an excellent prognosis, with an annual cardiac event rate <1% [7]. In these patients, in the absence of new symptoms and clinical conditions such as diabetes and known CAD, MPS may not need to be repeated for 3–5 years. Moreover, in patients with abnormal MPS, the severity and extent of perfusion may provide further prognostic information, considering that the annual event rate increases in accordance with both the severity and the extent of fixed or reversible perfusion defects [8]. One of the benefits of the wealth of evidence on prognostic evaluation by means of MPS is that the data can be easily integrated into risk-based patient management algorithms. A review of evidence suggests that high-risk findings are obtained on MPS in patients whose expected rate of major adverse cardiac events is 3%–5% or more and patients with moderately to severely abnormal perfusion abnormalities or a summed stress score greater than 8. Patients with a high-risk post-stress LVEF lower than 45% are at an elevated risk of major adverse cardiac events.

Risk stratification is widely used in the prognostic assessment of patients with a variety of clinical disorders, on the unquestioned

assumption that the intensity of treatment should be proportionate to the risk of an adverse event. A recent review evaluated the comparative ability of stress MPS risk markers using various iterative and risk classification approaches [9]. Other studies [10,11] have compared analytical approaches to assess the added value of MPS variables in estimating CAD outcomes in asymptomatic diabetic patients. At multivariable analysis, post-stress LVEF and stress MPS ischaemia were independent predictors of CAD death or myocardial infarction (MI) [11]. Moreover, the addition of MPS results to a prediction model based on traditional risk factors and ECG stress test data significantly improved the classification of risk. In particular, the addition of MPS data to pre-test CAD likelihood was important in estimating risk of CAD death or MI and effective in reclassifying a sizeable proportion (55%) of patients, yielding a significant net improvement compared with traditional approaches to prognostication [11]. More recent data showed that also different functional parameters obtained by MPS, such as TID, help to identify patients with higher mortality [12,13]. In particular, among patients with diabetes, when only subjects with post-stress LVEF >45% and no ischaemia were considered, TID was a strong predictor of cardiac events at long-term follow-up, with an event rate of 0.21% per year in those without TID and 4.9% per year in those with TID [13]. Interestingly, it emerged that the beneficial effect of revascularisation on hazard ratio is more evident in patients with TID, particularly in those with reduced post-stress LVEF and severe ischaemia [14].

The estimation of prognosis with an accurate and reproducible modality, such as MPS, allows a more precise linkage with efforts to reduce patient risk and therapeutic risk. In fact, a nuclear-based focus for decision-making concentrates on the physiological significance of the disease state and its relationship to event risk. In the long-term prognostic evaluation of patients with suspected or known CAD, serial stress MPS makes an important contribution to clinical decision-making. This is important in such patients when comparing a repeat study with a previous one: the interpreting physician should pay close attention to whether a new perfusion defect has developed or whether the extent of pre-existing ischaemia has substantially increased or decreased. Published reports have clearly shown that quantitative assessment of perfusion abnormality on MPS has a minimal intrinsic variability [15]. Software and scan reproducibility is extremely high because of the high degrees of automation of the algorithms. Different studies have provided quantitative criteria for ascertaining by means of MPS whether a meaningful change has occurred in an individual patient and these criteria should help guide clinical management decisions [15,16]. In the COURAGE nuclear sub-study, a change of ≥5% was used as the criterion for a significant serial change in ischaemic total perfusion defect in an individual patient [17].

Cardiac PET/CT

PET/CT systems were initially dedicated to oncology imaging. The increasing evidence of their clinical usefulness in cardiology is contributing in advancing the clinical role of PET/CT in cardiovascular imaging. Several technical advantages account for the improved image quality and diagnostic ability of PET compared with SPECT, including the high spatial resolution of reconstructed images (heart–background ratio), the high sensitivity in the identification of small concentrations of radiotracers, and above all the high temporal resolution, which allows dynamic sequences to be obtained in order to describe tracer kinetics and perform absolute measurements of myocardial blood flow (MBF). This last-mentioned feature also results in improved detection of multivessel CAD. Moreover, the appropriate attenuation correction obtained with simultaneous acquisition PET/CT technology decreases false-positives, increasing specificity, and provides a potential opportunity to delineate the anatomical extent and physiological severity of coronary atherosclerosis in a single setting. At the moment, cardiac PET/CT using perfusion tracers represents the gold standard for quantifying myocardial absolute perfusion (ml/min/g), at both rest and stress acquisition, and coronary flow reserve, defined as the ratio between MBF at peak stress and MBF at rest. Several PET myocardial perfusion tracers are available for clinical use, such as rubidium-82 (^{82}Rb) and nitrogen-13 (^{13}N) ammonia. The short physical half-life of PET perfusion tracers allows a reduction in the time required to complete rest and stress studies compared with MPS studies. Dynamic acquisitions are performed to obtain perfusion data while static perfusion images, as well as ECG-gated images, are acquired for the evaluation of LV function and wall motion. Modern PET systems are able to perform "list mode" acquisition, where spatial data for every coincident pair of photons are recorded sequentially with very high temporal resolution along with the associated electrocardiographic phase, providing maximal flexibility for the offline reconstruction of summed, gated or dynamic images. Through list-mode acquisitions, multiple images are reconstructed from a single acquisition. With this approach, image acquisition starts with the bolus injection of the radiopharmaceutical and continues for 6–7 min after ^{82}Rb injection and 10–20 min after ^{13}N-ammonia injection. Stress testing is most commonly performed with pharmacological agents.

Diagnostic and prognostic value of PET

The average weighted sensitivity for detection of at least one coronary artery with >50% stenosis is 90% (range 83–100%), while the average specificity is 89% (range 73–100%). The corresponding average positive predictive value (PPV) and negative predictive value (NPV) are 94% (range 80–100%) and 73% (range 36–100%), respectively, and the overall diagnostic accuracy is 90% (range 84–98%) [18]. Myocardial perfusion PET has higher diagnostic accuracy than SPECT [19]. This is because coronary vasodilator reserve

is globally reduced in patients with diffuse CAD, limiting detection of multivessel coronary artery stenosis. Diagnosis of multivessel CAD can be helped by PET measurements of MBF (ml/min/g) and coronary flow reserve. It has been demonstrated that estimates of coronary vasodilator reserve by PET are inversely and non-linearly related to the severity of stenosis [20]. Segments with reversible ischaemia and coronary stenosis had reduced hyperaemic MBF. Even segments that had significant coronary stenosis, but were negative for ischaemia, had reduced hyperaemic MBF compared with non-stenotic segments. Thus, MBF quantification by [82]Rb PET may provide additional diagnostic information in patients with CAD [21]. However, it is important to note that myocardial perfusion quantitation with PET methods cannot help in differentiating decreased perfusion due to epicardial coronary artery stenosis from that due to microvascular dysfunction. Hybrid PET/coronary CT angiography may be particularly helpful in this regard. It has been demonstrated that [82]Rb PET MPI provides independent and incremental information for the prediction of cardiac events and all-cause death. Risk-adjusted survival analysis showed that both statistical (increased chi-square and ROC analysis) and clinical enhanced risk stratification was achieved on the basis of the ischaemic burden and scar on PET MPI. The percentage of ischaemic or scarred myocardium on [82]Rb PET MPI added incremental value to the clinical data and rest LVEF in predicting cardiac event and all-cause death. Importantly,
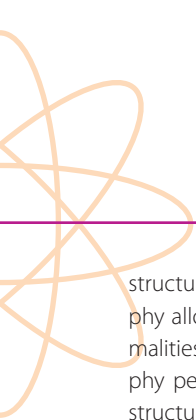
a novel finding in this study was that LVEF reserve is a significant independent predictor of these events [22]. In particular, LVEF reserve is inversely and independently related to the risk of events.

Comprehensive overviews of the role of [^{18}F]-2fluoro-2-deoxy-D-glucose (FDG) PET in the assessment of hibernating myocardium have recently been published (e.g. [23]). In the setting of persistent low-flow ischaemia, in which perfusion defects may show little evidence of reversibility, the ischaemic cardiac myocytes will utilise glycolysis and FDG uptake will increase, producing the classic mismatch pattern between blood flow, determined by perfusion PET, and metabolism. FDG PET assesses cellular metabolism, and thus also cellular integrity. As recently pointed out, techniques that detect presence of cellular integrity are likely to be more sensitive but less specific than techniques that detect contractile reserve, like dobutamine CMR, because a critical myocardial mass needs to be viable for a functional response to occur [24].

Other myocardial imaging modalities
Echocardiography
Echocardiography represents the most frequently performed cardiac imaging investigation and is an invaluable tool for accurate evaluation of cardiac structure and function. Numerous modalities are available for assessment of cardiac morphology and function: M-mode has a high temporal resolution and permits accurate depiction of rapidly moving

structures; 2D transthoracic echocardiography allows identification of structural abnormalities; transoesophageal echocardiography permits more detailed views of cardiac structures; and Doppler echocardiography is able to identify the direction, velocity, amplitude and timing of blood flow through the heart.

Stress echocardiography

Stress echocardiography (SE) has proved a useful diagnostic and prognostic tool in patients with known or suspected CAD. Several advances have helped to define this role, including the introduction of synchronised display of rest and stress images side by side using digital acquisition, the improvement of endocardial detection by tissue harmonic imaging, the use of contrast agent to achieve LV enhancement and detection of myocardial perfusion, 3D imaging and myocardial tissue quantitative techniques (tissue Doppler, myocardial strain and strain rate imaging). Stress ischaemia can be induced by exercise, pharmacological agents (such as dobutamine and vasodilator agents, e.g. dipyridamole or adenosine) or transoesophageal atrial pacing [25]. Evaluation of SE imaging is performed using qualitative assessment based on comparison of rest and stress images for global and regional dysfunction. Four response patterns are described: "normal", "inducible ischaemia", "fixed scar (necrosis)" and "stunned" or "biphasic response", as may be seen in dobutamine SE viability studies [26].

Compared with MPS, SE was found to display significantly superior specificity for detection of CAD, while nuclear perfusion had better sensitivity [27]. The ischaemic cascade can explain this finding, whereby the perfusion abnormalities precede wall motion abnormalities.

Coronary CT angiography

Coronary CT angiography has evolved into a robust and non-invasive tool for the assessment of CAD, being able to identify coronary anatomy, presence of obstructive and non-obstructive CAD and plaque characteristics. With the latest multislice CT scanners (64- and post-64-slice CT), coronary CT angiography has been reported to have high diagnostic and prognostic value for prediction of major cardiac events. It provides non-invasive visualisation of the coronary artery with a high sensitivity (>95%) and good specificity (82%) for detection of coronary artery stenosis [28]. Despite this, the presence of anatomically significant coronary stenosis does not always equate to functional significance. An alternative approach to assessment of the functional significance of a coronary stenosis is CT-based fractional flow reserve (CT-FFR) quantification. This method employs computational fluid dynamics to calculate pressure gradients across coronary lesions on standard CT coronary angiograms. Use of CT-FFR data improves diagnostic accuracy and discrimination of functionally significant stenosis over CT angiography alone [29]. Other

limitations of coronary CT angiography include inferior temporal resolution, motion-related artefacts and high false positive results due to severe calcification, presence of coronary stents and coronary artery bypass grafts, and arrhythmia.

Calcium score

The amount of coronary artery calcium, based on CT and traditionally expressed as the calcium score, is a marker of coronary atherosclerosis, correlated with the coronary atherosclerotic plaque burden. The coronary artery calcium score is associated with the risk of future cardiovascular events, and the detection of coronary artery calcification with cardiac CT has been used for risk stratification. Although coronary artery calcium scoring reflects the coronary atherosclerotic plaque burden, the absence of coronary artery calcification does not exclude obstructive CAD with non-calcified plaque.

Cardiac magnetic resonance

Magnetic resonance imaging has rapidly developed into a versatile tool for investigating CAD, being able to evaluate cardiac structure and ventricular function and to detect myocardial perfusion defects or infarction scar. CMR stress protocols are very useful for evaluation of myocardial perfusion and wall motion. For the assessment of myocardial perfusion, first-pass myocardial enhancement with gadolinium is performed using predominantly stress induced by a vasodilator, while stress-induced wall motion analysis most commonly employs dobutamine stress. Advantages of CMR are good specificity and sensitivity in detecting perfusion and wall motion abnormalities, concurrent assessment of cardiac structures and function and lack of radiation [30]. However, CMR has several limitations, including cost, test duration, variable centre expertise, patient claustrophobia, paramagnetic implants and gadolinium-associated nephrogenic systemic fibrosis. For the assessment of coronary anatomy, magnetic resonance angiography is used, but its operating characteristics are inferior to those of other available modalities.

New advances: PET/MR

The first available whole-body system for PET/MR hybrid imaging was introduced in 2010, based on two separate MR and PET imagers in one room. This system was followed by a fully integrated hybrid PET/MR system (Biograph mMR, Siemens AG, Healthcare Sector, Erlangen, Germany) that enables simultaneous PET/MR data acquisition. Integrated PET/MR appears a promising diagnostic tool for evaluation of cardiovascular disease because it combines the ability of MR to produce high-resolution images and provide information about anatomy, function, flow and perfusion with the strength of PET in quantifying physiological and metabolic processes.

References Chapter 1

References

1. Shaw LJ, Hage FG, Berman DS, Hachamovitch R, Iskandrian A. Prognosis in the era of comparative effectiveness research: where is nuclear cardiology now and where should it be? J Nucl Cardiol. 2012;19:1026–43. Erratum in: J Nucl Cardiol. 2012;19:1092–3.

2. Nakazato R, Berman DS, Hayes SW, Fish M, Padgett R, Xu Y, et al. Myocardial perfusion imaging with a solid-state camera: simulation of a very low dose imaging protocol. J Nucl Med. 2013;54:373–9.

3. Garcia EV, Faber TL, Esteves FP. Cardiac dedicated ultrafast SPECT cameras: new designs and clinical implications. J Nucl Med. 2011;52:210–7.

4. Schindler TH, Magosaki N, Jeserich M, Oser U, Krause T, Fischer R, et al. Fusion imaging: combined visualization of 3D reconstructed coronary artery tree and 3D myocardial scintigraphic image in coronary artery disease. Int J Card Imaging. 1999;15:357–68.

5. Shaw LJ, Iskandrian AE. Prognostic value of gated myocardial perfusion SPECT. J Nucl Cardiol. 2004;11:171–85.

6. Shaw LJ, Hendel R, Borges-Neto S, Lauer MS, Alazraki N, Burnette J, et al.; Myoview Multicenter Registry. Prognostic value of normal exercise and adenosine (99m)Tc-tetrofosmin SPECT imaging: results from the multicenter registry of 4,728 patients. J Nucl Med. 2003;44:134–9.

7. Hachamovitch R, Hayes S, Friedman JD, Cohen I, Shaw LJ, Germano G, Berman DS. Determinants of risk and its temporal variation in patients with normal stress myocardial perfusion scans: what is the warranty period of a normal scan? J Am Coll Cardiol. 2003;41:1329–40.

8. Sharir T, Germano G, Kang X, Lewin HC, Miranda R, Cohen I, et al. Prediction of myocardial infarction versus cardiac death by gated myocardial perfusion SPECT: risk stratification by the amount of stress-induced ischemia and the poststress ejection fraction. J Nucl Med. 2001;42:831–7.

9. Petretta M, Cuocolo A. Prediction models for risk classification in cardiovascular disease. Eur J Nucl Med Mol Imaging. 2012;39:1959–69.

10. Acampa W, Petretta M, Evangelista L, Daniele S, Xhoxhi E, De Rimini ML, et al. Myocardial perfusion imaging and risk classification for coronary heart disease in diabetic patients. The IDIS study: a prospective, multicentre trial. Eur J Nucl Med Mol Imaging. 2012;39:387–95.

11. Acampa W, Petretta M, Daniele S, Del Prete G, Assante R, Zampella E, Cuocolo A. Incremental prognostic value of stress myocardial perfusion imaging in asymptomatic diabetic patients. Atherosclerosis. 2013;227:307–12.

12. Petretta M, Acampa W, Daniele S, Petretta MP, Nappi C, Assante R, et al. Transient ischemic dilation in SPECT myocardial perfusion imaging for prediction of severe coronary artery disease in diabetic patients. J Nucl Cardiol. 2013;20:45–52.

13. Petretta M, Acampa W, Daniele S, Petretta MP, Plaitano M, Cuocolo A. Transient ischemic dilation in patients with diabetes mellitus: prognostic value and effect on clinical outcome after coronary revascularization. Circ Cardiovasc Imaging. 2013;6:908–15.

14. Acampa W, Cantoni V, Green R, Cuocolo R, Petretta MP, Orlandi M, Petretta M. Prognostic value of stress myocardial perfusion imaging in asymptomatic diabetic patients. Current Cardiovascular Imaging Reports. 2014;7:9268.

15. Xu Y, Hayes S, Ali I, Ruddy TD, Wells RG, Berman DS, et al. Automatic and visual reproducibility of perfusion and function measures for myocardial perfusion SPECT. J Nucl Cardiol. 2010;17 :1050–7.

16. Mahmarian JJ, Moyé LA, Verani MS, Bloom MF, Pratt CM. High reproducibility of myocardial perfusion defects in patients undergoing serial exercise thallium-201 tomography. Am J Cardiol. 1995;75:1116–9.

17. Shaw LJ, Berman DS, Maron DJ, Mancini GB, Hayes SW, Hartigan PM, et al.; COURAGE Investigators. Optimal medical therapy with or without percutaneous coronary intervention to reduce ischemic burden: results from the Clinical Outcomes Utilizing Revascularization and Aggressive Drug Evaluation (COURAGE) trial nuclear substudy. Circulation. 2008;117:1283–91.

18. Di Carli MF, Murthy VL. Cardiac PET/CT for the evaluation of known or suspected coronary artery disease. Radiographics. 2011;31:1239–54.

19. Bateman TM, Heller GV, McGhie AI, Friedman JD, Case JA, Bryngelson JR, et al. Diagnostic accuracy of rest/stress ECG-gated Rb-82 myocardial perfusion PET: comparison with ECGgated Tc-99m sestamibi SPECT. J Nucl Cardiol. 2006;13:24–33.

20. Anagnostopoulos C, Almonacid A, El Fakhri G, Curillova Z, Sitek A, Roughton M, et al. Quantitative relationship between coronary vasodilator reserve assessed by 82Rb PET imaging and coronary artery stenosis severity. Eur J Nucl Med Mol Imaging. 2008;35:1593–1601.

21. Yoshinaga K, Katoh C, Manabe O, Klein R, Naya M, Sakakibara M, et al. Incremental diagnostic value of regional myocardial blood flow quantification over relative perfusion imaging with generator-produced rubidium-82 PET. Circ J. 2011;75:2628–34.

22. Dorbala S, Hachamovitch R, Curillova Z, Thomas D, Vangala D, Kwong RY, Di Carli MF. Incremental prognostic value of gated Rb-82 positron emission tomography myocardial perfusion imaging over clinical variables and rest LVEF. JACC Cardiovasc Imaging. 2009;2:846–54.

23. Ghosh N, Rimoldi OE, Beanlands RS, Camici PG. Assessment of myocardial ischemia and viability: role of positron emission tomography. Eur Heart J. 2010;31:2984–95.

24. Shah BN, Khattar RS, Senior R. The hibernating myocardium: current concepts, diagnostic dilemmas, and clinical challenges in the post-STICH era. Eur Heart J. 2013;34:1323–36

25. Shah BN. Echocardiography in the era of multimodality cardiovascular imaging. Biomed Res Int. 2013;2013:310483. doi: 10.1155/2013/310483. Epub 2013 Jun 26.

26. Pellikka PA, Nagueh SF, Elhendy AA, Kuehl CA, Sawada SG; American Society of Echocardiography. American Society of Echocardiography recommendations for performance, interpretation, and application of stress echocardiography. J Am Soc Echocardiogr. 2007;20:1021–41.

27. Heijenbrok-Kal MH, Fleischmann KE, Hunink MG. Stress echocardiography, stress single-photon-emission computed tomography and electron beam computed tomography for the assessment of coronary artery disease: a meta-analysis of diagnostic performance. Am Heart J. 2007;154:415–23.

28. Paech DC, Weston AR. A systematic review of the clinical effectiveness of 64-slice or higher computed tomography angiography as an alternative to invasive coronary angiography in the investigation of suspected coronary artery disease. BMC Cardiovasc Disord. 2011;11:32.

29. Min JK, Leipsic J, Pencina MJ, Berman DS, Koo BK, van Mieghem C, et al. Diagnostic accuracy of fractional flow reserve from anatomic CT angiography. JAMA. 2012;308:1237–45.

30. Nandalur KR, Dwamena BA, Choudhri AF, Nandalur MR, Carlos RC. Diagnostic performance of stress cardiac magnetic resonance imaging in the detection of coronary artery disease: a meta-analysis. J Am Coll Cardiol. 2007;50:1343–53.

EANM

Chapter 2
Clinical Indications
Luka Lezaic

Introduction

Coronary artery disease (CAD) is a major cause of morbidity and mortality. Early and reliable detection of disease as well as assessment of its extent and severity have important implications for patient management.

Myocardial perfusion scintigraphy (MPS) is an essential clinical tool in patients with CAD. Initially, its main role was detection of disease and today it is still used extensively for this purpose. However, its role has gradually evolved to encompass risk assessment in patients with suspected or known CAD and/or cardiac risk factors; in specific patient subsets, it can effectively guide therapeutic decisions. Common clinical indications for MPS are discussed in the text.

Detection of ischaemic heart disease

Most common indication for MPS is detection of coronary artery disease.

Through a process of lipid deposition and calcification (atherosclerosis), coronary vessels are progressively narrowed by a local build-up (atheroma), allowing continued normal blood flow at rest but limiting the ability of the vessel to increase blood flow at increased demand (for example, at exercise, which increases cardiac contractility and heart rate). Normally, vessels adapt to increased demand by increasing their diameter (vasodilation). Myocardial perfusion scintigraphy is based on this pathophysiological principle that stenosed coronary arteries cannot increase blood flow by vasodilation in response to stress to the degree that normal vessels can (coronary flow reserve is decreased), whereas at rest blood flow in stenosed arteries is comparable to that in normal arteries until stenosis is far advanced (over 90% of luminal area). Regional uptake of radiopharmaceutical is dependent on regional blood flow. The difference in regional uptake (lower in areas supplied by a stenosed vessel) is a sign of regionally proportionally decreased blood flow (ischaemia).

For diagnostic purposes, stress is commonly induced in two ways: by exercise (on a stationary bicycle or treadmill) or by pharmacological agents. These options differ in terms of the mechanism by which they simulate changes induced by exercise: vasodilators, such as adenosine, dipyridamole and regadenoson, induce vasodilation, while dobutamine induces an increase in heart rate and contractility. Primarily, vasodilators are reserved for patients unable to exercise, but they are also used in patients with specific conditions (left bundle branch block, cardiac pacemakers, changes in resting ECG) in which exercise-induced increase in heart rate may induce changes in ECG and/or myocardial perfusion which could erroneously be interpreted as ischaemia [1, 2].

With all tracers in clinical use, extraction from blood pool and uptake in the myocardium is proportional to regional blood flow only at lower rates (up to approximately 2 ml/g cardiac tissue/min); at higher rates, it approaches a plateau. The non-linearity of tracer uptake is
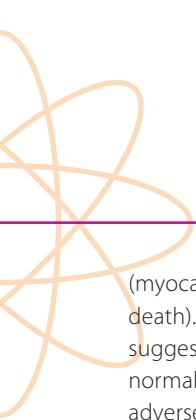
least expressed with thallium-201 (^{201}Tl), more so with technetium-99m (^{99m}Tc)-sestamibi and most with ^{99m}Tc-tetrofosmin. At exercise and particularly with pharmacological stress (which increases regional blood flow approximately 5 times above rest, while exercise-induced stress increases it to 2–3 times above rest), mild-to-moderate narrowing of coronary vessels may go undetected. Fortunately, significant (>70%) coronary stenoses result in a sufficient difference in myocardial uptake to be detected at imaging. In addition to detecting myocardial ischaemia, MPS is able to assess its location (and therefore predict the major epicardial vessel involved), extent (the amount of myocardium involved) and severity (level of ischaemia). MPS can be quantified: the left ventricle is divided into 17 segments using a universally accepted model for cardiac imaging [3] and segmental perfusion deficit is scored on a 0 (no defect) to 4 (no perfusion) scale by visual analysis or, preferably, by comparison to a normal database. Quantification adds to confidence, reproducibility and objective assessment of the degree of perfusion abnormality [4]. However, if all major epicardial vessels are equally affected (similar degree of stenosis), no relative difference in coronary flow reserve exists in different parts of the myocardium and therefore no ischaemia is detected, although coronary flow reserve is reduced ("balanced" ischaemia). In this case, absolute quantification of myocardial blood flow using positron-emitting flow tracers [rubidium-82 (^{82}Rb), nitrogen-13 ammonia (^{13}NH$_3$) or oxygen-15 labelled water (H$_2$^{15}O)] and positron emission tomography (PET) is able to detect diffuse reduction in coronary flow reserve.

Differences in kinetics of clinically used tracers do not result in clinically detectable differences. Overall, the substantial body of evidence accumulated over four decades shows that for detection of significant ischaemic heart disease, MPS yields a sensitivity of approximately 85% with a slightly lower specificity of approximately 70% [5–11]. Improvement in specificity can be achieved by the use of ECG-gated imaging and/or attenuation correction. ECG-gated imaging allows assessment of LV volumes, ejection fraction and regional contractility (wall motion and thickening). Regional contractility analysis is used for differentiation of attenuation artefacts from ischaemic changes through retained regional contraction, improving specificity (approaching 85%) [12]. Furthermore, extensive balanced ischaemia can be detected through relative reduction of ejection fraction at stress and/or increase in volume of the left ventricle (transient ischaemic dilation [13]). Attenuation correction also serves to differentiate attenuation artefacts from ischaemic changes and has been shown to improve specificity and overall accuracy [14]. Both techniques require constant quality control to provide reliable information.

Risk assessment/prognosis in ischaemic heart disease

Arguably the most important role of MPS is risk assessment – identification of patients at risk for major adverse cardiac events

(myocardial infarction, sudden cardiac death). Pooled data from numerous studies suggest that patients with normal or near-normal MPS are at a very low risk for a major adverse cardiac event (defined at <1% per year). Furthermore, the extent (amount of myocardium affected) and severity (level of ischaemia) of reversible perfusion abnormalities can further stratify patients in terms of risk for a cardiac event. However, these findings cannot be generalised to all patients referred for MPS. While patients without known prior CAD or known myocardial infarction and normal MPS have been reported to be at low annual risk (0.6%) for an adverse cardiac event [15], the predictive value of MPS may be lower in specific patient subsets (those with known CAD [16], the elderly [17], women [18] and patients with cardiac risk factors, particularly diabetes [19] and chronic kidney disease [20]). Nevertheless, in most clinical contexts in which patients are referred to MPS, additional risk stratification can be provided by the results of the examination. An additional advantage of MPS is the ability to guide therapeutic strategy according to quantitative assessment of ischaemic burden [21]. Observational data have shown that patients with a large amount of ischaemic myocardium (exceeding 10% of total myocardium) benefit from revascularisation, while in patients with a small amount of ischaemic myocardium appropriate medical therapy alone may suffice for improvement in survival [22].

An effective risk assessment and management strategy is essential in patients with known CAD treated by revascularisation [by either percutaneous coronary intervention (PCI) or coronary artery bypass grafting (CABG)]. Improvements in revascularisation techniques (such as drug-eluting stents and arterial grafts) have reduced the number of post-procedural major cardiac events, but a significant number of patients remain at high risk. After PCI, repeated occurrence of symptoms may be related to restenosis at a treated site or to disease progression at a different site; typically, symptoms within 6 months of the procedure occur due to restenosis and at 9 months and beyond due to progression of disease elsewhere. Notably, only about half of the patients with restenosis exhibit symptoms. MPS is able to detect ischaemia due to restenosis, residual stenoses and disease progression (representing high risk of a major adverse cardiac event) and should thus be performed in symptomatic patients. As ischaemia is frequently silent in patients after revascularisation, MPS may have a role in asymptomatic patients after PCI, taking clinical variables into consideration [23]. MPS should not be performed sooner than 3 (ideally 6) months after PCI to allow recovery of normal endothelial function and avoid false positive ischaemic findings. In patients after CABG, similar risk stratification is achieved by late (≥5 years post procedure) MPS, again with consideration of clinical variables (particularly diabetes, where early MPS may be

considered) [24]. Repeated revascularisation in these patients significantly reduces cardiovascular risk [25].

In patients considered for a major operative procedure, MPS aids in assessing risk of perioperative cardiac mortality. It is indicated in patients with moderate-to-high clinical risk and reduced exercise tolerance. In the presence of reduced left ventricular ejection fraction (LVEF), ischaemic changes signify a high perioperative risk [26].

Viability assessment

Severe ischaemia leads to transient regional contractile dysfunction ("stunning"), which persists beyond the ischaemic episode. Repeated episodes of stunning and progression of CAD lead to changes in regional myocardial perfusion, metabolism and eventually structure. Resulting myocardial adaptation through regional reduction in contractility (hypokinesis or akinesis) and metabolism shift (from free fatty acids to glucose as the main metabolic substrate) is termed "hibernation". Importantly, hibernating myocardium can regain function upon restoration of regional blood flow [27].

Myocardial functional impairment (degree of reduction in LVEF) is an important predictor of survival in patients with ischaemic cardiomyopathy. If coronary anatomy is amenable to a revascularisation procedure, assessment of myocardial viability should be performed. If a significant amount of viable, hibernating myocardium is present, revascularisation is likely to lead to improvement in symptoms, myocardial function and overall survival [28].

The role of MPS in viability assessment is well established. It relies on the physiological principle that tracer uptake in myocardium is related to preservation of the integrity of cell membranes and metabolism with maintenance of the internal cellular milieu (transmembrane pumps for ion analogues in the case of ^{201}Tl and transmembrane gradient in mitochondria in the case of ^{99m}Tc-labelled tracers) [29]. Patient preparation and imaging protocols are adapted to the selected myocardial perfusion tracer. With ^{201}Tl, a rest-redistribution protocol with delayed imaging after 4 h is usually employed. If ^{99m}Tc-labelled tracers are used, patient preparation with nitrates is performed; induction of vasodilation and increased collateral flow results in an increase in tracer uptake and augments detection of viable myocardium. Segmental tracer uptake is quantified to identify areas in which the amount of viable myocardium present is too small to result in a clinically observable benefit. Relative uptake of >50% of maximum myocardial uptake at rest and ≥10% increase in uptake at redistribution with ^{201}Tl and relative uptake >50–60% of maximum myocardial uptake on rest imaging with ^{99m}Tc-labelled tracers are considered to signify viable myocardium.

ECG-gated SPECT is an important integral part of viability assessment. By definition,

hibernating myocardium is regionally dysfunctional (hypokinetic or akinetic). Similarly to its role in the detection of ischaemic heart disease, ECG-gated SPECT assists in differentiation between regionally dysfunctional myocardium and attenuation artefacts. With the addition of low-dose dobutamine, the contractile reserve of dysfunctional segments can be assessed for complementary determination of viable myocardium [30]. In doubtful cases and advanced heart failure due to ischaemic heart disease (ischaemic cardiomyopathy), the gold standard for viability assessment remains fluorine-18 (^{18}F) fluorodeoxyglucose (FDG) PET, which identifies viable myocardium by the presence of preserved glucose metabolism, performed in conjunction with myocardial perfusion assessment with SPECT or, preferentially, PET tracers.

Conclusion

Myocardial perfusion scintigraphy is a well-established tool for assessment of various clinical manifestations of ischaemic heart disease. Information provided by the technique is highly dependent on appropriate indication, patient selection and implementation of the examination; ultimately, these factors determine its clinical usefulness.

References

1. Hesse B, Tägil K, Cuocolo A, Anagnostopoulos C, Bardiés M, Bax J, et al.; EANM/ESC Group. EANM/ESC procedural guidelines for myocardial perfusion imaging in nuclear cardiology. Eur J Nucl Med Mol Imaging. 2005;32:855–97.

2. Task Force Members, Montalescot G, Sechtem U, Achenbach S, Andreotti F, Arden C, Budaj A, et al. 2013 ESC guidelines on the management of stable coronary artery disease: the Task Force on the management of stable coronary artery disease of the European Society of Cardiology. Eur Heart J. 2013;34:2949–3003.

3. Cerqueira MD, Weissman NJ, Dilsizian V, Jacobs AK, Kaul S, Laskey WK, et al.; American Heart Association Writing Group on Myocardial Segmentation and Registration for Cardiac Imaging. Standardized myocardial segmentation and nomenclature for tomographic imaging of the heart. A statement for healthcare professionals from the Cardiac Imaging Committee of the Council on Clinical Cardiology of the American Heart Association. Circulation. 2002;105:539–42.

4. Berman DS, Kang X, Gransar H, Gerlach J, Friedman JD, Hayes SW, et al. Quantitative assessment of myocardial perfusion abnormality on SPECT myocardial perfusion imaging is more reproducible than expert visual analysis. J Nucl Cardiol. 2009;16:45–53.

5. Health Quality Ontario. Single photon emission computed tomography for the diagnosis of coronary artery disease: an evidence-based analysis. Ont Health Technol Assess Ser. 2010;10:1–64.

6. Mowatt G, Vale L, Brazzelli M, Hernandez R, Murray A, Scott N, et al. Systematic review of the effectiveness and cost-effectiveness, and economic evaluation, of myocardial perfusion scintigraphy for the diagnosis and management of angina and myocardial infarction. Health Technol Assess. 2004;8(30):iii-iv, 1–207.

7. Imran MB, Pálinkás A, Picano E. Head-to-head comparison of dipyridamole echocardiography and stress perfusion scintigraphy for the detection of coronary artery disease: a meta-analysis. Comparison between stress echo and scintigraphy. Int J Cardiovasc Imaging. 2003;19:23–8.

8. Kim C, Kwok YS, Heagerty P, Redberg R. Pharmacologic stress testing for coronary disease diagnosis: A meta-analysis. Am Heart J. 2001;42:934–44.

9. Heijenbrok-Kal MH, Fleischmann KE, Hunink MG. Stress echocardiography, stress single-photon-emission computed tomography and electron beam computed tomography for the assessment of coronary artery disease: a meta-analysis of diagnostic performance. Am Heart J. 2007;154:415–23.

10. O'Keefe JH Jr, Barnhart CS, Bateman TM. Comparison of stress echocardiography and stress myocardial perfusion scintigraphy for diagnosing coronary artery disease and assessing its severity. Am J Cardiol. 1995;75:25D–34D.

11. Fleischmann KE, Hunink MG, Kuntz KM, Douglas PS. Exercise echocardiography or exercise SPECT imaging? A meta-analysis of diagnostic test performance. JAMA. 1998;280:913–20.

12. Smanio PE, Watson DD, Segalla DL, Vinson EL, Smith WH, Beller GA. Value of gating of technetium-99m sestamibi single-photon emission computed tomographic imaging. J Am Coll Cardiol. 1997;30:1687–92.

13. McLaughlin MG, Danias PG. Transient ischemic dilation: a powerful diagnostic and prognostic finding of stress myocardial perfusion imaging. J Nucl Cardiol. 2002;9:663–7.

14. Hendel RC. Attenuation correction: eternal dilemma or real improvement? Q J Nucl Med Mol Imaging. 2005;49:30–42.

15. Klocke FJ, Baird MG, Lorell BH, Bateman TM, Messer JV, Berman DS, et al.; American College of Cardiology; American Heart Association Task Force on Practice Guidelines; American Society for Nuclear Cardiology. ACC/AHA/ASNC guidelines for the clinical use of cardiac radionuclide imaging--executive summary: a report of the American College of Cardiology/American Heart Association Task Force on Practice Guidelines (ACC/AHA/ASNC Committee to Revise the 1995 Guidelines for the Clinical Use of Cardiac Radionuclide Imaging). Circulation. 2003;108:1404–18.
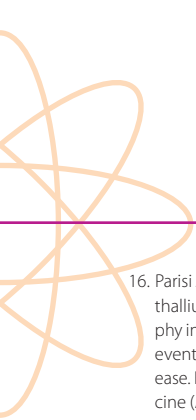
16. Parisi AF, Hartigan PM, Folland ED. Evaluation of exercise thallium scintigraphy versus exercise electrocardiography in predicting survival outcomes and morbid cardiac events in patients with single- and double-vessel disease. Findings from the Angioplasty Compared to Medicine (ACME) Study. J Am Coll Cardiol. 1997;30:1256–63.

17. Hachamovitch R, Kang X, Amanullah AM, Abidov A, Hayes SW, Friedman JD, et al. Prognostic implications of myocardial perfusion single-photon emission computed tomography in the elderly. Circulation. 2009;120:2197–206.

18. Cerci MS, Cerci JJ, Cerci RJ, Pereira Neto CC, Trindade E, Delbeke D, et al. Myocardial perfusion imaging is a strong predictor of death in women. JACC Cardiovasc Imaging. 2011;4:880–8.

19. Bourque JM, Patel CA, Ali MM, Perez M, Watson DD, Beller GA. Prevalence and predictors of ischemia and outcomes in outpatients with diabetes mellitus referred for single-photon emission computed tomography myocardial perfusion imaging. Circ Cardiovasc Imaging. 2013;6:466–77.

20. Al-Mallah MH, Hachamovitch R, Dorbala S, Di Carli MF. Incremental prognostic value of myocardial perfusion imaging in patients referred to stress single-photon emission computed tomography with renal dysfunction. Circ Cardiovasc Imaging. 2009;2:429–36.

21. Hachamovitch R, Di Carli MF. Methods and limitations of assessing new noninvasive tests: Part II: Outcomes-based validation and reliability assessment of noninvasive testing. Circulation. 2008;117:2793–801.

22. Hachamovitch R, Hayes SW, Friedman JD, Cohen I, Berman DS. Comparison of the short-term survival benefit associated with revascularization compared with medical therapy in patients with no prior coronary artery disease undergoing stress myocardial perfusion single photon emission computed tomography. Circulation. 2003;107:2900–7.

23. Acampa W, Evangelista L, Petretta M, Liuzzi R, Cuocolo A. Usefulness of stress cardiac single-photon emission computed tomographic imaging late after percutaneous coronary intervention for assessing cardiac events and time to such events. Am J Cardiol. 2007;100:436–41.

24. Acampa W, Petretta M, Evangelista L, Nappi G, Luongo L, Petretta MP, et al. Stress cardiac single-photon emission computed tomographic imaging late after coronary artery bypass surgery for risk stratification and estimation of time to cardiac events. J Thorac Cardiovasc Surg. 2008;136:46–51.

25. Rizzello V, Poldermans D, Schinkel AF, Biagini E, Boersma E, Elhendy A, et al. Outcome after redo coronary artery bypass grafting in patients with ischaemic cardiomyopathy and viable myocardium. Heart. 2007;93:221–5.

26. Weinstein H, Steingart R. Myocardial perfusion imaging for preoperative risk stratification. J Nucl Med. 2011;52:750–60.

27. Rahimtoola SH. The hibernating myocardium. Am Heart J. 1989;117:211–21.

28. Schinkel AF, Bax JJ, Poldermans D, Elhendy A, Ferrari R, Rahimtoola SH. Hibernating myocardium: diagnosis and patient outcomes. Curr Probl Cardiol. 2007;32:375–410.

29. Schinkel AF, Poldermans D, Elhendy A, Bax JJ. Assessment of myocardial viability in patients with heart failure. J Nucl Med. 2007;48:1135–46.

30. Leoncini M, Sciagrà R, Bellandi F, Maioli M, Sestini S, Marcucci G, et al. Low-dose dobutamine nitrate-enhanced technetium 99m sestamibi gated SPECT versus low-dose dobutamine echocardiography for detecting reversible dysfunction in ischemic cardiomyopathy. J Nucl Cardiol. 2002;9:402–6.

Chapter 3
Patient Preparation and Stress Protocols
Giuseppe Medolago and Adriana Ghilardi

Introduction

Non-invasive nuclear cardiology techniques for diagnosis and risk stratification of coronary artery disease (CAD) employ both exercise and pharmacological stressors to induce flow heterogeneity or functional abnormalities attributable to myocardial ischaemia.

The rationale is that an increase in oxygen demand (exercise) or in coronary blood flow (pharmacological stress) causes regional hypoperfusion or dysfunction in ischaemic myocardial segments supplied by stenotic coronary vessels (Fig. 1).
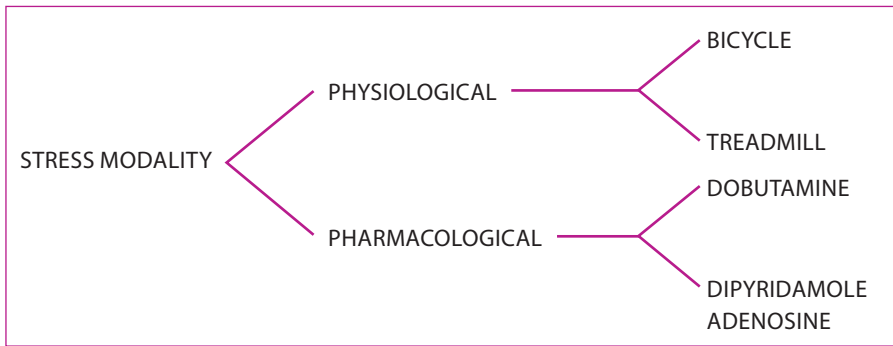

Figure 1: Stress modalities used in patients with CAD (from [1])

The room where the test procedure is performed should be equipped with a resuscitation cart, a defibrillator and appropriate cardioactive medication to allow prompt treatment of any emergency such as cardiac arrhythmias, atrioventricular block, hypotension or persistent chest pain. An intravenous line is mandatory for injection of the tracer at the peak of the exercise test or after administration of vasodilator drugs. The equipment and supplies in the cart must checked on a regular daily basis [2].

Exercise testing

Two main types of exercise test are distinguished:

1. Dynamic or isotonic exercise (bicycle ergometry)

2. Static or isometric exercise (treadmill protocol)

Exercise is preferred to pharmacological stress because it allows evaluation of physiological imbalance between oxygen supply and demand due to impaired flow reserve and identification of the ischaemic threshold

related to heart workload [calculated by multiplying the heart rate (HR) by the systolic blood pressure (BP) at the peak of exercise]. In patients without CAD, exercise test causes vasodilation and increases coronary blood flow to 2–2.5 times above baseline levels.

Bicycle ergometry

Bicycle protocols involve incremental workloads calibrated in watts (W) or kilopond (kp) metres/minute [1 W = 6 kp]. Electronically braked bicycles are preferred because they provide a constant workload regardless of changes in the pedalling rate (60-80 rpm). During the test the resistance to the pedalling is gradually increased following a standardised protocol while keeping the rate of pedalling constant, thereby controlling the workload the patient is performing.

Most protocols begin at a workload of 25 W, which is increased in 25-W increments every 2–3 min; Figure 2 shows an example of a protocol with larger, 50-W increments. It takes about 1–2 min for the cardiovascular system to adjust and stabilise HR and BP at each new workload. Usually exercise is completed when the patient reaches 85% of predicted maximum heart rate [(220 – age = max) × 0.85] (PMHR); at this time radiopharmaceutical is injected. The patient is then required to keep pedalling at a minor workload (25–50 W) for some more minutes (recovery) to obtain the resting values of HR and BP.

The patient is prepared with a standard 10- to 12-lead ECG setup. HR, BP and ECG are registered at rest, at the end of each stage and also during recovery. ECG monitoring is mandatory throughout the test.

Usually drugs that may interfere with the exercise test should be interrupted some days beforehand, though they may be maintained to evaluate efficacy of therapy.
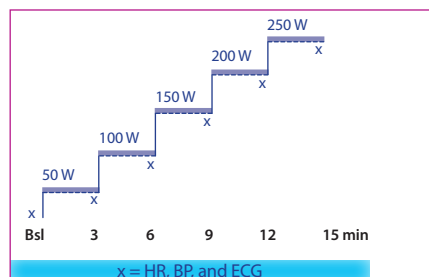

Figure 2: Bicycle protocol, with registration of HR, BP and ECG at the end of each stage (Bsl, baseline) (from [3])

Endpoints. The endpoints are as follows:

1. Reaching 85% of PMHR
2. Typical chest pain (angina) or equivalent (dyspnoea)
3. Ischaemic ECG abnormalities: diagnostic ST depression of >2-3 mm, horizontal or downsloping
4. Significant ventricular or supraventricular arrhythmia on ECG
5. Progressive decrease in systolic BP or abnormal elevation of systolic BP
6. Maximum stress: fatigue

Safety and risks. Bicycle ergometry is an extremely safe procedure. The risk is determined by the clinical characteristics of the patient. In non-selected patient populations the mortality is negligible and the morbidity less than 0.05%; the risk of complications is greater in patients with known CAD (infarction, multivessel disease) [4]. Indications, contraindications and limitations to exercise testing are shown in Tables 1 and 2. Exercise testing should always be undertaken under the supervision of a physician properly trained to perform such a test and able to deal with any emergency.

Treadmill

The treadmill protocol should be consistent with the patient's physical capacity. Several standardised treadmill exercise protocols exist (motor driven with variable speed and gradient steepness). The Bruce multistage maximal treadmill protocol is the most widely used [4].

An initially slow treadmill speed (1.7 mph) is gradually augmented until the patient has a good stride. The initial ramp angle is usually 10% and is progressively increased at fixed 3-min intervals (step) to achieve a steady state before increasing workload (Fig. 3).

The Bruce protocol can be modified to make it more suitable for elderly patients or those whose exercise capacity is limited in any way.

Usually exercise is completed when the patient reaches 85% of PMHR. Radiopharmaceutical is injected at the peak of exercise. The patient is required to keep on walking at a minor ramp angle for some more minutes (recovery) to obtain almost resting values of HR and BP.

The patient is prepared with a standard 10- to 12-lead ECG setup. HR, BP and ECG are registered at rest, at the end of each stage and also during recovery. ECG monitoring is mandatory throughout the test.
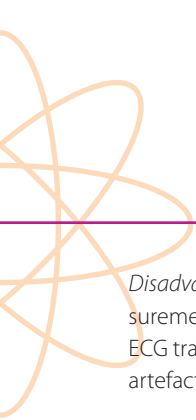
Usually drugs that may interfere with the exercise test should be interrupted some days beforehand, though they may be maintained to evaluate the efficacy of therapy.

Standard Bruce Protocol				
STAGE	DURATION (min)	TOTAL TIME	SPEED (mile/h)	GRADE (%)
1	3		1.7	10
2	3	6	2.5	12
3	3	9	3.4	14
4	3	12	4.2	16
5	3	15	5.0	18
6	3	18	6.0	20

Figure 3: Standard Bruce protocol (from [3])

Endpoints, safety and risks, and absolute and relative contraindications. These are the same for treadmill protocols as for bicycle exercise.

Advantage of treadmill protocols. Most patients find exercise by walking natural and easy to perform compared with cycling.

Disadvantages of both exercise tests. BP measurements are often difficult to obtain and ECG tracings may be subject to more motion artefacts.

Pharmacological testing

Pharmacological stress is increasingly employed as an alternative to exercise testing. Most patients referred to the nuclear cardiology laboratory are unable to perform a diagnostic exercise test owing to orthopaedic, neurological, systemic or vascular disease. In these patients, the presence of CAD can be evaluated on the basis of pharmacological vasodilation or chronotropic effect.

Three main types of pharmacological stressor are distinguished:

1. Dipyridamole
2. Adenosine/regadenoson
3. Dobutamine

Dipyridamole infusion protocol

More clinical experience has been gained with dipyridamole (a synthetic indirect vasodilator) than with the other pharmacological tests [5]. When intravenously infused, dipyridamole blocks cellular uptake (in vascular endothelium and red blood cell membranes) of the natural vasodilator adenosine (synthesised and released by endothelial cells), which regulates coronary blood flow to meet myocardial metabolic demands (by reacting with specific receptors which stimulate vascular smooth muscle cell relaxation).

In patients without CAD, dipyridamole infusion causes vasodilation and increases coronary blood flow 3–5 times above baseline levels. By contrast, in patients with significant CAD, the resistance vessels distal to the stenosis are already dilated, potentially even maximally, to maintain normal resting flow. Infusion of dipyridamole in the adjacent myocardium, supplied by normal vessels, causes a substantial increase in blood flow, producing heterogeneity in the myocardial blood flow (coronary steal).

Dipyridamole is infused over a 4-min period at a dose of 0.56 mg/kg diluted in normal saline solution. Maximal dilatory effect is achieved at 3–4 min after completion of the infusion: a slight increase in heart rate and decrease in systolic blood pressure may occur. Radiopharmaceutical is injected at the 7th–8th minute of the infusion (Fig. 4). In some laboratories, dipyridamole infusion is combined with handgrip exercise to reduce background activity of the radiotracer in the abdomen. After i.v. administration of the radiopharmaceutical, if necessary, the dipyridamole antidote aminophylline can be administered intravenously in order to reverse quickly any undesirable dipyridamole-associated side effects and/or stress blood flow discrepancy.

DIPYRIDAMOLE PROTOCOL
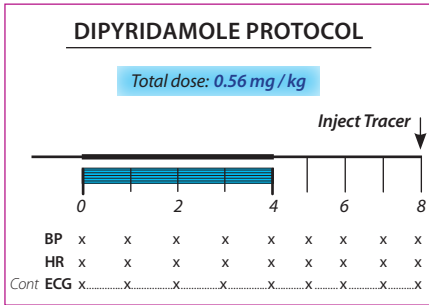
Total dose: 0.56 mg / kg

Inject Tracer

Figure 4: Dipyridamole infusion protocol (from [3])

The patient is prepared with a standard 10- to 12-lead ECG setup in the supine or semi-orthostatic (stress table) position. HR, BP and ECG are registered at rest and every minute throughout the test and also during recovery. ECG monitoring is mandatory throughout the test.

Usually cardiovascular drugs (calcium antagonists, nitrates) should be interrupted some days before the pharmacological test, as should caffeine and theophylline (adenosine receptor blockers).

The dipyridamole protocol is particularly well suited for patients with left bundle branch block, as it has a false positive rate of only 2–5% in such patients, compared with 30–40% for exercise testing [6].

Safety and risks. Even if side effects with dipyridamole are often more severe and more difficult to control, dipyridamole infusion is a safe procedure. The risk is determined by the

clinical characteristics of the patient referred for the procedure (Table 3). Dipyridamole infusion should be undertaken under the supervision of a physician properly trained to perform such a test and able to deal with any emergency.

Absolute contraindications. The absolute contraindications to dipyridamole testing are:

1. Bronchospasm
2. Drug intolerance

Limitations. Like any other drug, in some patients (non-responders) dipyridamole may display only slight or moderate pharmacological efficacy, thus reducing the accuracy of the stress testing.

Adenosine infusion protocol
Adenosine, unlike dipyridamole, is a natural vasodilator, synthesised (from ATP) in the vascular endothelium and metabolised through active cellular uptake and enzymatic degradation in myocardial cells and vascular smooth cells very quickly (the half-time of exogenously infused adenosine is about 10 s).

In the heart, endogenous and exogenous adenosine has an important role in the natural regulation of the coronary flow (vasodilation) and cardiac demand (lowering BP) by stimulating A2 purine receptors directly. It inhibits noradrenaline release from sympathetic nerve endings, reduces AV node conduction velocity and has negative inotropic and chronotropic effects by stimulating
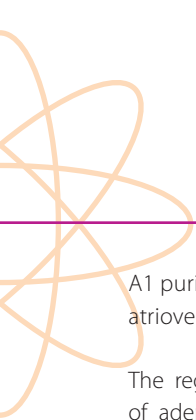
A1 purine receptors in the sinoatrial and the atrioventricular node.

The regional and systemic vascular effects of adenosine occur early (within 20–30 s) and quickly disappear after discontinuation of the infusion ($T_{1/2}$ in plasma is about 15 s). Maximal effect has been observed invasively after 60 s and continues as long as the drug is infused. These metabolic characteristics explain the lower rate of most side effects with adenosine in comparison with dipyridamole (Table 3).

Adenosine is infused over a 4- to 6-min period at a t the dose of 140 mg/kg per minute. A shorter-duration adenosine infusion, lasting 4 min, has been found to be equally effective for the detection of CAD compared to the 6-min infusion. Injection is at 3 min for a 6-min protocol and at 2 min for a 4-min protocol (Fig. 5).
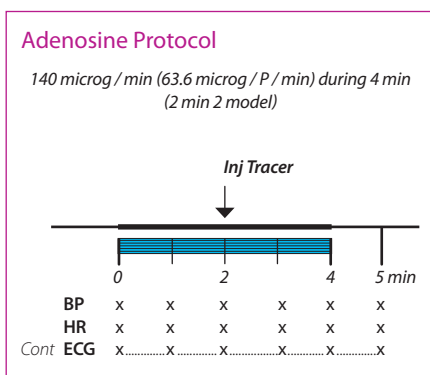
In some laboratories, adenosine infusion is combined with low-level exercise to reduce background activity of the tracer in the abdominal viscera. At the end of adenosine infusion and after intravenous administration of the radiopharmaceutical, the antidote aminophylline may be administered intravenously in order to reverse quickly any undesirable adenosine-associated side effects.

The patient is prepared with a standard 10- to 12-lead ECG setup in the supine or semi-orthostatic (stress table) position. HR, BP and ECG are registered at rest and every minute during the whole test and also during recovery. ECG monitoring is mandatory throughout the test.

Discontinuation of therapy is similar to that with dipyridamole.

Adenosine testing is the protocol of choice in patients with significant arrhythmias and with a history of psychiatric illness. Furthermore, adenosine testing is safe for stress testing early after acute myocardial reaction [8, 9].

Safety and risks, absolute contraindications and side effects. These are all similar to those for dipyridamole testing, even if bronchospasm is less frequent.

Figure 5: The 4-min adenosine infusion protocol (from [3])

Regadenoson protocol
Recently regadenoson, a selective A_{2A} adenosine receptor agonist, has become available. Regadenoson is less likely to cause the side effects associated with the other known receptors of adenosine. It is administered as a single standard dose of 400 μg in 5 ml over a full 10 s – with no dose adjustment for weight – into a peripheral vein using a 22-gauge or larger needle. This should be followed by a 5-ml saline flush, also over 10 s. Radiopharmaceutical is injected 10–20 s after the flush. In total it thus takes less than 1 min to complete the full administration protocol (Fig. 6).

Unlike adenosine or dipyridamole, regadenoson is not contraindicated in patients with asthma or COPD.
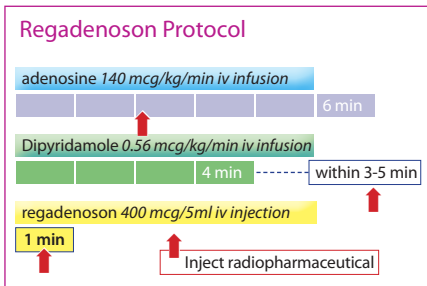

Figure 6: Regadenoson protocol

Advantages of regadenoson. Regadenoson has the following advantages:

- Selective A_{2A} adenosine receptor agonist
- Simplified dosing
    - 10-s injection
    - Single unit dosing
    - No weight determination or dose preparation
    - No need for an infusion pump
    - No need for an extension line or intravenous fluids
    - Reduces supplies and waste
- Improved tolerability over adenosine
- Alternative to dipyridamole stress for patients susceptible to a bronchonconstrictive response

Dobutamine infusion protocol
The dobutamine stress protocol is a demand/supply type protocol simulating a physical stress test. Dobutamine infusion produces systolic wall motion abnormalities because it increases myocardial oxygen demand by increasing heart rate, blood pressure and myocardial contractility. This results in a mismatch between oxygen supply and demand in the presence of a functionally significant coronary stenosis.

Dobutamine is a synthetic sympathomimetic a_1/b_1 and b_2 agonist. Cardiac b_1 adrenergic stimulation results in increased myocardial contractility and HR; the inotropic effect is greater. The stimulation of cardiac a_1 and b_1 receptors tends to offset the b_2 effect on the vascular arteriolar smooth muscle cells, leading to vasoconstriction, i.e. increase in BP.
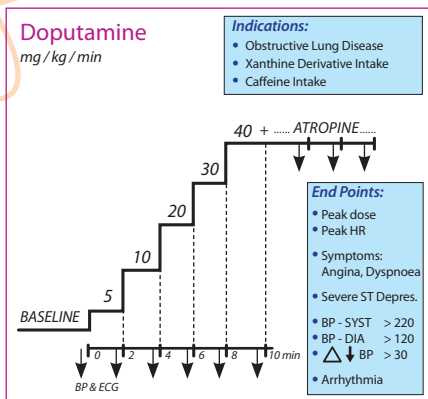
Doputamine
mg / kg / min

Indications:
• Obstructive Lung Disease
• Xanthine Derivative Intake
• Caffeine Intake

40 + ... ATROPINE ......

30

20

10

5

BASELINE

0 2 4 6 8 10 min

BP & ECG

End Points:
• Peak dose
• Peak HR
• Symptoms:
  Angina, Dyspnoea
• Severe ST Depres.
• BP - SYST   > 220
• BP - DIA   > 120
• △ ↓ BP   > 30
• Arrhythmia

Figure 7: Dobutamine infusion protocol

Dobutamine is infused at incremental doses of 5, 10, 20, 30 and 40 mg/kg per minute at 3-min intervals, until symptoms or target HR is reached. If target HR cannot be reached by dobutamine infusion alone (most often owing to ongoing beta-blocker medication), adjunctive low intravenous doses of atropine (0.25–0.50 mg/push) are necessary (Fig. 7). Radiotracer is injected when PMHR is reached.

The patient is prepared with a standard 10- to 12-lead ECG setup in the supine or semi-orthostatic (stress table) position. HR, BP and ECG are registered at rest and every minute throughout the test and also during recovery. ECG monitoring is mandatory throughout the test.

Dobutamine quickly clears from the blood ($T_{1/2}$ about 2 min). It should be emphasised that it is relatively common (15–20% of patients) to observe a fall in blood pressure at higher doses of dobutamine, both in patients with and in those without CAD, due to a mechanoreceptor reflex initiated in the left ventricle. This reaction does not carry the same significance as a fall in blood pressure during exercise testing. If symptoms occur, simple leg elevation will help; occasionally, in the presence of severe symptoms, a low dose of beta-blocker antidote is needed.

All side effects (Table 4) or severe symptoms are usually easily controlled with low intravenous doses of antidote beta-blockers.

Ongoing treatment with beta-blockers is often a problem when using the dobutamine protocol, because it may be very difficult (or impossible) to reach the target HR even after addition of atropine. In this situation, a pharmacological vasodilation protocol (dipyridamole or adenosine) should be used.

Contraindications to dobutamine testing. Absolute or relative contraindications are:

1. Presence of severe arrhythmias
2. Presence of psychiatric disorders

Table 5 summarises the properties of all the stressors (adenosine, dipyridamole and dobutamine).

Pharmacological stress for PET/CT myocardial perfusion imaging

Integrated X-ray CT angiography and PET perfusion imaging on hybrid PET/CT systems is an exciting new prospect. Complementary anatomical and functional information on atherosclerosis and ischaemia can be obtained in a single imaging session, permitting better diagnosis and risk stratification of patients with CAD. Use of the PET radiopharmaceuticals rubidium-82 (^{82}Rb), nitrogen-13 (^{13}N) ammonia and oxygen-15 labelled water (^{15}O-water) enables quantification of absolute myocardial blood flow and coronary reserve. In this context, taking into account the very short half-life of ^{82}Rb (<90 s), adenosine (or, still better, regadenoson) stress test is preferred, allowing the entire stress–rest protocol to be performed within 30 min at lower radiation doses and with a shorter examination time period [10] (Fig. 8).
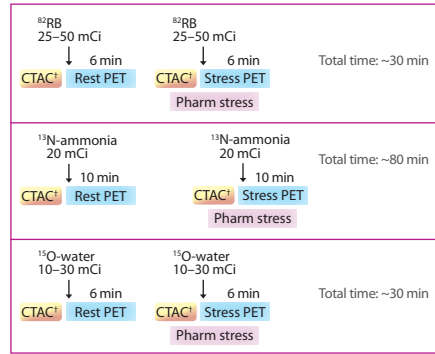

Figure 8: Examples of cardiac PET imaging protocols with ^{82}Rb, ^{13}N-ammonia and ^{15}O-water (from Nakazato et al. [10])

31

References Chapter 3

References

1. Escardio.org

2. Standard e VRQ per i laboratori di ergometria. G Ital Cardiol. 1999;29:1092–7.

3. Sochor H, Bourguinon M, Braat SH, et al. Pharmacological stress testing with 99mTc sestamibi. Dialogues in Nuclear Cardiology, vol. 3. Dordrecht: Kluwer, 1996. p. 1–31.

4. AHA exercise standards for testing and training. Circulation. 2001:104;1694-740.

5. Ranhosky A, Kempthorne-Rawson J. The safety of intravenous dipyridamole thallium myocardial perfusion imaging. Circulation. 1990;81:1425–7.

6. Lebtahi NE, Stauffer JC, Delaloye AB. Left bundle branch block and coronary artery disease: accuracy of dipyridamole thallium-201 single-photon emission computed tomography in patients with exercise anteroseptal perfusion defects. J Nucl Cardiol. 1997;4:266–73.

7. Verani MS, Mahmarian JJ, Hixson JB, Boyce TM, Staudacher RA. Diagnosis of coronary arter disease by controlled coronary vasodilation with adenosine and thallium-201 scintigraphy in patients unable to exercise. Circulation. 1990;82:80–7.

8. Bokhari S, Ficaro EP, McCallister BD. Adenosine stress protocols for myocardial perfusion imaging. Imaging Med. 2007;14:415–6.

9. Cerqueira MD, Verani MS, Schwaiger M, Heo J, Iskandrian AS. Safety profile of adenosine stress perfusione imaging: results of the Adenosine Multicenter Trial Registry. JACC. 1994;23:384–9.

10. Nakazato R, Berman DS, Alexanderson E, Slomka P. Myocardial perfusion imaging with PET. Imaging Med. 2013;5:35–46.

Table 1: Absolute and relative contraindications to exercise testing (from [4])

Absolute contraindication	Relative contraindication
Acute myocardial infarction or recent change on resting ECG	Less serious non-cardiac disorder
Active unstable angina	Significant arterial or pulmonary hypertension
Serious cardiac arrhythmias	Tachyarrhythmias or bradyarrhythmias
Acute pericarditis	Moderate valvular or myocardial heart disease
Endocarditis	Drug effect or electrolyte abnormalities
Severe aortic stenosis	Left main coronary obstruction or equivalent
Severe left ventricular dysfunction	Hypertrophic cardiomyopathy
Acute pulmonary embolus or pulmonary infarction	Psychiatric disease
Acute or serious non-cardiac disorder	
Severe physical handicap or disability	

Table 2: Limitations to exercise testing

Peripheral arteriosclerotic vascular disease

Disabling arthritis; orthopaedic problems

History of stroke

Chronic pulmonary disease (except asthma)

Extremity amputations

Before kidney, liver transplant

Poor exercise capacity due to non-cardiac endpoints (e.g. fatigue)

Beta-blocking drugs limiting heart rate response

Left bundle branch block (false positive exercise perfusion scans)

Early post-myocardial infarction (<5 days)

Table 2: Limitations to exercise testing

	Dipyridamole (Ranhosky et al. [5])	Adenosine (Verani et al. [7])
Cardiac		
Fatal/non-fatal MI	0.10	0
Chest pain	19.7	57
ST-T changes on ECG	7.5	12
Ventricular ectopy	5.2	?
Tachycardia	3.2	?
Hypotension	4.6	?
Blood pressure liability	1.6	?
Hypertension	1.5	?
AV block	0	10
Non-cardiac		
Headache	12.2	35
Dizziness	11.8	?
Nausea	4.6	?
Flushing	3.4	29
Pain (non-specific)	2.6	?
Dyspnoea	2.6	15
Paraesthesia	1.3	?
Fatigue	1.2	?
Dyspepsia	1.0	?

Table 4: Reported side effects (% of patients) of intravenous dobutamine infusion (from [3])

Side effect	%
Cardiac	
Chest pain	19.3
Arrhythmias (all types)	15.0
Ventricular premature beats	15.0
Atrial premature beats	3.0

Side effect	%
Non-cardiac	
Headache	3.0
Nausea	3.0
Dyspnoea	3.0

Table 5: Summary of the properties of all stressors

	Adenosine	Dipyridamole	Dobutamine
Mechanism of action	Direct vasodilator	Indirect vasodilator	Inotrope
May cause heart block/arrhythmias	Yes	Yes	Yes
Patient groups	No asthma/COPD	No asthma/COPD	Asthma/COPD only
Administration	Infusion	Infusion	Stepped infusion
Weight-based dosing	Yes	Yes	Yes
Timing of radiopharmaceutical	3 min	3-5 min post infusion	Variable

Chapter 4
Multidisciplinary Approach and Advanced Practice
Anil Vara

Introduction

A multidisciplinary team (MDT) with responsibility for formulation of patient care pathways is composed of members from different healthcare professions who have specialised skills and expertise. A patient being examined for cardiology-related issues will be seen by a group of general practitioners, cardiologists, technologists, nurses, healthcare assistants and cardiac surgeons, who jointly provide an integrated care approach appropriate for that patient. Within nuclear medicine, too, such an approach is adopted, with the MDT team consisting of the professional groups shown in Fig. 1.
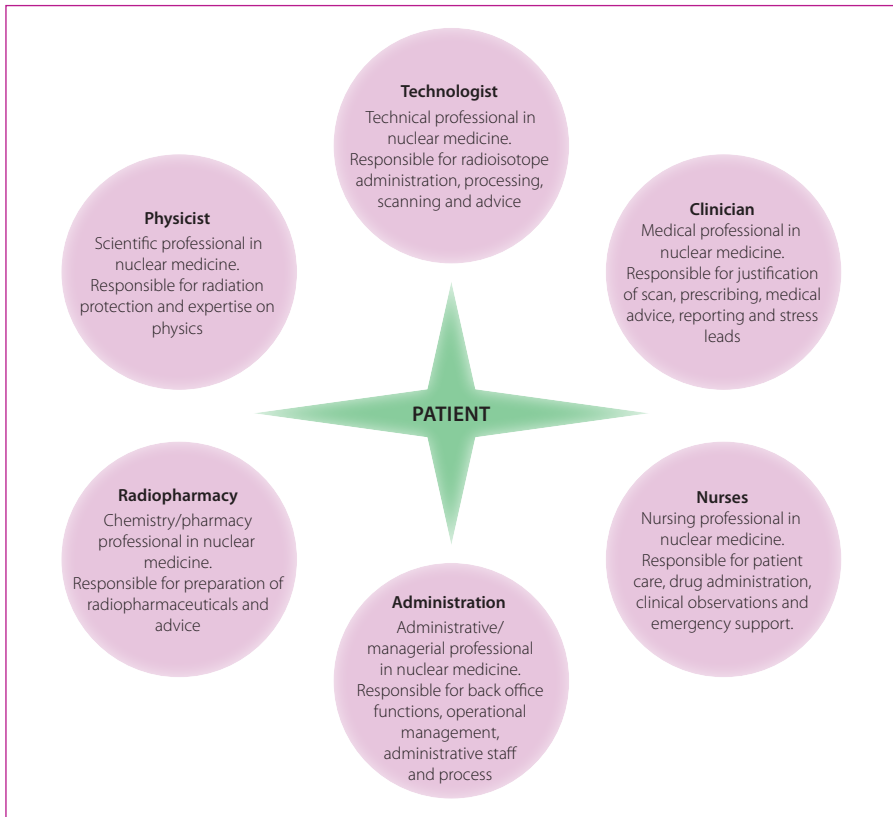
Figure 1: The professional groups involved in the MDT team and their roles

Nature of the multidisciplinary approach in myocardial perfusion imaging

Myocardial perfusion imaging (MPI) is a complex examination that is often very daunting for the patient, given the discomfort during exercise stress testing and the requirement to keep still for long periods and to lie flat for the scan. The MDT approach to MPI reassures the patient that they are being cared for by professionals with the requisite competencies and with clear responsibility for individual roles during the MPI exam. Figure 1 outlines the key professions and briefly describes how they contribute to the overall MPI exam.

The main advantages and disadvantages of the MDT approach in MPI are outlined in Table 1. Overall, the advantages do outweigh the disadvantages, and it is important to remember that the MDT approach is considered more effective given the higher levels of quality and efficiency that it can provide. In addition, there are many emerging challenges to the delivery of healthcare in Europe, and without an MDT approach there is a high risk that MPI exams will be overtaken by other diagnostic approaches and become obsolete.

What is advanced practice?

Recently, boundaries between the professions represented in MDTs have started to break down, and it is becoming more common for professionals responsible for healthcare delivery to have overlapping responsibilities (e.g. in the United Kingdom). "Advanced practice" is the term used to describe the situation where technologists develop a set of competencies that allows them to perform tasks previously within the boundaries of other professionals. Advanced practice is impacting on MPI as it is becoming more common for technologists to adopt enhanced roles after learning the appropriate set of nuclear cardiology competencies (as set out, for example, for the "Nuclear Medicine Advanced Associate" in the SNM's *Nuclear Medicine Advanced Associate Curriculum Guide, 1st Edition* [1]; see Appendix).

The introduction of advanced practice is not unique to technologists, as many other professionals such as radiographers and nurses have also increased their contribution to patient care through the adoption of advanced practice. In the United Kingdom, the introduction of the NICE 73 appraisal in the management and diagnosis of angina resulted in large numbers of patients being referred for MPI. The guidelines outlined an expectation that service provision to 4000 patients per million population would be achieved. This level of provision, coupled with the aim of performance of MPI within 6 weeks following referral, would have placed tremendous pressure on hospital services in the absence of modification of practices. The challenge led nuclear medicine services to adopt new ways of working through service configuration and skill mix within existing professional groups. Through the adoption of an enhanced technologist role in stress testing, the nuclear cardiology service was

able to effectively increase the capacity for stress sessions and allow clinicians to focus their resources on reporting, clinical developments/research, and development of the clinical service.

The nursing profession had already established an advanced practice role through the acquisition of skills in cardiac physiology, and nurses could easily gain further competencies in advising on and managing clinical issues arising from pharmacological and exercise-induced stress. However, such nursing support has often been limited to large hospitals where nurses rotate through all of the imaging modalities. In contrast, technologists remain solely responsible to the nuclear cardiology department, which facilitates skill development and acquisition of the competencies required for advanced practice roles in the performance of stress studies. It remains the case, however, that these advanced practice roles are adopted only to complement the MDT involved in MPI in order to enhance patient care, reduce costs and provide more efficient service [2].

Advanced practice competencies for technologists in MPI

Technologists with an advanced practice role within nuclear cardiology would normally have acquired competencies to an enhanced level in nuclear medicine [1]. The core competencies required for such a role have been published by the British Nuclear Medicine Society (BNMS) and the Society of Nuclear Medicine, both of which have pub-
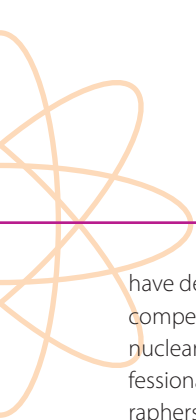
lished a competency framework that provides a useful guide for training.

The fundamental competency framework set out by the BNMS [3] should ensure the technologist can take responsibility for diverse specific aspects of a stress test:

• Communication – with patients, the MPI team, clinical referrers and other professionals

• Clinical assessment – taking a patient history, examination, justification and authorisation, obtaining patient consent, examination of the patient's clinical notes and drug charts

• Physical preparation – venous cannulation, ECG and blood pressure interpretation, stress equipment and pharmaceuticals

• Selection of the appropriate stress test – correct method, individual variations, plans for adverse events

• Conducting a stress test – safety, observations and interpretation, handling radionuclides, knowledge and safe administration of stress drugs, use of equipment, patient needs and documentation

The appendix to this chapter provides a detailed list of the competencies listed in the *Nuclear Medicine Advanced Associate Curriculum Guide, 1st edition* [1], which represent good guidelines for delivery of a suitable technologist training programme. In the United Kingdom, some academic centres

have developed courses that deliver the core competencies for advanced practice within nuclear cardiology for a wide group of professionals, including technologists, radiographers and nurses. These courses comprise both theoretical and work-based practical components, with case studies, assessments and written assignments.

Possibility of building a career ladder for the technologist practising MPI

Technologists partaking in advanced practice within nuclear cardiology are professionally accountable to their nuclear medicine consultant, who must ensure that the technologist's practice is routinely audited to reassure patients that they are receiving an appropriate quality of care. It must be emphasised that such technologists are operating as part of an MDT. They should always have adequate medical support available and must work in accordance with the written protocols and seek medical advice when difficult issues arise.

In the United Kingdom, technologists are not yet state registered and therefore advanced practice can often pose difficulties in respect of assurance to the employing organisation and the patient, compared with other professional groups such as radiographers and nurses. This should not, however, deter the technologist from developing a career in advanced practice. In the United Kingdom, certain professional groups will provide indemnity as well as an infrastructure to ensure maintenance of continuing professional development. The technologist's role in MPI might be further advanced to include authorisation of request forms, prescription of drugs as part of MPI and possibly even reporting of MPI scans. Such a level of practice for technologists could be accomplished by ensuring that state registration is available for nuclear medicine technologists and by embedding the technologist's role more deeply within the MDT delivering the MPI service.

Appendix Chapter 4

Appendix

Detailed nuclear cardiology competencies for a Nuclear Medicine Advanced Associate as set out in the SNM's *Nuclear Medicine Advanced Associate Curriculum Guide 1st Edition.*

1. Successfully complete Advanced Cardiac Life Support credentialing

2. Assess normal electrocardiogram to determine patient safety for stress testing

3. Assess abnormal electrocardiographic conduction in preparation for stress testing

4. Develop procedural policies and standards for pre-cardiac arrest emergencies that might occur within the department as directed by institutional policy and practice standards

5. Identify the signs and symptoms of symptomatic bradycardia and symptomatic tachycardia

6. Follow a step-by-step course of action for the patient who develops asymptomatic bradycardia or tachycardia while in office (before, during or after the stress test)

7. Follow a step-by-step course of action for the patient who develops signs and symptoms of bradycardia or tachycardia while in office (before, during or after the stress test)

8. Identify the proper medications and dosages for stable cardiac rhythms

9. List contraindications and precautions of common cardiac medications

10. Follow a step-by-step approach to handling an ST elevated myocardial infarction

11. Follow a step-by-step approach to handling a stroke situation

12. Follow a step-by-step approach to handling other patient incidents

13. Identify and delegate personnel to perform various tasks in preparation for cardiac emergencies

14. Incorporate the appropriate guidelines into departmental policies and procedures

15. Develop procedural policies and standards for cardiac arrest emergencies that occur within the department as directed by institutional policy and practice standards and provide indicated intervention for a cardiac emergency event

16. Establish intravenous access

17. Identify and administer the appropriate medications for commonly occurring cardiac arrhythmias under the direction of the supervising physician

18. Perform cardiac compression or defibrillate patient if required

19. Facilitate the ordering of laboratory tests or other tests as needed for a cardiac arrest event under the direction of the supervising physician

20. Facilitate admission of the patient to the hospital if necessary

21. Provide indicated intervention for non-cardiac emergency events

22. Manage crash cart for compliance

23. Follow the appropriate guidelines in implementing regulation for managing the department's crash cart

24. Inventory crash cart components according to institutional policy

25. Properly dispose of expired drugs

26. Replace expired drugs

27. Perform quality assurance testing on defibrillator and document results

28. Take comprehensive patient history and evaluate for patient pathology

29. Interview the patient and document on department form a complete past and current cardiac history

30. Review non-cardiac history for prevalence to study requested

31. Perform physical assessment

32. Evaluate patient laboratory biochemical markers relevant to cardiac pathology

33. Review most recent laboratory test results relevant to cardiovascular diseases

34. Order relevant blood tests if necessary (including pregnancy testing)

35. Evaluate patient medications for contraindications to stress testing

36. Understand contraindications to each type of stress test and evaluate for each

37. Review patient medications for contraindications to exercise stress testing

38. Obtain patient informed consent as required for nuclear cardiology procedures according to state law and hospital policy

39. Understand the ethical and legal underpinnings of informed consent

40. Determine the capability of the patient to give informed consent

41. Explain the procedure to the patient, including all components of a valid informed consent

42. Obtain the patient's or guardian's signature

43. Conduct treadmill testing per all protocol options under the direction of the supervising physician

44. Prepare the patient for exercise protocol

45. Determine type of exercise stress test

46. Monitor electrocardiographic tracings and blood pressure for specific pathology and cardiac events during stress testing

47. Use the appropriate termination protocols

48. Prescribe and administer interventional drugs for pharmacologic stress under the direction of the supervising physician

49. Explain the indications and contraindications for each pharmacological stress agent

50. Identify the physiological action of each pharmacological agent as it relates to stress testing

51. Calculate total dose, volume and dose rate for each of the most common pharmacological stress agents

52. Set up drug administration pump

53. Prepare pharmacological agents for administration utilising sterile technique

54. Administer pharmacological agents

55. Monitor patient response to pharmacological agents and treat the patient appropriately in the event of an adverse effect

56. Analyse results of the stress test and imaging portion of the examination and prepare a preliminary description of findings for the supervising physician

57. Create a preliminary description of findings detailing the results of the stress portion of the test

58. Examine rotating raw data from both stress and resting image acquisitions and evaluate image quality

59. Review data for incidental finding outside of the heart

60. Compare and contrast stress versus resting processed images for perfusion defects

61. Determine whether the heart-to-lung ratio and transient ischaemic dilation are abnormal

62. Evaluate the wall motion of stress and resting images for ejection fraction and kinetic abnormalities

63. Review and evaluate bull's eye polar maps and summed stress scores

64. Create a preliminary description of findings detailing the results of the imaging portion of the test

65. Facilitate or recommend patient-specific cardiac-related procedures based on nuclear cardiology examination results (outcome management) according to the supervising physician

66. Order or facilitate scheduling of complementary diagnostic procedures as indicated

References Chapter 4

References

1. Advanced Practice Task Force of the SNMTS. Nuclear Medicine Advanced Associate curriculum guide, 1st ed. SNM, 2008.

2. Waterstram-Rich K, Hogg P, Testanera G, Medvedec H, Dennan SE, Knapp W, et al. Euro-American discussion document on entry-level and advanced practice in nuclear medicine. J Nucl Med Technol. 2011;39:240-8.

3. British Nuclear Medicine Society. Clinical competence in myocardial perfusion scintigraphic stress testing. 2005.

Table 1: Advantages and disadvantages of the MDT

Advantages	Disadvantages
Ensure quality is maintained within the MPI exam	Expensive to resource many staff in smaller units that perform a low volume of MPI procedures
Working as a cohesive team improves the scope for innovation and developments within the different professions, thereby enhancing the quality of MPI	Teams can become fragmented owing to competition among the various professionals, resulting in loss of cohesiveness and impairment of ability to pursue an integrated approach
Increased job satisfaction and development of the professional role	Poor communication within the team can reduce the effectiveness of decision making, and often the different professional groups are not equally involved in or do not contribute equally to the decision-making process

Chapter 5
Advances in Radiopharmaceuticals for Myocardial Perfusion Imaging

James R. Ballinger and Jacek Koziorowski

Introduction

Myocardial perfusion imaging (MPI) is one of the greatest success stories of nuclear medicine, growing continuously since the late 1970s to now constitute more than 50% of imaging procedures in some countries such as the United States[1,2]. This success resulted from the development of improved imaging agents, the direct impact of the test results on patient prognosis and the technique being embraced by cardiologists. With single-photon emission computed tomography (SPECT) myocardial imaging now being firmly entrenched, we may see a similar growth in cardiac positron emission tomography (PET).

Properties of the ideal agent

The objectives of MPI are to detect abnormal perfusion to the heart, to differentiate permanent defects (due to blockage of coronary arteries such as following a myocardial infarction) from reversible defects (due to coronary artery disease, CAD), to determine which coronary arteries are involved and to estimate the extent of the defect. Permanent and reversible defects are differentiated by performing the test with the patient at rest and again following exercise or pharmacological stress. Detection and quantification of CAD are important in determining the prognosis of patients. In particular, a normal MPI scan is associated with an extremely low risk of cardiac events [1].

An ideal agent for MPI would have the following properties [3]:

- Efficient extraction from the blood on first pass in proportion to regional perfusion

- Linear relationship between perfusion and accumulation, particularly at high flow rates

- Retention in initial distribution for long enough that a SPECT or PET image can be acquired

- Rapid clearance from adjacent organs, particularly the lungs and liver, to achieve a high heart/background ratio

- Suitable emission energy for imaging, and absence of other emissions which increase radiation dose or degrade the image

- Physical half-life appropriate to the study

- Cost effectiveness and convenience of supply

It will be seen that the MPI tracers in current use vary in their conformity to these ideal properties.

History of MPI

The first approach taken was to use radioisotopes of potassium, particularly ^{43}K, making use of the sodium-potassium (Na^+/K^+) ATPase pump as a mechanism for efficient entry of the radiotracer into the cell. For clinical use, thallium-201 (^{201}Tl) was introduced in the mid

1970s as a potassium analogue. Its 3-day half-life made it convenient to supply, but limited the administered activity because of concerns about radiation dosimetry. The initial distribution of ^{201}Tl reflects regional MPI; however, over time there is redistribution from storage depots in other tissues, resulting in the filling in of transient defects. This property allows stress and rest images to be obtained at different times after a single injection.

At the time, ^{201}Tl was relatively expensive, so there was interest in finding a technetium-99m (^{99m}Tc)-labelled tracer which would be suitable for MPI. In the late 1970s a group of inorganic chemists began to explore the chemistry of technetium and to develop compounds in which the ^{99m}Tc atom was hidden inside the molecule and functional groups on the exterior of the molecule determined its biological properties. This was unlike the metal chelates which had been used previously. For targeting the Na^+/K^+ ATPase, it was believed that a monovalent cation was required. The first promising compound was bis(1,2-dimethylphosphino)ethane (DMPE), developed by Deutsch et al. in Cincinatti. Images of a dog heart were published in *Science* but the compound failed in humans due to binding to a protein in blood which did not allow activity to clear from the circulation. Davison and Jones in Boston developed the isonitrile complexes, of which sestamibi (Cardiolite) was brought to market by DuPont Pharma, becoming the most commercially successful radiopharmaceutical in

history. Deutsch et al. continued work with the phosphines and developed furifosmin, which Mallinckrodt brought to market, but its properties were definitely inferior to those of sestamibi. Radiochemists at the University of Cardiff developed another monovalent cation, tetrofosmin (Myoview), with Amersham International and it became a rival to sestamibi. Ironically, it turned out that these tracers entered the heart by passive diffusion rather than active transport, though their retention was due to the positive charge causing them to localise in the mitochondria.

The group of Nunn et al. at Squibb developed the boronic acid adduct of technetium oxime (BATO) compound teboroxime (Cardiotec), a neutral complex which showed good myocardial extraction but rapid washout, meaning that SPECT imaging had to be performed soon after injection. It was licensed in the United States at the same time as sestamibi but dropped out of the market within a few years. Ironically, its properties are well suited to the solid state cardiac cameras now in use. Pasqualini et al. at CIS Bio International developed [99m]Tc(N)-N-ethoxy-N-ethyl dithiocarbamate (NOEt), a neutral complex which showed good extraction and retention by the myocardium. Although it was very promising, it was not brought to market because sestamibi and tetrofosmin were too well established by that time.

PET imaging of myocardial perfusion can be performed using ^{13}N-ammonia and
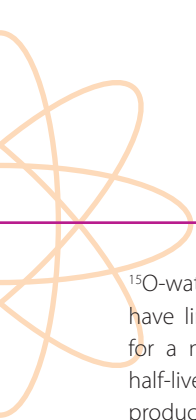
¹⁵O-water, as described below, though both have limitations including the requirement for a nearby cyclotron due to their short half-lives. As an analogue of ²⁰¹Tl, generator-produced rubidium-82 (²⁸²Rb) was marketed by Squibb (later Bracco) and became widely used in the United States. Its use is gradually increasing in Europe. More recently, Lantheus Medical Imaging has developed an ¹⁸F-labelled mitochondrial targeting agent, flurpiridaz, which may come to market in the near future.

Mechanisms of accumulation

The tracers used for MPI accumulate in the myocardium by different mechanisms. They will be categorised with respect to their mechanisms of localisation rather than their types of emission (i.e. SPECT vs PET). The three main mechanisms are active transport, passive diffusion and mitochondrial targeting.

Active transport

The Na^+/K^+ ATPase pump regulates the balance of these two cations in the heart.

Both ²⁸²Rb and ²⁰¹Tl are biological analogues of potassium and are thus extracted by the same mechanism as potassium from the blood pool and transported into the myocyte (Fig. 1). ²⁰¹Tl has a slower clearance time from the myocardium than potassium; this facilitates the imaging of the myocardium by gamma cameras. In a standard MPI procedure, ²⁰¹Tl is injected when the patient is undergoing peak stress, either exercise or pharmacological [4,5]. The initial distribution of ²⁰¹Tl reflects perfusion, due to its high extraction, and thus ischaemic and infarcted regions are evident as defects (low activity). However, ²⁰¹Tl is not retained in its initial distribution and as the patient rests it diffuses into regions which had been ischaemic due to increased demand. Repeat imaging 4 h after injection provides an image in which only infarcted areas will be seen as defects. However, the imaging properties of ²⁰¹Tl are not ideal, with its gamma photons in low abundance and the more abundant X-rays being subject to attenuation and scatter. Furthermore, its long half-life and poor dosimetry limit the amount of activity which can be administered and hence the image quality. It has largely been replaced by the ⁹⁹ᵐTc agents, though it is useful during times of molybdenum-99 shortage.

²⁸²Rb is a generator-produced positron emitter which is taken up by the same mechanism as ²⁰¹Tl [6,7]. However, its half-life is too short for redistribution images to be performed so separate injections are required for stress and rest images, but the entire procedure, including attenuation correction by CT, takes less than 30 min. The generator is relatively expensive and must be replaced monthly, so a high throughput of patients is required to make the test cost effective [7]. However, the quantitative nature of the results obtained more than justify the cost of the test by producing a more accurate diagnosis with savings on alternative treatments [7]. ²⁸²Rb is eluted from the generator with saline and infused directly into the patient.
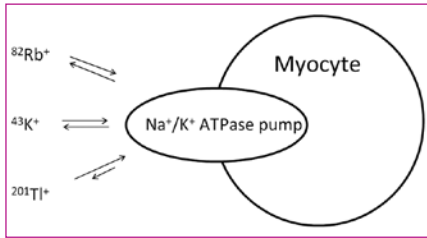
Figure 1: Mechanism of myocardial accumulation of [43]K, ^{201}Tl and [82]Rb

[201]Tl thallous chloride

Production: Cyclotron

Physical half-life: 73 h

Principal gamma emissions (abundance): 135 keV (3%), 167 keV (10%), 60-80 keV (Hg X-rays, 95%)

First-pass extraction: 85%

Half-life of retention in myocardium: 4 h

Routes of excretion: 8% in urine in 24 h; whole-body retention half-life 10 days

Typical administered activity: 80 MBq

Effective dose: 14 mSv

Advantages: High extraction efficiency; convenience of supply due to long half-life; redistribution allowing rest and stress information to be obtained from single injection

Disadvantages: Suboptimal imaging characteristics; poor counting statistics because of the low administered activity necessitated by its long physical half-life; imaging must be performed immediately after stress before redistribution takes place.

[82]Rb rubidium chloride

Trade name: CardioGen (Bracco)

Production: Obtained from [82]Sr generator (half-life 25 days) by elution with saline and infusion directly into patient

Physical half-life: 75 s

Maximum positron energy: 3.3 MeV

First-pass extraction: 65%

Half-life of retention in myocardium: 90 s

Routes of excretion: Irrelevant with 75-s half-life

Typical administered activity: 1500 MBq

Effective dose: 7.2 mSv

Advantages: Good for obese patients because of less attenuation compared with ^{99m}Tc photons; convenient availability from generator; virtually unlimited number of patients; short stress-rest protocol (~30 min) convenient for patients; absolute quantification, allowing detection of triple-vessel disease

Disadvantages: High patient throughput required for test to be cost effective because generator is expensive; high positron energy degrades spatial resolution; generator has to be replaced monthly; problems with breakthrough of the parent radionuclide [82]Sr and radionuclidic contaminant [85]Sr have occurred; only pharmacological stress is possible due to the short half-life.

Passive diffusion

Oxygen-15 labelled water (^{15}O-water) is freely diffusible and efficiently extracted by the heart, but rapid washout occurs, which necessitates dynamic imaging and subtraction of blood pool activity [8] (Fig. 2). Each set of rest or stress images requires 5 min of dynamic acquisition, with a period of about 10 min between injections. ^{15}O-water is generally administered as a bolus, although ^{15}O-carbon dioxide can be inhaled and converted to ^{15}O-water by carbonic anhydrase in vivo. Following bolus injection, the first-pass information can be used to delineate the blood pool in order to produce subtraction images of the myocardium. Alternatively, ^{15}O-carbon monoxide can be given by inhalation to generate a blood pool image. Neither approach is ideal. The first-pass information from a slow bolus will overestimate blood pool activity because of early extraction into the myocardium, while patient motion between the perfusion and blood pool images can result in artefacts [9]. Overall, image quality is poorer with ^{15}O-water than with the other PET agents discussed.

In contrast, nitrogen-13 labelled ammonia (^{13}N-ammonia) equilibrates with ammonium ion in the bloodstream. The neutral ^{13}N-ammonia species crosses the vascular epithelium by passive diffusion and is trapped intracellularly by enzymatic conversion to glutamine [7,10] (Fig. 3). After clearance of activity from the lungs and blood pool, imaging commences 3–5 min post injection and continues up to 20 min. Following a delay of 30–60 min for decay of the radionuclide, a stress protocol is performed.
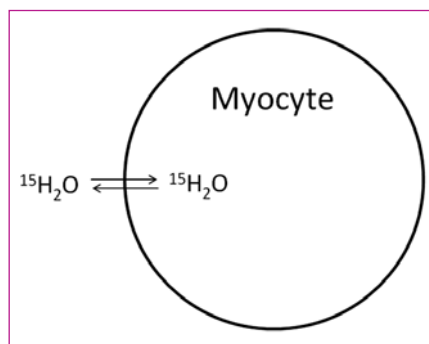
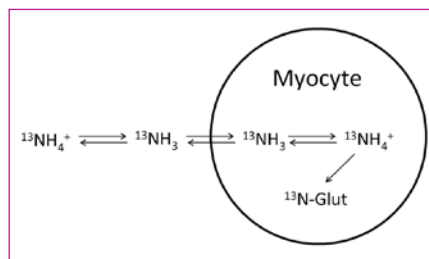Figure 2: Mechanism of myocardial accumulation of ^{15}O-water

Figure 3: Mechanism of myocardial accumulation of ^{13}N-ammonia

^{15}O-water

Production: Cyclotron

Physical half-life: 2 min

Maximum positron energy: 1.7 MeV

First-pass extraction: 100%

Half-life of retention in myocardium: Washes out freely

Routes of excretion: Irrelevant with 2-min half-life

Typical administered activity: 2200 MBq

Effective dose: 2.6 mSv

Advantages: Does not require high patient throughput; absolute quantification can be performed; high extraction, not affected by flow; due to short half-life, studies can be repeated after 15 min with physiological intervention

Disadvantages: Requires on-site cyclotron; blood pool activity must be subtracted; poor counting statistics due to short half-life

^{13}N-ammonia

Production: Cyclotron

Physical half-life: 10 min

Maximum positron energy: 1.2 MeV

First-pass extraction: 80%

Half-life of retention in myocardium: 4 h

Route of excretion: Hepatobiliary

Typical administered activity: 740 MBq

Effective dose: 1.7 mSv

Advantages: Convenient for small number of patient studies; absolute quantification can be performed

Disadvantages: Requires nearby cyclotron; rest-stress protocol requires 1 h between tests to allow for decay; intense liver activity can mask inferior wall of heart

Mitochondrial targeting

The two most commercially successful and widely used ^{99m}Tc-labelled agents for MPI both target the mitochondria, though this was not intentional (Fig. 4). They were developed as lipophilic cations, intended to be substrates for Na^+/K^+ ATPase as a transport pump. However, in vitro studies early in their development demonstrated that their uptake was not inhibited by pretreatment with ouabain, which blocks Na^+/K^+ ATPase. It was later determined that both compounds enter cells by passive diffusion due to their lipophilicity. Once in the cell they home to the mitochondria, where they are trapped by their positive charge. Both sestamibi and tetrofosmin consist of a ^{99m}Tc core hidden within a lipophilic structure with methoxy or ethoxy groups on the exterior to fine tune the biodistribution of the complex. Following intravenous injection at rest or during peak exercise or pharmacological stress, both are extracted quickly into the heart; however, imaging cannot begin until activity has cleared from the lungs and clearance has begun from the liver [1,5,11,12]. This occurs

somewhat more rapidly with tetrofosmin, allowing imaging after rest or pharmacological stress injection within 30–45 min whereas a 45- to 60-min delay is required with sestamibi. The time pattern is similar for exercise stress, with a 10-min delay for tetrofosmin and a 20-min delay for sestamibi before imaging begins [13]. Both undergo extensive hepatobiliary excretion while tetrofosmin also has a degree of urinary elimination. Both are reported to be excreted unchanged.

Until recently, MPI with PET required either an on-site cyclotron (for production of ^{15}O-water or ^{13}N-ammonia) or an ^{82}Rb generator (which is expensive and requires high patient throughput to make it cost-effective). The networks set up for distribution of fluorine-18 fluorodeoxyglucose (^{18}F-FDG) could be utilised to provide an ^{18}F-labelled MPI tracer. Rotenone is an inhibitor of mitochondrial complex I (MC-I) and labelled rotenone showed promising characteristics for MPI. Pyridaben, a functional analogue of rotenone, has been labelled with ^{18}F and evaluated for MPI under the name flurpiridaz [3] (Fig. 5).
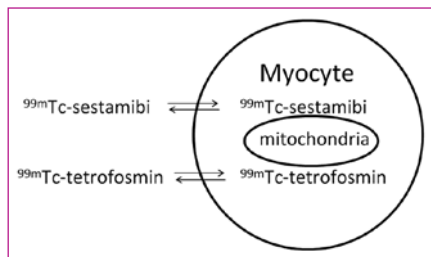

Figure 4: Mechanism of myocardial accumulation of ^{99m}Tc-sestamibi and ^{99m}Tc-tetrofosmin
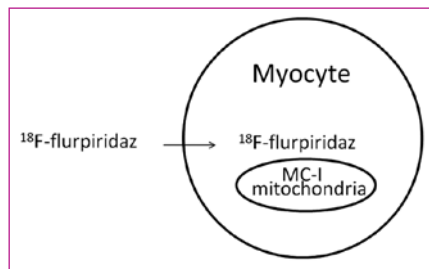

Figure 5: Mechanism of myocardial accumulation of ^{18}F-flurpiridaz

^{99m}Tc-sestamibi

Chemical name: methoxyisobutyl isonitrile, MIBI

Trade name: Cardiolite (Lantheus); generic equivalents available

Production: Prepared from kit using ^{99m}Tc-pertechnetate eluted from generator; kit preparation requires heating at 100°C for 10 min

Physical half-life: 6 h

Principal gamma emissions (abundance): 140 keV (89%)

First-pass extraction: 65%

Half-life of retention in myocardium: 11 h

Route of excretion: Primarily hepatobiliary

Typical administered activity: 800 MBq

Effective dose: 8 mSv

Advantages: High-quality images; relatively inexpensive due to availability of generic products; long retention of initial distribution; has additional uses such as imaging parathyroid adenoma, scintimammography and assessment of P-glycoprotein expression

Disadvantages: Preparation requires heating; hepatobiliary excretion delays imaging and can compromise cardiac resolution

99mTc-tetrofosmin

Chemical name: 6,9-bis(2-ethoxyethyl)-3,12-dioxa-6,9-diphosphatetradecane

Trade name: Myoview (GE Healthcare)

Production: Prepared from kit using 99mTc-pertechnetate eluted from generator and incubation at room temperature

Physical half-life: 6 h

Principal gamma emissions (abundance): 140 keV (89%)

First-pass extraction: 55%

Half-life of retention in myocardium: 4.5 h

Routes of excretion: Hepatobiliary and renal

Typical administered activity: 800 MBq

Effective dose: 6 mSv

Advantages: High-quality images; room temperature preparation is more convenient; faster background clearance than sestamibi, allowing earlier imaging

Disadvantages: Slightly lower first-pass extraction than sestamibi

18F-flurpiridaz (aka flupiridaz)

Chemical name: 2-tert-butyl-4-chloro-5-[(4-(2-[18F]fluoroanylethoxymethyl)phenyl) methoxy]pyridazin-3-one, BMS747158-02, RP1012, Lantheus Medical Imaging)

Production: Cyclotron

Physical half-life: 109 min

Maximum positron energy: 1.6 MeV

First-pass extraction: 90%

Half-life of retention in myocardium: 6 h

Route of excretion: Renal

Typical administered activity: 100 MBq (rest), 300 MBq (stress)

Effective dose: 6 mSv (rest + stress)

Advantages: Available as unit dose; high extraction, no flow limitation

Disadvantages: Expensive for high throughput

Production and quality assurance aspects
Licensed products
201Tl is a fully licensed product which arrives ready to use. The end user only needs to check the documentation and verify the radioactivity measurement. 18F-flurpiridaz will eventually be in the same class.

99mTc products prepared on site
Sestamibi and tetrofosmin are prepared on site or at a central radiopharmacy from licensed kits and a licensed 99Mo/99mTc generator under national regulations. Appropriate facilities are required and radiochemical purity testing may be performed.
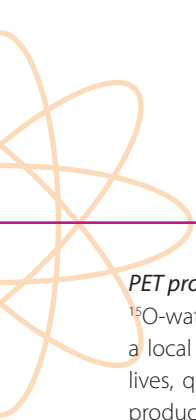
PET products prepared on site

^{15}O-water and ^{13}N-ammonia are prepared in a local cyclotron. Because of the short half-lives, quality testing is performed on a test production immediately prior to the clinical production. ^{15}O-water is particularly problematic as it can be produced adjacent to the patient and infused directly.

Generator-produced PET products

^{82}Rb is obtained from a generator and infused directly into the patient. Problems have occurred with breakthrough of the parent radionuclide ^{82}Sr and radiocontaminant ^{85}Sr. As a result it is now imperative that radionuclidic purity testing is performed on a test elution prior to clinical use each day.

Summary and future directions

MPI with SPECT is an extensively validated test which is useful for cost-effective risk stratification and patient management[14]. It is widely available in the outpatient setting using relatively inexpensive technology. Protocols are standardised and there are excellent procedural and clinical utilization guidelines published by professional medical societies internationally [14]. However, SPECT suffers the limitations that the radiotracers are not optimal and are subject to attenuation artefacts,the test is time inefficient (stress-rest requires 4 h) and attenuation correction is not robust and, as a result, may underestimate the extent of CAD [7].

MPI with PET offers a number of real or potential advantages. There is higher spatial and temporal resolution of images, with fewer attenuation defects. Diagnostic accuracy is reported to be higher and thus better for risk stratification[15]. In most cases the procedure is shorter (30–90 min). PET/CT allows the potential for complementary information such as calcium scoring [14]. However, on the downside there are higher capital costs and, at present, more limited availability [14,15].

The properties of the discussed SPECT and PET agents are compared in Tables 1 and 2.

Current research in MPI tracers

There is great interest in developing MPI tracers for PET using the generator-produced radionuclides copper-62 (^{62}Cu) (half-life 10 min) and gallium-68 (^{68}Ga) (half-life 68 min). ^{62}Cu-pyruvaldehyde-bis(N^4-methylthiosemicarbazone (^{62}Cu-PTSM) produced good myocardial images in patients but accumulation was non-linear with relation to blood flow due to binding to albumin in the circulation [16]. An optimal ^{68}Ga-labelled agent remains to be identified. A series of ^{68}Ga-labelled salicylaldimine ligands failed to show suitable behaviour in a pig model [17]. However, the immense potential benefits of generator-produced PET radionuclides will ensure that this research continues.

Alternatives to flurpiridaz are under development, including BFPET (4-^{18}F-fluorophenyl) triphenylphosphonium ion, FluoroPharma), a lipophilic cationic mitochondrial targeting agent currently in phase 2 clinical trials. Other ^{18}F-labelled cations are also under development [18].

In contrast, there has been relatively little recent interest in novel SPECT agents as the market is felt to be mature, with sestamibi and tetrofosmin being well established. Recently an iodine-123 labelled analogue of rotenone has shown promising characteristics for mitochondrial targeting [19].

Competing modalities

Competing modalities include cardiac magnetic resonance (CMR), echocardioradiography (ECR) and multi-detector computed tomography (MDCT) or dual-source CT (DSCT) [14,20]. CMR and ECR provide good diagnostic accuracy but variable intra- and inter-observer agreement for the presence or exclusion of CAD [21]. CMR cannot be performed in most patients with pacemakers and implantable cardiac devices. Unlike PET/CT, these methods cannot provide absolute quantification (mL/g per minute), which is necessary to calculate the myocardial perfusion reserve (MPR), and have lower sensitivity for the detection of balanced ischaemia, multi-vessel disease and other pathological conditions that cannot be easily visualised by relative perfusion [7]. MDCT/DSCT has so far proven to be clinically feasible only for the detection of CAD (stenosis), and has shown limited success with MPI [21]. There is also concern about the radiation dose associated with the CT techniques.

Prospects

MPI with SPECT is a well-established procedure used widely around the world. MPI with PET/CT offers some potential advantages but at a cost. Competing modalities are being developed, but it will be a number of years before these replace MPI.

References Chapter 5

References

1. Notghi A, Low CS. Myocardial perfusion scintigraphy: past, present and future, Br J Radiol. 2011;84:S229-36.

2. Reyes E, Wiener S, Underwood SR. Myocardial perfusion scintigraphy in Europe 2007: a survey of the European Council of Nuclear Cardiology. Eur J Nucl Med Mol Imaging.2012;39:160-4.

3. Yu M, Nekolla SG, SchwaigerM, Robinson SP. The next generation of cardiac positron emission tomography imaging agents: discovery of flurpiridaz F-18 for detection of coronary disease.SeminNucl Med.2011;41:305-13.

4. Ritchie JL, Albro PC, Caldwell JH, TrobaughGB, Hamilton GW. Thallium-201 myocardial imaging: a comparison of the redistribution and rest images.J Nucl Med.1979;20:477-83.

5. Hesse B, Tägil K, Cuocolo A, Anagnostopoulos C, Bardiés M, Bax J, et al. and EANM/ESC Group. EANM/ESC procedural guidelines for myocardial perfusion imaging in nuclear cardiology.Eur J Nucl Med Mol Imaging.2005;32:855-97.

6. Selwyn AP, Allan RM, L'Abbate A, Horlock P, Camici P, Clark J, et al. Relation between regional myocardial uptake of rubidium-82 and perfusion: absolute reduction of cation uptake in ischemia. Am J Cardiol.1982;50:112-21.

7. Machac J. Cardiac positron emission tomography imaging.SeminNucl Med.2005;35:17-36.

8. Bergmann SR, Herrero P, Markham J, WeinheimerCJ, Walsh MN.Noninvasive quantitation of myocardial blood flow in human subjects with oxygen-15-labeled water and positron emission tomography.J Am CollCardiol.1989;14:639-52.

9. Bergmann SR. Clinical applications of myocardial perfusion assessments made with oxygen-15 water and positron emission tomography. Cardiology.1997;88:71-9.

10. Schelbert HR, Phelps ME, Hoffman EJ, Huang SC, SelinCE, Kuhl DE. Regional myocardial perfusion assessed with N-13 labeled ammonia and positron emission computerized axial tomography. Am J Cardiol.1979;43:209-18.

11. Wackers FJ, Berman DS, Maddahi J, Watson DD, Beller GA, Strauss HW, et al. Technetium-99m hexakis 2-methoxyisobutyl isonitrile: human biodistribution, dosimetry, safety, and preliminary comparison to thallium-201 for myocardial perfusion imaging.J Nucl Med.1989;30:301-11.

12. Kelly JD, Forster AM, Higley B, Archer CM, Booker FS, Canning LR, et al. Technetium-99m-tetrofosmin as a new radiopharmaceutical for myocardial perfusion imaging.J Nucl Med.1993;34:222-7.

13. BaggishAL, Boucher CA. Radiopharmaceutical agents for myocardial perfusion imaging. Circulation.2008;118:1668-74.

14. Flotats A, Knuuti J, Gutberlet M, Marcassa C, Bengel FM, Kaufmann PA, et al., Cardiovascular Committee of the EANM, the ESCR and the ECNC. Hybrid cardiac imaging: SPECT/CT and PET/CT. A joint position statement by the European Association of Nuclear Medicine (EANM), the European Society of Cardiac Radiology (ESCR) and the European Council of Nuclear Cardiology (ECNC).Eur J Nucl Med Mol Imaging.2011;38:201-12.

15. McArdle BA, Dowsley TF, deKemp RA, Wells GA, Beanlands RS.Does rubidium-82 PET have superior accuracy to SPECT perfusion imaging for the diagnosis of obstructive coronary disease? A systematic review and meta-analysis.J Am CollCardiol.2012;60:1828-37.

16. Herrero P, Hartman JJ, Green MA, Anderson CJ, Welch MJ, Markham J, Bergmann SR. Regional myocardial perfusion assessed with generator-produced copper-62-PTSM and PET.J Nucl Med.1996;37:1294-300.

17. Tarkia M, Saraste A, Saanijoki T, Oikonen V, Vähäsilta T, Strandberg M, et al. Evaluation of 68Ga-labeled tracers for PET imaging of myocardial perfusion in pigs.Nucl Med Biol.2012;39:715-23.

18. Kim DY, Kim HJ, Yu KH, Min JJ. Synthesis of [18F]-labeled (2-(2-fluoroethoxy)ethyl)tris(4-methoxyphenyl) phosphoniumcation as a potential agent for positron emission tomography myocardial imaging.Nucl Med Biol.2012;39:1093-8.

19. Wei L, Bensimon C, Lockwood J, Yan X, Fernando P, Wells RG, et al. Synthesis and characterization of 123I-CMICE-013: a potential SPECT myocardial perfusion imaging agent.Bioorg Med Chem.2013;21:2903-11.

20. Greenwood JP, Maredia N, Younger JF, Brown JM, Nixon J, Everett CC, et al. Cardiovascular magnetic resonance and single-photon emission computed tomography for diagnosis of coronary heart disease (CE-MARC): a prospective trial.Lancet.2012;379:453-60.

21. Pakkal M, Raj V, McCann GP. Non-invasive imaging in coronary artery disease including anatomical and functional evaluation of ischaemia and viability assessment. Br J Radiol.2011;84:S280-95.

Tables

Table 1: Comparison of properties of SPECT agents

	Thallium	**Sestamibi**	**Tetrofosmin**
Availability	Long half-life makes supply convenient	Kit preparation with boiling	Kit preparation at room temperature
Image quality	Poor emissions, low count density	Optimal for gamma cameras	Optimal for gamma cameras
Imaging flexibility	Stress imaging must begin immediately	Stress and rest on same or different days	Stress and rest on same or different days
Imaging protocol	Stress and rest data from single injection	Separate injections at stress and rest	Separate injections at stress and rest

Table 2: Comparison of properties of PET agents

	Water	**Ammonia**	**Rubidium**	**Flurpiridaz**
Availability	Requires on-site cyclotron	Requires on-site cyclotron	Generator produced	Unit dose supplied from commercial cyclotron
Image quality	High positron energy, poor counting statistics	Good image quality	High positron energy	Good image quality
Imaging flexibility	Good for small numbers of patients	Good for small numbers of patients	Unlimited number of patients	Available as unit dose; no special infrastructure required
Imaging protocol	Separate injections at stress and rest	Separate injections at stress and rest with 1 h between	Rapid rest-stress protocol	Separate injections at stress and rest

Chapter 6
SPECT and SPECT/CT Protocols and New Imaging Equipment
Andrea Santos and Edgar Lemos Pereira

Cardiac SPECT
Overall protocol
When using thallium-201 (^{201}Tl), because of redistribution, stress imaging starts 5–10 min after radiopharmaceutical injection and finishes at 30 min after administration. Acquisition of the redistribution image (rest image) should start 3–4 h afterwards, with the patient at rest during the interval. To access viability, re-injection must be considered, at rest and under nitrates [1–3].

When using technetium-99m (^{99m}Tc) radiopharmaceuticals, such as tetrofosmin or sestamibi, no redistribution occurs. The protocol preferably starts with a stress study. If needed, a rest study is performed on the same day (one-day protocol) or a different day (two-day protocol). Images should be acquired 30–60 min after injection on both studies; if the stress test is done on a treadmill, image acquisition can start as soon as 15–30 min after injection. The two-day protocol is preferred for reasons relating to dose and image quality. When applying the one-day protocol, injections should be separated by a 2-h period [1–3]. Figure 1 illustrates the general protocol for myocardial perfusion imaging (MPI).
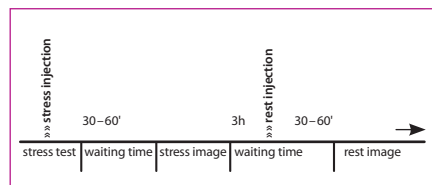

Figure 1: General cardiac MPI protocol

Imaging parameters
Table 1 shows gamma camera and acquisition parameters for SPECT. It is possible to perform circular rotation; however, non-circular rotation minimises the distance between the patient and the detectors. Step-and-shoot mode is more commonly used than continuous or continuous step-and-shoot mode. Acquisition time should take into consideration the count rate in order to obtain a good-quality image.

Patient positioning
Usually, the supine position is preferred, with the arms raised above the head, particularly the left arm. In order to reduce the patient's movement during the acquisition, technologists should make sure that the patient is comfortably positioned. For patients who cannot tolerate the supine position, the prone or lateral position should be used. A pillow can be placed under the knees, and the shoulders and arms should also be comfortably positioned in order to reduce both movement and pain, especially in older patients. Female patients should be imaged without a bra, and a chest band can be used to reduce breast attenuation and ensure reproducibility of images between stress and rest studies. Patients should be positioned in the same way for stress and rest studies; for this reason, i.e. to ensure reproducibility, use of a systematic method for patient positioning is recommended [1–4].

Image optimisation

In order to maximise the quality of the images acquired, with the lowest absorbed dose possible, awareness of some important factors is essential.

Gamma camera detectors

Nowadays, inorganic crystals are used in nuclear medicine to detect gamma rays. Ideally, the detector should have high detection efficiency, good energy resolution, good intrinsic spatial resolution and low dead time. The most commonly used crystal in SPECT systems is NaI(Tl). More recently, a CdZnTe (CZT) solid state camera has been developed with better energy resolution than NaI(Tl) cameras. This newer technology, due to its better physics characteristics (better sensibility and efficiency), is considered the best choice for MPI as it enables both faster SPECT acquisition (reducing motion and maximising patient throughput) and lower radiopharmaceutical administered activity. Moreover, recently developed gamma cameras use multiple-detector gantries that can be used in dedicated systems, like cardiac SPECT dedicated gamma cameras, because the equipment's architecture is optimised to acquire only one type of study. One example of the specific design on such equipment relies on the detector and/or patient positioning system. The so-called D-SPECT systems consist of several collimated CZT modules. A fast scout scan is first performed to locate the heart and the detector modules can confine their sampling to the heart. The main advantages of these systems are their increase sensitivity and improved spatial resolution [5, 6]. The properties of detectors used in SPECT are summarised in Table 2.

Administered activity and count statistics

The activity administered in each part of the exam (rest/stress, one-day/two-day protocol) affects the image quality, if a standard time per projection is established. If the time per projection can be adapted, depending on the left ventricle count rate, the administered activity may be less important than if a rigid time per view protocol is established. In the latter case, the administered activity has to be better adapted to the patient's weight or body mass index (BMI). In larger patients, higher activity must be used and in patients with lower BMI, lower activity must be administered in order to attain similar total counts on every SPECT study acquired in the same department. In the one-day protocol, the second injection should be given with an activity that triples the count rate [7–10].

According to EANM's guidelines, the recommended administered activities for both [99mTc] agents and [201Tl] are as follows:

[99mTc]-sestamibi or -tetrofosmin [1]:

- Two-day protocol: 600–900 MBq/study
- One-day protocol: 400–500 MBq for the first injection and, as mentioned above, three times greater for the second injection.

[201Tl]:

- Stress redistribution: 74–111 MBq
- Re-injection: 37 MBq

Dedicated cameras

Dedicated cameras are already being used for cardiac SPECT. Image acquisition is focused on the heart of the patient with highly efficient acquisition. These detectors are smaller and can acquire images with a smaller pixel matrix size. NaI(Tl) crystals can be used, but the solid state detectors are more commonly used in these dedicated cameras, such as CZT [7].
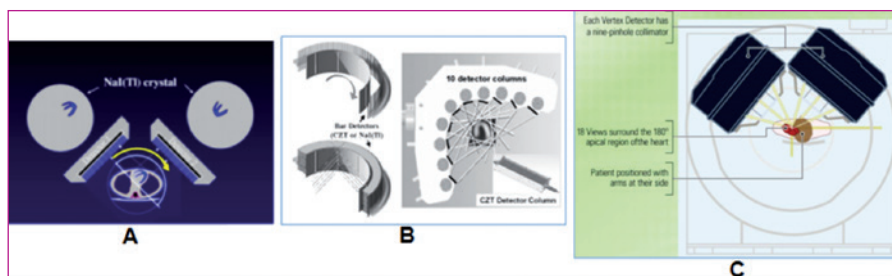
Figure 2 A – C: A Conventional gamma camera with dual-detector system (from Garcia et al. [8]). B Dedicated NaI(Tl) or CZT multiple detector gamma camera (from Madsen [16]). C Multiple-pinhole collimator (from Eagle Heart Imaging, LLC)

Several new types of gamma camera, with differing characteristics, are available from various vendors. There are dedicated gamma cameras, with or without CT, smaller equipment, in some cases with three detection heads, cameras with multiple detectors and even dedicated multi-pinhole collimators (Fig. 2). Some equipment allows acquisition with the patient seated, potentially reducing patient movement and, therefore, artefacts. With these dedicated systems, the acquisition can be faster (2–4 min vs the conventional 15–20 min), enhancing the patient's tolerance and consequently allowing better image quality [8, 9].

Software

Improved software can also enhance the image quality. Filtered back-projection is commonly used in MPI. In addition, iterative reconstruction algorithms are available and can improve image quality, one example being wide beam reconstruction. This subject is further explored in another chapter.

Attenuation correction

Patient body attenuation is one of the factors that can degrade image quality, especially in patients with higher BMI. For example, soft tissue can absorb or scatter radiation. In order to minimise the effect of attenuation, it is fundamental to perform attenuation correction. This compensation can be done by applying a mathematical algorithm that provides information about known and developed attenuation maps. Numerous attenuation correction algorithms have been proposed;

the most commonly used algorithms are the Chang algorithm (from 1978) and the maximum-likelihood expectation-maximisation (MLEM) reconstruction algorithm [10].

There is also a more patient-specific method to correct or compensate attenuation: estimation of patient-specific attenuation maps. This method is more accurate as it develops a patient-personal attenuation map. This type of attenuation correction can be applied by co-registration of the maps of *another modality* (such as computed tomography), or obtained by the estimation of attenuation maps with the emission data. Use of the attenuation map generated by the CT image is one of the most accurate methods of attenuation correction but it must be very carefully used owing to both the increased radiation burden and the need for perfect emission and transmission alignment, systematically controlled. In the absence of the latter, motion artefacts between the images can cause a mismatch between the attenuation correction map from CT and the emission image [10].

Gating

Gated studies should be acquired whenever possible despite the slight increase in acquisition time. This technique allows evaluation of functional parameters such as ejection fraction, left ventricle volumes and regional wall motion and improves the diagnostic accuracy of perfusion imaging. For gating purposes, only the systolic signal is needed (usually the R wave), as it is not a diagnostic ECG. Usually, a 20% window of acceptance

is allowed, without reduction of the study quality. One can define 8–32 images per cardiac cycle (usually 8–16), depending on the desired information. The larger the number of images per cycle, the longer the exam will take. It is important that the heart rate remains stable and consistent during the entire procedure; an arrhythmic/dysrhythmic heart rate can significantly decrease the accuracy of the study [1, 4, 5].

Cardiac SPECT/CT

SPECT/CT combines SPECT MPI with a CT scan in the same gantry. It allows acquisition of a SPECT scan and/or a CT scan, registration and fusion of the two images, and hybrid imaging, which adds specificity. Hybrid images can also be achieved by registering and fusing scans from different equipment. Adequacy of the registration process is crucial, to avoid reconstruction artefacts. Some authors recommend the acquisition of a different CT scan at stress and rest for the purpose of attenuation correction [11–14].

Attenuation correction can be achieved with CT attenuation maps from linear attenuation coefficients. Table 3 summarises the general characteristics of CT for non-diagnostic and diagnostic purposes. When used for a non-diagnostic purpose, CT is performed only for attenuation correction as an alternative to the mathematical methods previously discussed (it offers a more accurate method to correct attenuation, but at the cost of an increase in radiation burden). If CT is performed for a diagnostic
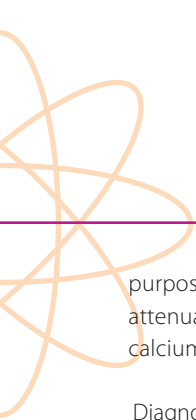
purpose, it maintains the ability to correct attenuation but can also be used to assess calcium scores or coronary angiography.

Diagnostic calcium scoring allows the detection of calcified plaques within the coronary vessels and can thus help in the early detection of coronary artery disease. Since the presence of calcified plaques does not mean that the myocardium is already in ischaemia, the information provided by this method is complementary to that acquired by MPI.

CT coronary angiography (CTCA) provides detailed anatomical information on coronary vessels, which, when combined with the functional information offered by SPECT, increases diagnostic accuracy. CTCA is performed in several steps. Prior to CTCA, technologists should instruct the patient on breath-hold technique. First, a scout scan is performed for anatomical localisation of the heart, to define the start and end location of the CTCA scan. The scan should extend from 2.5–5 cm above the aortic root to below the bottom of the heart, in accordance with the scout image. It is important that scan length is optimised for the purpose of dose optimisation. The aim is to minimise the distance scanned from above to below the heart, while avoiding excessive restriction of the scan volume. CT coronary angiography is a contrast-enhanced scan: the scan starts about 10 s after intravenous contrast administration as a single CT slice, with acquisition of one image every 2 s until a decrease in opacification of the aorta is observed [13, 14].

Calcium scoring CT and CTCA are complementary exams and the information provided by each one should be considered in conjunction with the results of MPI in order to maximise the information available regarding possible heart disease in each patient.

Radiation dose
Nowadays, the reduction of radiation doses related to myocardial scintigraphy is an important issue. New reconstruction methods and modern detectors and/or collimators optimised for cardiac SPECT may provide a solution. Exclusion of the rest study when stress is normal can also appreciably reduce the radiation dose. CT for the purpose of attenuation correction (non-diagnostic) does not increase the radiation dose significantly. In any case, physicians and technologists must always pay due attention to adjusting CT protocols to the patient's BMI, respecting the ALARA principle.

The estimated radiation dose due to CTCA ranges from 8 to 18 mSv. However, modern cardiac CT protocols (step-and-shoot ECG triggering, ECG-controlled current modulation that reduces the tube current by 80% during systole and body mass-adapted tube voltage that reduces the tube voltage to 100 kV in patients under 90 kg) allow reduction of the radiation dose by 60–80%. Some studies have reported a radiation dose of 5.4 mSv at stress-only hybrid ^{99m}Tc-tetrofosmin SPECT/CT [11].

References Chapter 6

References

1. Hesse B, Tägil K, Cuocolo A, Anagnostopoulos C, Bardies M, Bax J, et al. EANM/ESC procedural guidelines for myocardial perfusion imaging in nuclear cardiology. Eur J NUcl Med Mol Imaging. 2005;32:855–97.

2. Strauss HW, Miller DD, Wittry MD, Cerqueira MD, Garcia EV, Iskandrian AS, et al. Procedure guideline for myocardial perfusion imaging 3.3. J Nucl Med Technol. 2008;36:155–61.

3. Lecoultre R, Jorge JP. Preparation and use of imaging equipment. In: Myocardial perfusion imaging – a technologist's guide. EANM. 2004:29–35.

4. Holly TA, Abbott BG, Al-Mallah M, Calnon DA, Cohen MC, DiFilippo FP, et al. ASNC imaging guidelines for nuclear cardiology procedures. J Nucl Cardiol. 2010.

5. Pedroso de Lima J. Física em Medicina Nuclear: Temas e aplicações. Coimbra: Coimbra University Press; 2008:159–86.

6. Arlt R, Ivanov V, Parnham K. Advantages and use of CdZnTe detectors in safeguard measurements. Accessed in January, 2014. Available from http://www.evproducts.com/pdf/Applications/Advantages%20and%20use%20of%20CdZnTe.pdf

7. Frans J, Wackers T. Cardiac single-photon emission computed tomography myocardial perfusion imaging: finally up to speed. J Am Coll Cardiol. 55:1975–8.

8. Garcia EV, Faber TL, Esteves FP. Cardiac dedicated ultra-fast SPECT cameras: new designs and clinical implications. J Nucl Med. 2011;52:210–7.

9. Sharir T, Slomka PJ, Berman DS. Solid-state SPECT technology: fast and furious. J Nucl Cardiol. 2010;17:890–6.

10. King M, Glick S, Pretorius P. Attenuation, scatter and spatial resolution compensation in SPECT. In: Wernick M, Aarsvold J. Emssion tomograph: The fundamentals of PET and SPECT. USA: Elsevier Academic Press; 2004:473–85.

11. Flotats A, Knuuti J, Gutberlet M, Marcassa C, Bengel FM, Kaufmann PA, et al. Hybrid cardiac imaging: SPECT/CT and PET/CT. A joint position statement by the European Association of Nuclear Medicine (EANM), the European Society of Cardiac Radiology (ESCR) and the European Council of Nuclear Cardiology (ECNC). Eur J Nucl Med Mol Imaging 2011;38:201–12.

12. Delbeke D, Coleman RE, Guiberteau MJ, Brown ML, Royal HD, Siegel BA, et al. Procedure guidelines for SPECT/CT imaging 1.0. SNM. 2006.

13. Dorbala S, Di Carli MF, Delbeke D, Abbara S, DePuey EG, Dilsizian V, et al. SNMMI/ASNC/SCCT guideline for cardiac SPECT/CT and PET/CT 1.0. J Nucl Med. 2013;54:1485–507.

14. Mariani G, Flotats A, Israel O, Kim EE, Kuwert T. Clinical applications of SPECT/CT: New hybrid nuclear medicine imaging system. IAEA-TECDOC-1597. 2008.

15. Patton JA, Turkington TG. SNM SPECT/CT physical principles and attenuation correction. J Nucl Med Technol. 2008;36:1–10.

16. Madsen MT. Recent advances in SPECT imaging. J Nucl Med. 2007;48:661–73.

Table 1: Gamma camera and imaging parameters for SPECT

Isotope	Protocol	Collimator	Energy	Energy window	Rotation	Nr. projections	Angles	Projection time	Pixel matrix	Zoom
^{99m}Tc	1 day	LEHR or LEGP	140 keV	15–20%	180º (360º if 3-head gamma camera)	64 or 128	3–6º; 45º RAO to 45º LPO	1st acquisition: 25 s/frame 2nd acquisition: 20 s/frame	64×64 or 128×128	1.0 (higher if necessary)
	2 day							25 s/frame		
^{201}Tl	1 day	LEGP or LEHR	70 keV	20–30%	180º (static images if necessary)	32 or 64		20–25 s/frame		
			167 keV	20%						

Table 2: Properties of detectors used in SPECT (adapted from Arlt et al. [6])

Property	Energy per e-h pair (eV)	Atomic number	Density (g/cm³)	Maximal volume (cm³)	Resolution FWHM (keV)
Influences:	Resolution	Photo peak/Compton	Efficiency	Efficiency	Separation of lines
Ge	296	32	5.35	100	0.4–2
Si	3.61	14	2.33	0.1	0.2–1
CdTe	4.43	50	6.2	0.1	0.2–20
Cd$_{0.9}$Zn$_{0.1}$Te	4.64	49.1	5.78	3.4	0.2–20
HgI$_2$	4.15	63	6.4	40	0.2–30
GaAs	4.3	32	5.3	0.1	3
NaI	–	–	3.67	>100	15–50

Table 3: Acquisition modalities: CT scanners for hybrid imaging [11–13, 15]

Scan type	Non-diagnostic (low resolution)	Diagnostic	
Modality	AC only	AC and/or calcium score	AC and/or CTCA
Acquisition protocol	Non-enhanced Non-gated Free tidal breath	Non-enhanced Gated Breath hold (inspiration)	Contrast-enhanced Gated Breath hold
Slice thickness	5 mm	Depending on equipment, 2–3 mm	Depending on equipment, 0.4–0.75 mm
Nr. of slices	Less than 4	≥4 (≥6 recommended)	≥16 (≥64 recommended)
Resolution	Low	Good	Excellent
Spatial resolution	Depending on equipment, can be higher than 3 lp/cm	Depending on equipment, 13–15 lp/cm (2-slice to 64-slice multidetector row CT)	
Temporal resolution	0.6–1.5 s		<0.5 s (preferably ≤0.35 s)
Tube current[a]	Depending on equipment, usually from 1 to 2.5 mA	Depending on equipment and purpose, 20–500 mA	
Tube voltage[a]	80–140 kVp	100 kVp	120–140 kVp
Additional radiation dose	Very low/low (0.1–1 mSv)	Usually intermediate (1–10 mSv)	Intermediate/high (1–10 mSv)
Scan duration	<5 min		

[a] Dose optimisation, tube current and voltage can be lowered for patients with lower body mass index. However, manufacturer and guideline recommendations should be consulted to guarantee that the scan stills accomplishes its purpose [13]

AC, Attenuation correction; CTCA, CT coronary angiography

Chapter 7
PET/CT Protocols and Imaging Equipment
April Mann and Scott Holbrook

Introduction

Myocardial Imaging with hybrid positron emission tomography/computed tomography (PET/CT) is an evolving discipline exhibiting growth influenced by improvements in instrumentation, novel radiopharmaceuticals which provide unique clinical information, and an expanding knowledge necessary to overcome logistical and technical challenges amongst imaging experts. In order to successfully implement a cardiac PET/CT imaging programme special attention must be given to the short half-life of radiotracers, safety considerations associated with radiation exposure due to computed tomography, and the normal or abnormal bio-distribution of specific biomarkers. Numerous peer-reviewed publications have suggested appropriate patient preparation for myocardial PET/CT imaging and protocols to ensure accurate and reproducible data, and the factors influencing image optimisation have been well documented.

Perhaps the first consideration in successful acquisition of a myocardial PET/CT exam relates to radiopharmaceutical availability and characteristics. The two most commonly available radiopharmaceuticals at the time of this publication are rubidium-82 (^{82}Rb) chloride and Nitrogen-13 (^{13}N) ammonia. Stress protocol, patient and staff radiation exposure, and image acquisition parameters relate directly to the relative half-lives of ^{82}Rb (75 s) and ^{13}N (9.96 min). Technical factors associated with image optimisation are influenced not only by patient body habitus but also by the energy associated with beta decay and beta max for each radionuclide. The energy for ^{82}Rb, beta max of 3.35 MeV, is such that there is degradation in image resolution when compared with that of ^{13}N, beta max 1.19 MeV. Kinetic energy associated with initial beta decay must be lost before an annihilation reaction will occur resulting in collinear photons to be detected by the PET/CT system. It is the movement associated with the loss of kinetic energy and prior to the resultant annihilation reaction that accounts for a decrease in image resolution.

Rubidium-82 cardiac PET perfusion imaging

PET myocardial perfusion imaging utilising ^{82}Rb is considered a highly accurate procedure to detect hemodynamically significant coronary artery disease and is well established within the literature [1]. Rubidium-82 is a potassium analogue produced with commercially available generators and is the product (daughter) from decay of strontium-82 (^{82}Sr). ^{82}Sr has a half-life ($T_{1/2}$) of 25.5 days and decays by electron capture. The generator contains accelerator-produced ^{82}Sr absorbed on stannic oxide in a lead-shielded column [2]. The introduction of saline through the columns produces a sterile non-pyrogenic solution of rubidium chloride (^{82}RbCl) for injection. The resulting activity of ^{82}Rb is dependent on the potency of the generator but is usually in the range of 1110–2220 MBq and should not exceed 2220 MBq.

Rubidium-82 decays by positron emission and associated gamma emission. Once produced, it has a half-life ($T_{1/2}$ of 75 s and, since it is generator produced, an on-site cyclotron is not required [1–4]. ^{82}Rb decays into krypton-82 (^{82}Kr) by emitting a neutron and a positron. The annihilation photons released following the positron emission have a mean energy of 511 keV and are used for image acquisition. The very short half-life allows the generator to be eluted every 10 min, making ^{82}Rb suitable for repeated and sequential perfusion studies [1–4].

The short half-life requires rapid image acquisition to occur shortly after tracer administration reducing the total study duration to approximately 30–45 min depending on the type of PET or PET/CT system and protocol used for imaging [1, 3]. This time is significantly reduced compared with the standard one-day rest/stress technetium-99m (^{99m}Tc) labelled radiotracer study, which takes approximately 3–4 h depending on the protocol and system used for image acquisition. Further, the short half-life, results in a limited radiation exposure for patients (5.5 mSv for 2220 MBq compared with a standard one-day rest/stress ^{99m}Tc-labelled radiotracer study (10.6–12.0 mSv for 370/1110 MBq) or thallium-201 (^{201}Tl) stress-rest study (18.8 mSv for 111 MBq) [2].

Rubidium-82 has been well studied as a perfusion tracer since the 1950s. As a blood flow tracer, it is rapidly extracted from the blood and taken up by the myocardium. Since it is a potassium analogue, ^{82}Rb uptake occurs via the Na^+/K^+-ATPase transporter similar to ^{201}Tl. ^{82}Rb has been recorded to have an extraction rate of 50–60% at normal flow rates. However, its extraction is documented to be less than that of ^{13}N-ammonia and decreases with increased blood flow to as low as 20–30%. It has also been noted that hypoxia, myocardial cell integrity, severe acidosis and myocardial ischaemia may also decrease ^{82}Rb extraction rates [1–4].

Quality control for rubidium-82

The ^{82}Rb generator is stored in an automatic infusion system that produces accurate and reproducible constant-activity elution profiles (Fig. 1) [2]. In order to utilise the ^{82}Rb generator, the manufacturer has training and education requirements that must be completed by both physicians and technologists prior to initiating a cardiac PET programme. In addition, there are mandatory quality control procedure requirements for radiochemical purity and eluate volume that must be performed on the generator and documented daily before patient use.

Approximately 75 min is required in order to complete the ^{82}Rb generator quality control using the following steps [2]:

1. Elute the generator with 50 mL normal saline

2. Measure the eluate for the activity of ^{82}Rb *(MBq)*

3. Allow sample to sit for an hour and measure activity again *(Bq)*

4. Decay the ratio of $^{85}Sr/^{82}Sr$ from the calibration lot information to current time *(R)*

5. ^{82}Sr = (dose calibrator reading)/[1+(R)*(F)*]

   a. *Where F is a constant 0.478 to eliminate higher counts coming from ^{85}Sr*

6. THEN, Bq of ^{82}Sr/MBq of ^{82}Rb= *(N)*

7. The $^{82}Sr/^{82}Rb$ ratio *(N)* is multiplied by *R* to get amount of Bq ^{85}Sr/ MBq ^{82}Rb.

As part of the daily documentation and quality control, it is also necessary to measure for each generator eluate waste, test and cumulative eluate volumes and determine ^{82}Rb, ^{82}Sr and ^{85}Sr eluate levels once daily prior to patient administration. In addition to these quality control requirements, Alert and Expiration Limits have been established in order to eliminate the possibility of any unintended radiation exposure to patients from ^{82}Sr or ^{85}Sr. ^{85}Sr content cannot be more than 740 Bq/kBq of ^{82}Rb at the end of elution time and ^{85}Sr content cannot be more than 7400 Bq/kBq of ^{82}Rb at the end of elution time. Both of these limits are well below the established legal breakthrough limits set by the Nuclear Regulatory Commission (NRC).

Additional daily testing on the generator is necessary after detection of an *Alert Limit*:

- 14 L for the cumulative eluate volume, *or*
- An eluate ^{82}Sr level of 74 Bq/kBq ^{82}Rb, *or*
- An eluate ^{85}Sr level of 740 Bq/kBq ^{82}Rb

Use of a generator must **STOP** at an *Expiration Limit*:

- 17 L for the generator's cumulative eluate volume, *or*
- 42 days post generator calibration date, *or*
- An eluate ^{82}Sr level of 370 Bq/kBq ^{82}Rb, *or*
- An eluate ^{85}Sr level of 3700 Bq/kBq ^{82}Rb

Figure 1: ^{82}Rb generator and infusion cart

Imaging and acquisition parameters
Preparation for patients undergoing an ^{82}Rb myocardial perfusion study is similar to that for other myocardial perfusion imaging exams. Patients should not have anything to eat or drink, except water, for at least 6 h prior to the scheduled examination time. Caffeine should be withheld for at least 12 h prior to the procedure and medications such as theophylline and aminophylline should be withheld for at least 48 h. In patients referred for diagnosis or CAD, beta-blocker and other cardiac medication should be withheld for at least 48 h prior to the exam. If patients are referred for evaluation of medical therapy,

withholding cardiac medication may not be necessary.

When performing myocardial perfusion imaging with [82]Rb, it is recommended to perform the rest images first in order to reduce any residual stress effects (ischaemic stunning or coronary steal. It is also necessary to consider that 80% of all useful counts are acquired in the first 3 min, 95% in the first 5 min and 97% in the first 6 min when imaging with [82]Rb. Therefore, it is not necessary to acquire images for longer than 6 min. After the infusion of [82]Rb (approximately 30 s) in patients with normal left ventricular ejection fraction (LVEF) >50%, imaging should begin 70–90 s post injection [1]. In patients with known decreased LVEF (30–50%), imaging should begin 90–110 s post injection, and in those with LVEF <30%, 110–130 s post injection [1]. If imaging begins sooner than suggested, counts not cleared from the residual blood pool may interfere with true counts within the myocardium, decreasing the diagnostic accuracy of the study.

The short half-life of [82]Rb poses a challenge for achieving optimal image quality, and acquisition parameters vary widely and are dependent on the type of PET or PET/CT system being used. Acquisition of the scout for attenuation correction will also depend on the type of imaging system being used. The short half-life of [82]Rb also requires the patient's image acquisition to begin quickly following injection. Therefore, myocardial perfusion imaging with [82]Rb is primary limited to pharmacologic stress. Figure 2 demonstrates an example of an imaging protocol performed with a PET/CT system and dipyridamole used as the stress agent.
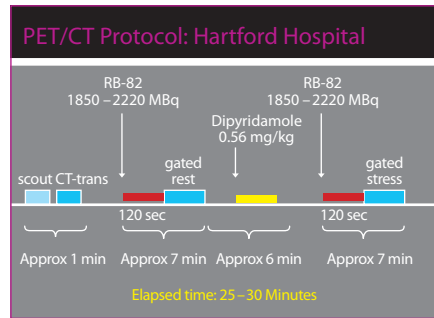
Figure 2: PET/CT protocol for myocardial perfusion imaging with [82]Rb at Hartford Hospital in Hartford, Connecticut

Limitations of [82]Rb imaging

There are many advantages to the use of [82]Rb PET protocols for myocardial perfusion imaging including improved image quality, spatial and temporal resolution and diagnostic accuracy compared with SPECT imaging. Also, [82]Rb PET imaging is well validated in the literature, provides reliable prognosis and risk stratification for patients and offers a rapid imaging procedure with lower patient radiation exposures. However, [82]Rb PET imaging does have some limitations, including: it is cost prohibitive with low patient volumes (fewer than four patients/day); it is not possible to perform exercise testing in patients; and quality control requirements are extensive (greater than 60 min/day).

Stress testing with cardiac PET

The best test to evaluate haemodynamic changes during stress is an exercise test. It provides independent prognostic value and allows for assessment of symptoms and exercise capacity. Furthermore, combining exercise data with perfusion data results in the best risk stratification of patients. Standard clinical indications for stress testing include but are not limited to:

- Evaluation of patients with chest pain or other findings suggestive of CAD

- Determination of prognosis and severity of disease

- Evaluation of effects from medical and surgical therapy

- Screening for latent CAD (only approx. 30% of patients with ischaemia have chest pain)

- Evaluation of arrhythmias, functional capacity or congenital heart disease

More specifically, common clinical indications for stress myocardial perfusion imaging include but are not limited to:

- Diagnosis of suspected CAD

- Risk stratification of known CAD

- Assessment of medical or surgical therapies used to treat known CAD

- Pre-operative assessment in patients with cardiac symptoms

- Myocardial viability assessment

Stress protocols for cardiac PET imaging are similar and generic to all perfusion tracers. The differences for ^{82}Rb and ^{13}N-ammonia are related to the half-life and clearance of the specific tracers [1]. Given the short half-life (75 s) of ^{82}Rb, physical exercise is not currently possible. Therefore, only pharmacological stress is performed with the ^{82}Rb imaging protocol.

Standard stress protocols and patient preparation should be in compliance with ACC/AHA guidelines for stress testing. Before performing any stress test, it is necessary to ensure patients do not have an absolute or relative contraindication to the procedure. When performing stress tests in conjunction with perfusion imaging it is necessary to have at least two qualified individuals present during the procedure: one person to monitor the patient and the other individual to perform the injection of the radiotracer.

Various types of protocol are used to perform physical exercise tests, including Bruce, Modified Bruce, Naughton and Chung. For PET perfusion imaging, the standard protocol followed in most laboratories is the Bruce (Fig. 3). During the procedure, it is necessary to measure and document the patient's heart rate and blood pressure at 2 min into every stage. The radiotracer should be injected when the patient has achieved at least 85% of the maximum predicted heart rate and is no longer able to continue. As discussed earlier, due to the short half-life of ^{82}Rb, treadmill stress testing in patients is not possible.

Stage	Speed (MPH)	Grade (%)	Time (min)	Cum. Time
1	1.7	10	3	3
2	2.5	12	3	6
3	3.4	14	3	9
4	4.2	16	3	12
5	5.0	18	3	15
6	5.5	20	3	18
7	6.0	22	3	21

*   Inject trace 1 min. prior to termination

Figure 3: Standard Bruce protocol for treadmill exercise

Considering pharmacological stress, dipyridamole has the longest history of use and has the most data available in the literature in relation to myocardial perfusion imaging (Fig. 4). It is a potent coronary vasodilator that acts by blocking cellular adenosine uptake. During infusion, dipyridamole causes coronary vasodilatation and hyperaemia at blood flow rates 3–5 times baseline.
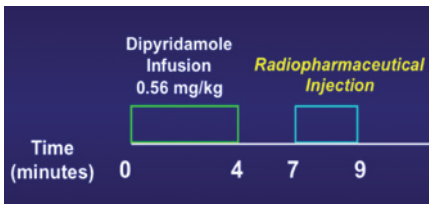
Figure 4: Dipyridamole infusion protocol

Adenosine is another pharmaceutical used for stress testing (Fig. 5). It is a potent coronary vasodilator that acts by directly activating adenosine receptors on cell membrane surfaces. During infusion it causes blood flow rates 4–6 times resting blood flow. Similar to dipyridamole, its use is well validated in the literature.
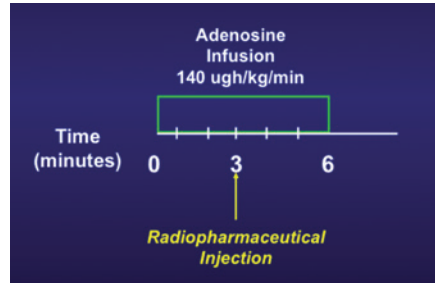
Figure 5: Adenosine infusion protocol

Finally, regadenoson is another option for pharmacological stress testing (Fig. 6). It is a selective A_2A receptor coronary vasodilator that causes blood flow rates 4–6 times resting blood flow. It is supplied in a single-use vial or pre-filled syringe and it does not require dose adjustment for body weight. It is given as a rapid (10 s) intravenous injection, causing maximum hyperaemia at 30 s post injection.
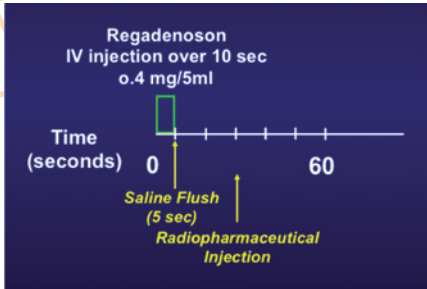
Figure 6: Regadenoson infusion protocol

Cardiac PET perfusion imaging with ^{13}N-ammonia

Considered to be the gold standard for myocardial perfusion imaging due to very high image resolution and quantitative characteristics, cardiac PET perfusion imaging with ^{13}N-ammonia has grown in utilisation despite the relatively short half-life of ^{13}N, which necessitates the availability of a nearby cyclotron and PET drug manufacturing facilities (Fig. 7).
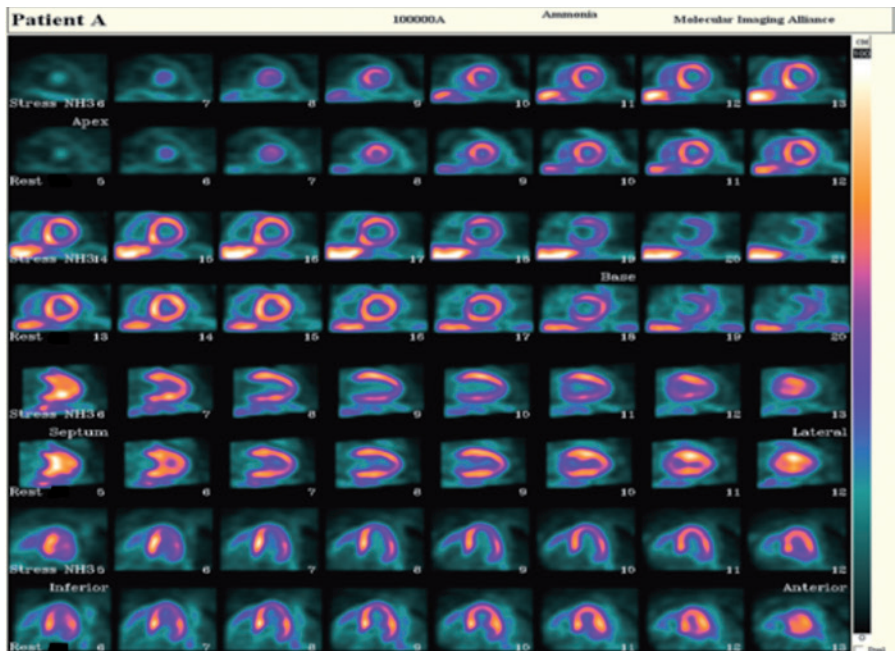

Figure 7: A 204-kg male patient with chest tightness and shortness of breath upon exertion. Despite a very high body mass index, ^{13}N-ammonia cardiac perfusion images provide data of excellent technical quality

Preparation for patients undergoing a ^{13}N-ammonia cardiac PET perfusion studies is similar to that for other myocardial perfusion imaging exams. Patients should not have anything to eat or drink, except water, for a minimum of 6 h prior to the scheduled examination time. Foods containing caffeine should be withheld for at least 12 h prior to the procedure. Medications such as theophylline and aminophylline should be withheld for at least 48 h and beta-blockers for 24 h. Patients should be dressed in comfortable non-attenuating clothing without metal zippers or buttons if possible [1].

Stress protocols are the same as previously mentioned (Fig. 8). The radioactive half-life of ^{13}N does potentially allow for treadmill exercise protocols unlike with ^{82}Rb. ^{13}N-ammonia doses are 370–740 MBq per injection. Once injected, ^{13}N-ammonia accumulates in myocardium, as with other radiotracers, in proportion to blood flow, extraction and retention. ^{13}N-ammonia is transported intracellularly through active transport via the sodium-potassium pump and becomes trapped as ^{13}N-glutamine. Patients should be positioned supine with arms raised and out of the PET field of view in order to avoid artefacts. Electrocardiogram electrodes and a blood pressure cuff should be placed on the patient's arm, and care should be taken to ensure that intravenous lines will not interfere with the study acquisition. Also, in order to ensure that the myocardium is centred within the field of view, a scout scan may be performed utilising CT or the camera's laser positioning device and the xiphoid process as an anatomical landmark. With a dedicated PET system, a small point source of ^{13}N-ammonia may also be used to verify correct patient positioning.

The ^{13}N-ammonia should be administered in less than 30 s, and a delay after injection of 1.5–3 min should occur prior to initiation of imaging. However, if myocardial blood flow is measured, imaging should begin immediately after injection. A sufficient difference between stress and rest radiopharmaceutical counts may be achieved by decay and/or administered activities to ensure the data from the second image set overcome data from the first. Images may be gated to reflect myocardial wall motion and should be acquired in either static or dynamic list mode. Emission images should be acquired for 10–15 min while the patient is instructed to remain very still. Transmission imaging for attenuation correction is conducted with CT or ^{68}Ge rod sources and may be completed before emission images are acquired. Transmission scans obtained with ^{68}Ge rod sources should take into account the age and energy of the rod sources. Transmission scan time should be increased when the energy of the sources is low or the rod sources are older. Data should be processed using filtered back-projection or iterative reconstruction and examined for artefacts associated with transmission-emission misregistration or patient motion [1].
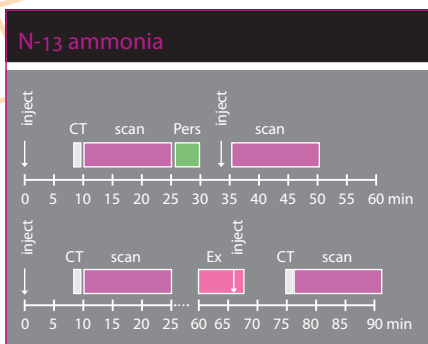
N-13 ammonia

Figure 8: Example of exercise (top) and dipyridamole $^{13}NH_3$ PET protocol (bottom)

Increased availability and utilisation of ^{13}N-ammonia has led to variations of the aforementioned protocol in routine clinical practice. Previously, batches of ^{13}N-ammonia at end-of-synthesis were commonly produced with a total activity of 5550 MBq. New in-target production methods now routinely produce total batch activities of greater than 37,000–55,500 MBq. Furthermore, cyclotrons equipped with more than one ^{13}N target may be capable of producing several batches per hour. Sufficient batches sizes of ^{13}N-ammonia allow for higher dosing of patients with extremely large body mass index. For example, patients who weigh less than 159 kg may receive 370–740 MBq of ^{13}N-ammonia compared with an injection of 1110–1665 MBq of ^{13}N-ammonia for patients who weigh greater than 159 kg. Also of note, many PET and PET/CT scanners have recommended maximum patient table weights of 204.5 kg, and patients with a very large body mass index often benefit from cardiac PET perfusion imaging over SPECT.

Cardiac metabolic imaging with fluorine-18 fluorodeoxyglucose

Unlike other tissues under normal physiological circumstances, the myocardium preferentially metabolises free fatty acids rather than glucose. Approximately 70% of available energy for the typical myocyte is derived from long chain fatty acid metabolism compared with 30% from glucose metabolism. The percentage contribution of substrate metabolism within the myocardium can shift depending on various circumstances such as the presence of endogenous insulin due to exercise or carbohydrate digestion, the administration of insulin in diabetics, and the presence of anaerobic metabolism, as with ischaemia. Understanding this metabolic shift is of great importance when engaging in myocardial metabolic imaging. When properly utilised, fluorine-18 fluorodeoxyglucose (^{18}F-FDG) cardiac imaging is a valuable tool in distinguishing viable myocardium that has undergone an acute ischaemic event, may be hypokinetic and is metabolising glucose rather than fatty acids from myocardium that has infarcted, is no longer viable and is not metabolising glucose [1]. In order to evaluate viability myocardial tissue, it is first necessary to normalise the metabolic environment for all of the myocardium to ensure glucose metabolism will occur within viable tissue. This may be accomplished through oral administration of glucose after a fasting period resulting in an endogenous release of insulin or, in the case of diabetics, through the administration of insulin.

Fluorine-18 fluorodeoxyglucose, an analogue for dietary glucose, is transported across cell membranes via glucose transporter proteins such as GLUT-1. Once in the intracellular space, glucose is acted upon by the enzyme hexokinase and converted to two molecules of pyruvate (glycolysis) that then proceed to the Krebs cycle and subsequent steps associated with oxidative metabolism. Alternatively, 18F-FDG becomes converted to 18F-FDG-6-phosphatase, which is not a suitable substrate for oxidative metabolism and cannot pass to subsequent steps associated with glucose metabolism. Additionally, 18F-FDG-6-phosphatase becomes trapped within the intracellular space and serves as an excellent marker for relative glucose metabolism.

On the day of the scheduled procedure, patients should arrive with nothing by mouth for at least 6 h prior to the scheduled examination time. An initial blood serum glucose measurement should be taken prior to administration of glucose. If initial blood serum glucose values are less than 250 mg/dl, then the protocol may proceed with 25–100 mg of oral glucose. Subsequent blood serum glucose measurements should be taken until a blood serum glucose level of 100–140 mg/dl is obtained. The increase in blood serum glucose associated with oral administration of glucose and its subsequent decrease indicate the release of endogenous insulin by the pancreas, creating a suitable environment for administration and imaging of 18F-FDG. If the patient's initial fasting blood serum glucose

measurement is greater than 250 mg/dl, no further oral glucose loading is necessary. However, it may be necessary to administer insulin to achieve the desired effect [5]. Once the desired blood serum glucose/insulin response has been achieved, 185–555 MBq 18F-FDG should be administered.

Image acquisition typically begins 45–60 min post injection. Certain patient populations such as diabetics may present glucose management challenges because insulin resistance may result in the need to delay imaging up to 2 or 3 h. Patients should be instructed to wear comfortable, non-attenuating clothing and be positioned supine with arms above the head and outside of the camera field of view. Scout scans may be performed with 18F-FDG data or CT data in the case of PET/CT. Images may be acquired for 10–30 min in static or dynamic list mode. Attenuation correction may be performed immediately before or after the emission scan, prior to patient movement, using either CT or 68Ge rod sources. Data are reconstructed with filtered back-projection or iterative reconstruction [1].

Cardiac PET images obtained with 18F-FDG are often compared with resting perfusion images in order to identify tissue that was not readily detectible based on potassium transport or other mechanisms relied upon by cardiac perfusion radiopharmaceuticals but still participates in active glucose metabolism and is therefore viable. This mismatch represents viable myocardium that is either

71

"stunned" or hibernating and would benefit from revascularisation. Myocardium that does not demonstrate glucose metabolism as represented by ^{18}F-FDG accumulation following a lack of perfusion tracer concentration represents infarcted tissue (Fig. 9).
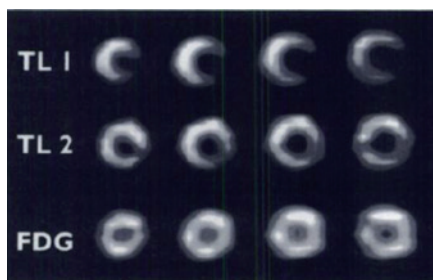

Figure 9: Corresponding series of ^{201}Tl rest-redistribution SPECT and FDG PET short-axis slices. The early ^{201}Tl slices (top) show a defect in the lateral wall and redistribution on late ^{201}Tl images (middle). FDG slices (bottom) show increased uptake in the lateral wall compared with early ^{201}Tl images. Lateral wall was akinetic on resting echocardiography and improved in function with revascularisation

Future directions

The unquestionable benefits of cardiac PET have led to efforts to increase the availability of PET radiopharmaceuticals. The requirement for a nearby cyclotron for ^{13}N-ammonia and the supply costs associated with ^{82}Rb generators have placed an emphasis on cardiac PET radiotracers labelled with ^{18}F. The ideal radiotracer for cardiac PET imaging would exhibit a high extraction proportional to regional cardiac flow even at very high flow rates, have a sufficient half-life to allow for optimal logistics and work-flow, entail reasonable radiation exposure for staff and patients and provide the ability to conduct quantification and excellent image quality in all patient populations. The cardiac PET perfusion agent [^{18}F]BMS747158 or Flurpiridaz, still in clinical trials, has thus far demonstrated these tracer characteristics and has been well tolerated by subjects and provides high-resolution cardiac PET perfusion images (Fig. 10). A rotenone analogue, this agent has affinity for the mitochondrial complex found in abundance within myocardial tissue. ^{18}F-Flurpiridaz has also exhibited excellent myocardial extraction fraction and flow rate characteristics [5].
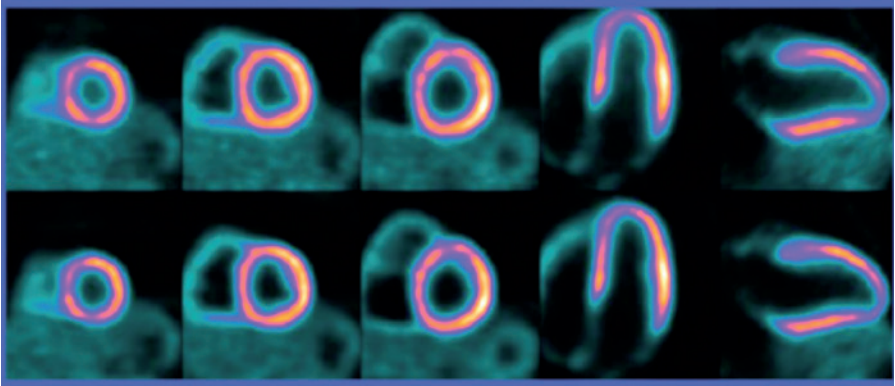
Figure 10: Cardiac imaging with [18F]BMS747158. Top row, standard reconstruction. Bottom row, high-definition cardiac perfusion PET

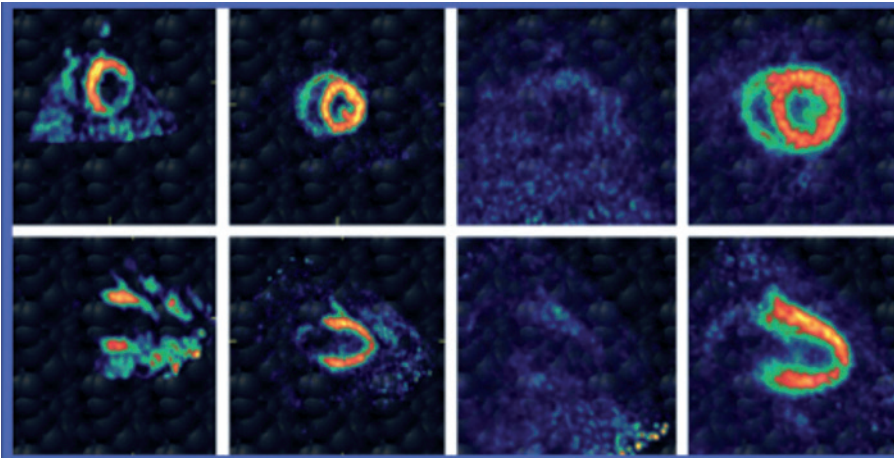Figure 11: Representative cardiac PET images of LMI1195 (first and third columns) and [18F] BMS747158 (second and fourth columns) in rabbits with and without regional (phenol directly painted on the heart, left four images) and systemic (intravenous injection of 6-OHDA to destroy cardiac neurons, right four images) cardiac sympathetic denervation. The denervated area in the heart was clearly detected by imaging with LMI1195 but not [18F]BMS747158 in the same rabbit. With normal perfusion images in the denervated rabbit, decreased LMI1195 heart uptake resulted from reduced neuronal function, not changes in myocardial perfusion

Future opportunities in cardiac imaging will offer unique information to clinicians that will aid in patient stratification for therapy and intervention. The novel biomarker LMI1195 (Fig. 11) has demonstrated the ability to differentiate normal myocardial tissue from tissue that exhibits neuronal dysfunction and remodelling. Neuronal dysfunction following an ischaemic event has been show to contribute to arrhythmias [5]. Identification of this cardiac remodelling may assist with patient stratification for implantable cardioverter defibrillator (ICD). Additional future directions in cardiac PET imaging include detection of ischaemic injury by imaging the metabolic shift from ^{18}F-labelled fatty acids to glucose. Areas of injured myocardium preferentially metabolise glucose rather than free fatty acids during and after periods of ischaemia. Initial image sets associated with flow may be compared to delayed images associated with metabolism (Fig. 12). Myocardial segments associated with normal flow but decreased fatty acid metabolism are potentially indicative of a recent ischaemic event [6].
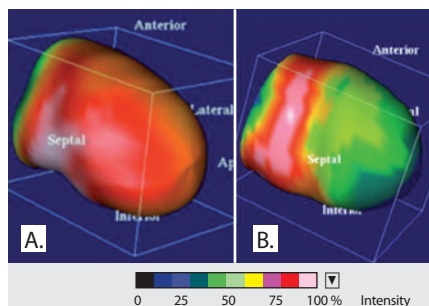
Figure 12 A, B: PET/CT images of free fatty acid analogue ^{18}F-fluoro-cyclopropyl hexadecanoic acid (^{18}F-CPHA). A Normal myocardium with homogeneous distribution of ^{18}F-CPHA associated with normal free fatty acid metabolism. B Abnormal myocardium with areas of decreased fatty acid metabolism from metabolic shift associated with anaerobic metabolism and injury

Conclusion

Successful implementation of a cardiac PET imaging programme requires consideration of many issues. The availability of radiotracer, whether as a result of a local cyclotron with sufficient capabilities and staffing or the acquisition of ^{82}Rb generator, may be the first important factor to consider. Availability of ^{13}N-ammonia may provide the opportunity to conduct exercise cardiac PET procedures but necessitates planning for adequate treadmill space in close proximity to the PET or PET/CT unit. Stress testing and image acquisition protocols will be determined by the radiotracer utilised. The half-life of the administered radiopharmaceutical will determine dosage as well as radiation exposures to staff and patients. Adequate shielding, size and weight-bearing characteristics of the imaging room must be accounted for when considering installation of a PET or PET/CT unit. Patient scheduling may be complicated when performing cardiac perfusion and cardiac viability procedures at a facility also providing oncology and neurology services due to differences in patient preparations, imaging start times post dose administration and the requirements for different staff to be present. The development of new ^{18}F-labelled cardiac imaging agents may improve image quality, quantification and access to cardiac PET imaging. However, these agents may present additional logistical challenges such as radiation exposure to staff, that must be addressed. While the establishment of a cardiac PET service presents unique challenges, they have been successfully addressed at many facilities and the benefit to patients makes this endeavor worthwhile.

References Chapter 7

References

1. Dilsizian V, Bacharach SL, Beanlands RS, et al. PET myocardial perfusion and metabolism clinical imaging. ASNC Imaging Guidelines for Nuclear Cardiology Procedures. American Society of Nuclear Cardiology J Nucl Cardiol. 2009:16.

2. CARDIOGEN-82® (Rubidium Rb82 Generator) package insert. Bracco Diagnostics, Princeton, New Jersey. 2012.

3. Yoshinaga K, Kein R, Tamaki M. Generator-produced rubidium-82 positron emission tomography myocardial perfusion imaging – From basic aspects to clinical applications. J Cardiol. 2010;55:163–73.

4. Heller GV, Hendel R, Mann A. Nuclear cardiology: Technical applications. 2009. New York: McGraw Hill, 2009.

5. Sherif HM, Nekolla SG, Saraste A, Reder S, Yu M, Robinson S, Schwaiger M. Simplified quantification of myocardial blood flow reserve with Flurpiridaz F 18: Validation with microspheres in a pig model. J Nucl Med. 2011;52:617–24.

6. Gropler RJ, Beanlands RS, Dilsizian V, Lewandowski ED, Villanueva FS, Ziadi MC. Imaging myocardial metabolic remodeling. J Nucl Med. 2010; 51 Suppl 1:885–1015.

Chapter 8
Image Processing and Software
Sérgio Figueiredo and Pedro Fragoso Costa

Introduction

Myocardial perfusion imaging (MPI) has become a relatively common diagnostic test in the clinical field of nuclear medicine [1]. In particular, gated single-photon emission computed tomography (G-SPECT) has become a part of mainstream practice, mostly being used in the non-invasive assessment of patients with known or suspected haemodynamically significant coronary artery disease (CAD) [1,2].

Procurement of test results with optimal quality depends on technical issues relating to image acquisition, processing and quantification. Despite "soft" inter-lab differences, a dynamic workflow process similar to that shown in Fig. 1 is generally followed.

DATA ACQUISITION
› Attenuation Correction
› Scatter Correction
› Resolution Recovery

IMAGE EVALUATION
› Patient motion
› Objects surrounding the heart
› Hot gastro-intestinal activity encroaching on the LV inferior wall
› Inaccurate ECG gating
› Injection site
› Issues related to the detection and mechanical physics

IMAGE PROCESSING
› Filtering
› Reconstruction algorithms
› Slice orientation

IMAGE QUANTIFICATION

Left Ventricle Segmentation Algorithm

PERFUSION	FUNCTION
POLAR MAPS	POLAR MAPS
3D - PERFUSION SAMPLING DISPLAY	3D - GATED MOTION SURFACE DISPLAY
DEFECT EXTENT and SEVERITY	LVEF, ESV and EDV
REVERSIBILITY STRESS-REST	RWM and RWT; PHASE ANGLE ANALYSIS
CATEGORICAL SUMMED SCORES	CATEGORICAL SUMMED SCORES

REPORT
› Diagnosis
› Prognosis

Figure 1: Generic cardiac imaging workflow. LVEF, left ventricular ejection fraction; ESV, end-systolic volume; EDV, end-dystolic volume; RWM, regional wall motion; RWT, regional wall thickening

After the data acquisition, with or without attenuation and scatter correction, the planar projection images should be inspected immediately by the technologist in order to identify technical problems that might require repetition of the acquisition. This step is referred to as "image evaluation" and parameters to consider may include: patient motion, inaccurate ECG gating, hot gastro-intestinal activity encroaching on the left ventricular (LV) inferior wall, injection site, objects surrounding the heart and issues related to detection and mechanical physics (Fig. 1). Only after proper evaluation of these parameters and correct validation of the acquisition is it possible to proceed to the next steps of the flowchart: image reconstruction, image quantification and report.

Image reconstruction

Image reconstruction has traditionally been performed using filtered back-projection (FBP), but reconstruction algorithms such as iterative methods can be applied in MPI [3]. Similarly, filtering techniques help improve image clarity by, potentially, removing noise and blur after back-projection of the raw data [4]. Recently, improvements in hardware and software have been introduced in an attempt to meet the challenges of modern healthcare MPI studies through the implementation of resolution recovery (RR) and noise suppression (NS) algorithms [5]. After reconstruction, reorientation of stress and rest data can be displayed and images should be appropriately aligned in a format that allows ready comparison of corresponding tomograms [6].

Analytical and iterative reconstruction

Filtered back-projection is an analytical reconstruction method that has been widely used in clinical cardiac G-SPECT because of its simplicity, speed and the fact of being relatively simple to compute. However, it has gradually declined in importance compared with iterative methods, mainly because of its inability to model basic physical processes in emission tomography, e.g. attenuation and scatter [7, 8].

Figure 2A illustrates the practical steps involved in reconstruction by FBP. In a 2D acquisition, each row of projections represents the sum of all counts along a straight line through the depth of the object, and all projections are organised as a function of the angle in a sinogram. The back-projection technique redistributes the number of counts uniformly at each particular point along the line from which they were originally detected, for all pixels and all angles. Star artefacts and blurring of the image are the main consequences of this process. In order to eliminate these problems, the projections are filtered with a window filter, in the frequency domain, before being back-projected onto the image matrix, mathematically using the fast Fourier transform (FFT). The back-projection takes place in the spatial domain in order to obtain the final image [4, 8].
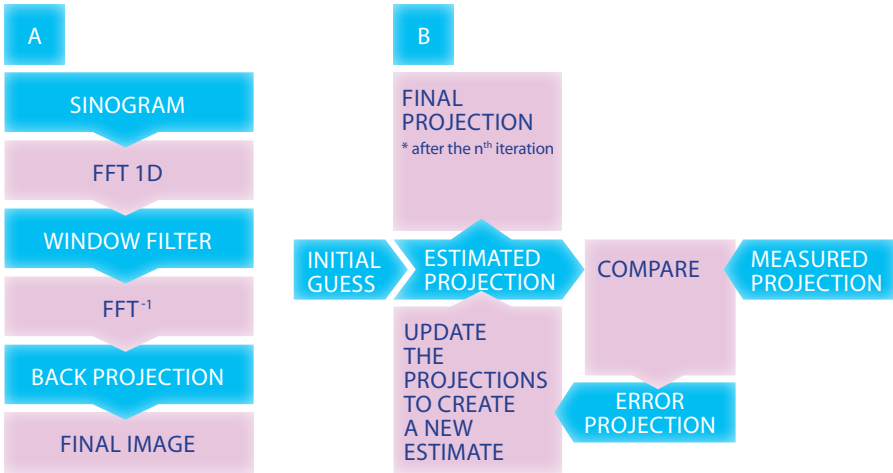
A

SINOGRAM

FFT 1D

WINDOW FILTER

FFT^{-1}

BACK PROJECTION

FINAL IMAGE

B

FINAL PROJECTION
* after the nth iteration

INITIAL GUESS

ESTIMATED PROJECTION

COMPARE

MEASURED PROJECTION

UPDATE THE PROJECTIONS TO CREATE A NEW ESTIMATE

ERROR PROJECTION

Figure 2 A, B: A Typical FBP algorithm. B Iterative reconstruction, general schematisation. FFT, Fast Fourier transform

Iterative reconstruction is based on the algebraic reconstruction technique and allows the incorporation of more accurate image models rather than the Radon model assumed in the FBP algorithm (Fig. 2B). These include attenuation and scatter corrections as well as collimator response and more realistic statistical noise models [8, 9]. Fuelled by increases in computer speed and performance, these methods are gaining wider acceptance in the field of nuclear cardiology.

These algorithms, as illustrated in Fig. 2B, start with a rudimentary initial first guess (usually by FBP) of the activity distribution, generate projections from the guess and compare these projections with the acquired ones. The guess is refined based on the differences between the generated and actual projections, and the process is repeated (hence the term "iterative") until the differences between the calculated and measured data are smaller than a specified preselected value [3, 6].

Diverse iterative algorithms have been developed, such as the maximum likelihood expectation maximisation (MLEM), assuming Poisson noise is present in the projection data but with long computational times. Currently, the most widely used iterative technique is based on the ordered subsets expectation maximisation (OSEM) approach, which is an accelerated version of MLEM; its main advantage is the decreased reconstruction time, which is consistent with routine clinical use [8, 10].

New trends in iterative image reconstruction
Although it is a well-established medical imaging modality, MPI suffers from some fundamental limitations, including long image acquisition time, low image resolution (depending on scanner/camera photon sensitivity, primarily controlled by the type of collimator and imaging detection geometry) and patient radiation dose [11]. Typically, to balance the binomial resolution–sensitivity (higher resolution images require lowering of image sensitivity), the scan time is about 15–20 min for each stress and rest acquisition, resulting in frequent artefacts due to patient motion [2, 11]. Additionally, the traditional dual-head cameras with standard parallel hole collimators are over 50 years old and the basic FBP algorithm is even older, dating from 90 years ago [2]. Recently, however, new imaging systems and iterative reconstruction algorithms have gone through several stages of development with the aim of increasing signal to noise ratio (SNR) and system resolution, which will simultaneously allow higher photon sensitivity and improve both image quality and resolution [2, 5, 11].

For this purpose various methods have been implemented in the RR reconstruction algorithms. Resolution recovery integrates the detector's physics into the iterative algorithm so as to compensate for the distance-dependent blurring, illustrated in Fig. 3, which is known to be the main factor affecting the resolution and noise properties of nuclear medicine images [2, 5, 12]. The modelling of this phenomenon is often called point spread function (PSF).
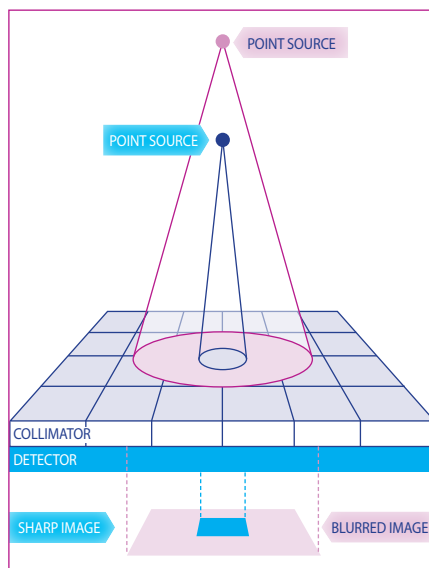
Figure 3: Point spread function and the subsequent distance-dependent blurring

Knowledge of the distance from the patient to the elliptical path of the detector and the collimator detector response (CDR) permits inclusion of correct compensation for the blurring effect in the iterative reconstruction process [5]. During the course of image reconstruction, specific information needs to be incorporated in respect of the CDR, i.e. collimator design parameters (hole length and diameter, septa thickness), detector characteristics (intrinsic resolution, crystal thickness, collimator–detector gap) and acquisition parameters (centre of rotation to collimator face distances for every projection collected and geometric orbit of radius acquisition) [5, 12].

For each combination of systems, equipment-related information for different collimators is stored in an additional look-up table, which is part of the reconstruction package and is measured previously to ensure correct modulation of the *a priori* physical aspects, while the acquisition parameters are retrieved from raw projection data [2, 12]. The modelled physical information (instrumentation and imaging parameters) is then integrated in the estimated projections of the overall iterative method, eliminating the main degrading effects of the line spread function (LSF) and thereby resulting in improved SNR and enhanced spatial resolution [2, 11]. Regarding these new trends in image reconstruction, the initial clinical results that are being reported demonstrate potential for equivalent diagnostic performance by MPI scans obtained in *half-time* sampling mode [11, 13, 14].

Commercial software approach

With the recent development of nuclear cardiology and its increasing application in the clinical field, the need for processing and acquisition dedicated software has increased. Apart from the main scanner manufacturers, who develop such software suited to their products and dedicated cameras, there are also stand-alone software applications with "solutions" for image reconstruction using conventional hardware scanners. Most modern software uses iterative reconstruction methods; each developer uses a specific approach to produce high-resolution images, reduced noise acquisitions or shorter acquisition times in order to achieve diagnostically valuable images. Table 1 lists the main manufacturers and the reconstruction algorithms applied.

Table 1: Most widely available commercial reconstruction software

Software	Reconstruction algorithm	Manufacturer
Astonish	3D-OSEM	Philips
Evolution for Cardiac	OSEM-RR (MAP)	GE
IQ·SPECT	Conjugate gradient (CG)	Siemens
WBR	OSEM-RR	UltraSPECT

MAP, Maximum a posteriori

Astonish™

Philips (Milpitas, CA) has developed a fast SPECT reconstruction algorithm, Astonish, that includes corrections for the major factors degrading SPECT image quality [11]. This software package is based on a three-dimensional ordered subsets expectation maximisation (3D-OSEM) method. Astonish uses a distance compensation method to model the varying resolution at different distances from the detector; such corrections allow the visualisation of sharper details. Additionally, it corrects for Compton scattering and for photon attenuation by means of the ESSE method described by Kadrmas et al. [15], which improves lesion contrast and provides a more accurate representation of lesions at varying depths [16].
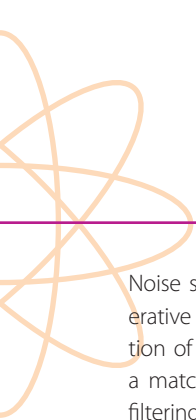
Noise suppression – one problem that all iterative methods must address is amplification of statistical noise – is attained through a matched filtering. This process consists of filtering before reconstruction and using an identical filter to forward project the information. This avoids the dissipation of features that could have been "smoothed away" and the increased iteration-associated noise [11, 16].

EvolutionTM for Cardiac
GE Healthcare (Waukesha, WI) has also developed a modification of the OSEM algorithm that incorporates RR named "Evolution for Cardiac" [11]. Focussed on CDR modeling, the Evolution approach is able to achieve resolution recovery by integration of the collimator and detector response in an iterative reconstruction algorithm [13]. The CDR compensation technique is accomplished by convolving the projected photon ray with the corresponding LSF during iterative projection and back-projection. The following compensation parameters are taken into account: collimator hole length and septa thickness, intrinsic resolution, crystal thickness and collimator–detector gap. Acquisition parameters, including the distance from the centre of rotation to the collimator for every acquired projection, obtained from the raw data, also contribute for modulation [11, 12].

Noise suppression is achieved with a maximum a posteriori (MAP) algorithm. This algorithm is a modification of the EM. It operates in order to maximise the similarity between estimated and measured projections and to ensure that reconstructed images are not too noisy [5].

IQ·SPECTTM
This software package works in synergy with a dedicated collimator (SMARTZOOM), the design of which enables a cardio-centric orbit at a fixed radius of 28 cm. While most software designs are based in the EM optimisation method, IQ·SPECT uses a preconditioned conjugate gradient (CG) [17]. This algorithm is based on the minimisation of the Poisson noise function. In the CG method the aim is not to maximise the likelihood that the objective function is an answer to the system but to minimise the objective function; for this purpose, steps conjugate to one another are taken in the direction in which the objective function decreases more quickly [7].

Similarly to EM, an increase in iterations with the CG results in noise accumulation on the produced images, and to diminish the extent of this the CG is preconditioned with a nearly complete description of the imaging system, from emission to collimator acceptance: scatter and attenuation correction are included, a vector map of the collimator angles in included

in the matrix, PSF is modulated based on the radius of rotation and a post filter is applied to the final reconstructed images [17, 18].

WBR™

UltraSPECT Limited (Haifa, Israel) has developed a stand-alone workstation (Xpress.cardiac) that utilises the patented Wide Beam Reconstruction (WBR) algorithm [11]. The WBR technique is an OSEM-based algorithm that models the physics and geometry of the acquisition for resolution recovery [19] in a similar fashion to the previously described methods. Using a segmentation algorithm, the distance from the detector to the body can be extrapolated and integrated in the CDR model. Noise suppression is achieved using a likelihood function with a combination of the Poisson (high frequency recovery) and Gaussian (high frequency suppression) distributions, accomplished by Fourier analysis of a projection to determine the approximate SNR, thus avoiding post-reconstruction filtering (the standard approach to overcome noise) [11, 19, 20].

WBR utilises a stand-alone running hardware platform and can reconstruct data acquired from most scanners with standard collimator design [20].

Importance of reconstruction filters

Once a Fourier spectrum has been generated for an image, it can be filtered so that certain spatial frequencies can be modified, enhanced or suppressed. The filtered spectrum can then be inverse transformed, using a mathematical operator (inverse Fourier transform), to generate a filtered image with, for example, sharpened or smoothed features [8].

These operations are commonly applied in order to obtain good quality images, and specifically to maximise the SNR, which describes the relative strength of the signal component compared with noise. The SNR is much higher at low spatial frequencies (broad features that are constant over many pixels, such as large uniform objects) and decreases at higher spatial frequencies (features that change over a few pixels, such as edges) [1, 3]. Window filters are such tools; those most frequently used in nuclear cardiology are passive filters, of which low-pass and high-pass are representative examples [4].

In order to achieve an optimal compromise between the extent of noise reduction and suppression of fine detail, the typical star artefact from FBP can be reduced by applying

a Ramp filter [3]. This mathematical window is a high-pass filter that does not permit low frequencies that cause blurring to appear in the image and enhances the geometric contours of the object. In frequency domain, its mathematical function is given by the equation [8]:
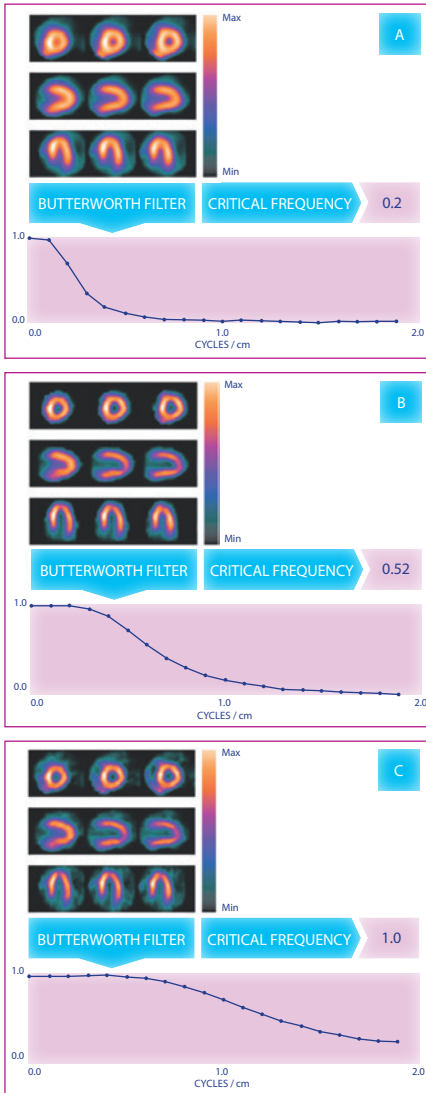
$$H_R(k_x,k_y) = k = (k_x^2 + k_y^2)^{1/2}$$

where k_x, k_y are the spatial frequencies.

The main disadvantage of the Ramp filter is that it amplifies the high-frequency statistical noise present in the measured counts, and as a consequence it is usually combined with a low-pass filter [1]. A low-pass filter is the common method to reduce or remove statistical noise in an FBP cardiac image because it allows low spatial frequencies to be unaltered and attenuates the high frequencies, where noise predominates. Hanning and Butterworth are the most popular low-pass filters used in nuclear cardiology. Because of the flexibility and ease of design, Butterworth filters are the more usual choice in nuclear cardiology routine procedures [8]. They are characterised by two parameters: the "cut-off frequency" and the "order" (or the "power") and are described, in the spatial domain, by the equation:

$$Bw(f) = \frac{1}{1 + \left(\dfrac{f}{f_c}\right)^{2n}}$$

where f is the spatial frequency domain, f_c the critical (or cut-off) frequency and n the order of the filter.

The cut-off frequency (or roll-off frequency) defines the frequency above which the noise is eliminated. The Nyquist (Nq) frequency – the highest frequency that can be displayed in an image – is apparently the highest cut-off frequency for a filter. Its importance is related to the fact that the critical frequency is expressed in cycles per pixel (or cm) or as a fraction of the Nq frequency [4, 7]. Typically the cut-off frequency varies from 0.2 to 1.0 times the Nq frequency, and because of the variability in notations, any measurement expressed in frequency terms must always be accompanied by knowledge of the pixel size [4, 8]. Therefore, a high *fc* will improve the spatial resolution and, consequently, much detail can be seen, but the image will remain noisy. Furthermore, a low *fc* will increase smoothing but will degrade image contrast in the final reconstruction [3, 6] (Fig. 4).

BUTTERWORTH FILTER   CRITICAL FREQUENCY   0.2

BUTTERWORTH FILTER   CRITICAL FREQUENCY   0.52

BUTTERWORTH FILTER   CRITICAL FREQUENCY   1.0

Figure 4 A – C : Influence of cut-off frequency on reconstructed slices and filter graphical representation on the frequency domain.

The order controls the slope of the filter function and characterises the steepness of the roll-off. A high n will result in a sharp fall, while a low n is responsible for a smooth fall [8].

Nuclear cardiology images, because of their relatively low count statistics and dependence on the ramp filter (FBP), tend to have great amounts of statistical noise. Additionally, balanced selection of parameters n and fc may optimise the SNR and improve image quality. Traditionally, the manufacturer's recommendations, e.g. fc =0.5 cycles·cm^{-1} (n=5 or n=10) or 0.75 cycles·cm^{-1}, can be chosen [4].

In contrast to FBP, the iterative techniques such as OSEM take into account the Poisson distribution and the filters are applied mostly post-processing in 3D. Post-filtering with a Butterworth filter may result in higher contrast compared to reconstructions without filtering [3, 7].

Only professionals thoroughly familiar with the potential effects of these changes on the image should adjust filter cut-off and order in FBP and perform post-processing filtering in OSEM. Such adjustments should only be carried out in accordance with the manufacturer's recommendations and in the presence of sufficient guiding documentation on the subject [3, 21].

General recommendations regarding reconstruction technique

The same reconstruction technique should be used consistently for all studies unless modifications are needed in specific cases

to retain a comparable count density/image appearance in both sets of stress and rest images, and not in order to maintain a consistency of appearance (Table 2) [6, 21].

Table 2: General reconstruction recommendations. Adapted from [21]

Filtered back projection					
		Pre-filter			
		Butterworth		Hanning	
Radioisotope	Activity (MBq)	Cut-off[a] (cm^{-1})	Order	Cut-off (cm^{-1})	α
^{99m}Tc	296–444	0.3–0.4	6	0.30–0.45	0.5
	888–1332	0.4–0.5	6	0.45–0.60	0.5
Iterative					
MLEM	Iterations: 10–15	No prefiltering needed[b]			
OSEM	Iterations: 2–5; Subsets: 8	No prefiltering needed[b]			

[a] Some individuals prefer to express the critical frequency as a 0–1 numeric range, with 1 being the highest attainable frequency, or 100% of the Nyquist frequency. Others point out that the Nyquist frequency is, by definition, equivalent to 0.5 cycles per pixel and adopt a 0–0.5 range instead. The same critical frequency can be reported as 0.3 or 0.6 on two different camera systems. In any event, whether a critical frequency is expressed in cycles per pixel or as a fraction of the Nyquist frequency, any measurement expressed in frequency terms must, clearly, always be accompanied by knowledge of the pixel size [4].

[b] Usually no pre-filtering is needed, but post-filtering techniques can be applied.

Reorientation and display

A critical phase of myocardial processing is reorientation of tomographic data into the natural approximate symmetry axes of the patient's heart.

The output of "reconstruction" is a set of transaxial images. It is customary to reorient transaxial images perpendicularly to the long axis of the LV, creating short-axis images that have standardised orientation. This is performed either manually or automatically and results in sectioning the data into vertical long-axis (VLA), horizontal long-axis (HLA) and short-axis (SA) planes, based on the cardiac plane definition and on the criteria for display of tomographic post-reconstruction slices. Both options, manual and automatic, should allow long-axis orientation lines to be parallel to long-axis walls of the myocardium and should be consistent between rest and stress studies. Preferentially, automated methods of

reorientation are applied, making use of the software widely available in clinical practice. In addition to the "zoom reconstruction" tools, these automated methods have been shown to be at least as capable as trained operators in achieving improved reproducibility [1, 21]. An example of correct automatic reorientation is shown in Fig. 5.
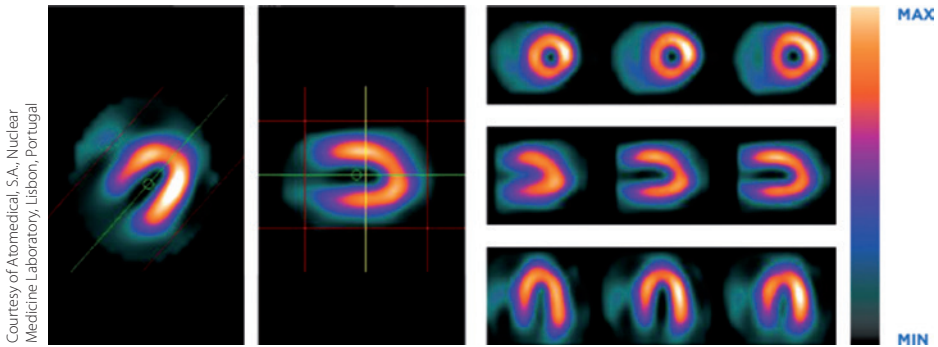
Courtesy of Atomedical, S.A., Nuclear Medicine Laboratory, Lisbon, Portugal

Figure 5: Correct reorientation and adjusted alignment in a WBR gated-stress half-time acquisition.

Evidently, as shown in Fig. 6, inappropriate reorientation and plane selections can result in misaligned myocardial walls between rest and stress datasets, potentially resulting in artefacts and further incorrect interpretation.

Courtesy of Atomedical, S.A., Nuclear Medicine Laboratory, Lisbon, Portugal
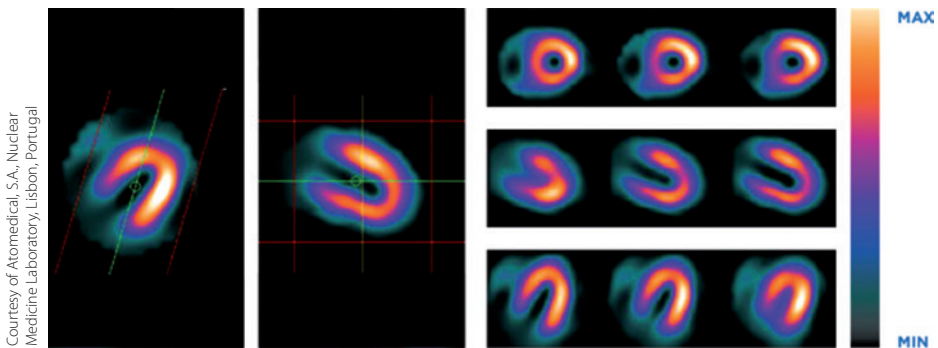
Figure 6: Inappropriate reorientation and inadequate alignment in a WBR gated-stress half-time acquisition.

Stress and rest images should be appropriately aligned and sequentially adjacent to each other, and presented in a format that allows ready comparison of the parallel corresponding tomograms. Conventional stress-rest display should show the apical slices to the left and the base at the right, considering the SA plan. The VLA tomograms should be displayed with septal slices on the left and lateral slices on the right. Similarly, the HLA tomograms should be displayed with inferior slices on the left and anterior slices on the right. Figure 7 shows an example of this traditional display.
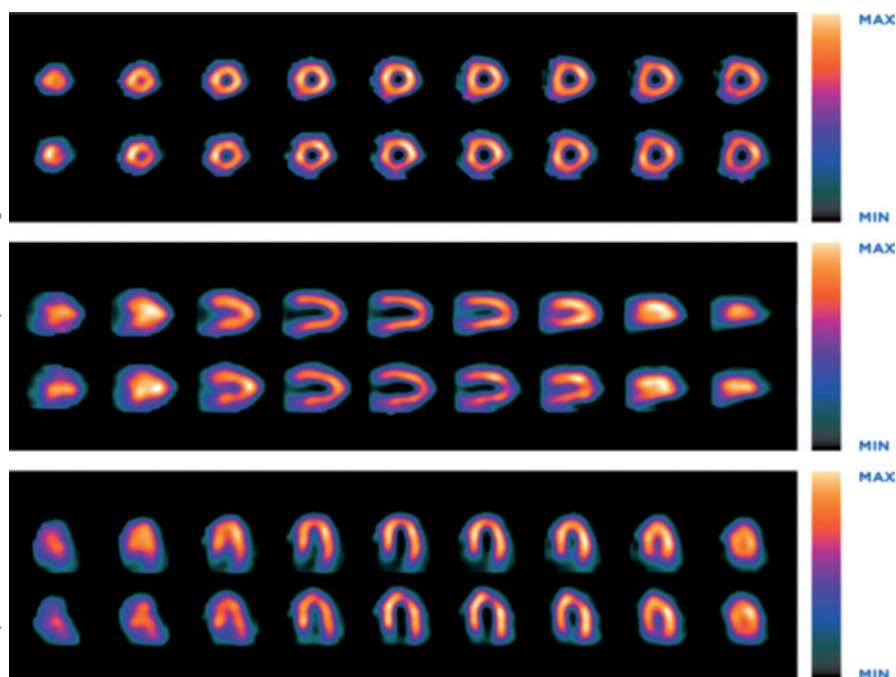
Figure 7: Conventional stress-rest display in a WBR™ half-time gated acquisition. Top: Stress-rest SA slices; middle: stress-rest VLA slices; bottom: stress-rest HLA slices.

Different colour maps can be used depending on the operator's expertise, but use of a linear or a grey colour scale is classically recommended [6, 21]. Additionally, the same colour map should always be used for rest images and stress slices.

Each study should be displayed with the top of the colour scale at the maximum counts/pixel within the myocardium for each set of images. Each series (VLA, HLA and SA) may be normalised to the brightest pixel in the entire image set, providing the most intuitively easy way to evaluate the perfusion defects. However, this approach is very sensitive to focal hot spots, so if the pixel with maximum counts lies outside the myocardium, care should be taken and manual adjustment or masking of extracardiac activity may be required.

Sometimes, the stress-rest display can include 3D-rendered data sets of regional myocardial perfusion. These may help less experienced readers to identify coronary distributions associated with perfusion defects but should be used only as an adjunct, not a replacement.

Image quantification

Image quantification is an extremely valuable tool in MPI and usually involves the extraction of quantitative parameters derivable from a rest-stress gated perfusion SPECT protocol. After correct implementation of the *left ventricle segmentation algorithm*, it is possible to obtain the perfusion parameters, i.e. defect extent, severity values with polar map display, reversibility stress-rest, percent hypoperfused myocardium, percent ischaemic myocardium, categorical summed scores (rest, stress and difference), and even total perfusion deficit. Likewise, the left ventricle (LV) global functional parameters, i.e. left ventricle ejection fraction (LVEF), end-diastolic volume (EDV) and end-systolic volume (ESV), and the LV regional parameters, i.e. regional wall motion and thickening, in conjunction with phase analysis and 3D gated surface display, may contribute significantly to the final report.

Commercial software approach

Table 3: Most popular quantitative algorithms for gated perfusion SPECT. Adapted from [1]

	Cedars-Sinai Medical Centre	Emory University	University of Michigan	Yale University
Commercial name	QPS/QGS; AutoQuant	EGS; ECTb	Corridor 4DM	GSCQ
Operation	Automatic	Automatic	Automatic	Automatic
Dimensionality	3D	3D	3D	3D
Method	Gaussian fit	Partial volume	Gradient	Maximal pixel; partial volume

In order to obtain the LV perfusion and functional parameters several software packages are commercially available, among which three have become the most popular [1, 11]: QPS™/QGS™, developed at Cedars-Sinai Medical Centre (Los Angeles, California), ECT-b™, developed at Emory University (Atlanta, Georgia), and Corridor 4DM™, developed at the University of Michigan (Invia, Ann Arbor, Michigan). A fourth method also used commercially is the Wackers-Liu CQ software (GSCQ™), developed at Yale University (New Haven, Connecticut) [1, 11] Table 3 provides a brief summary of these algorithms.

Further factors have been very important in the growth and popularity of these commercially available software packages: (a) they are automated, (b) they integrate different image display techniques, permitting simultaneous assessment of LV perfusion and function in one package, and (c) they are well validated, with excellent reproducibility of the results [11, 22]. However, it is important to understand that the implementation of these programs varies from vendor to vendor and even between versions of the same program. It is nevertheless well accepted that in general the automation in these programs is quite robust and that they yield similar results [11, 23]. Different image display results can be found in the sections "Polar maps", "Perfusion imaging quantification" and "Left ventricular function imaging quantification" (below) , as examples of these methods.

Most recently, as described in the section "Commercial software approach" (above), vendors have introduced novel noise reduction and/or resolution recovery protocols based on iterative reconstruction methodology, leading to a significant improvement in image quality. The above quantification algorithms are being optimised to take account of the new reconstruction methods and, furthermore, the new current fast digital systems.

Left ventricle segmentation algorithm

When using a software package, segmentation is a crucial step (Fig. 1). Segmentation refers to the separation of a region or a structure of interest from the remainder of an image. In nuclear cardiology, this kind of algorithm detects the myocardial surface of the LV out of a myocardial perfusion image [1, 24].

In general, the segmentation process is dependent on the "correctness" of the reorientation of the SA slices and the geometric boundaries of the LV, based on various computational techniques. The algorithm flow is roughly composed of a cascade of consecutive computational steps, including initial centre of mass calculation and final valve plan fit [1, 25, 26].

Regardless of the computational techniques applied, there are several challenges that the algorithm needs to overcome. In particular, its *robustness* depends on three key criteria: hot gastro-intestinal activity, valve plane detection and under-perfused

tissue. Hot gastro-intestinal activity can sometimes be extremely close to myocardial activity and even bind to myocardial uptake [26]. Figure 8A shows an example in which, although the intestinal activity attaches to the myocardium itself, the geometric contours of the LV are unaffected; in contrast, in the example in Fig. 8B, the hot gastro-intestinal activity influences the segmentation process.
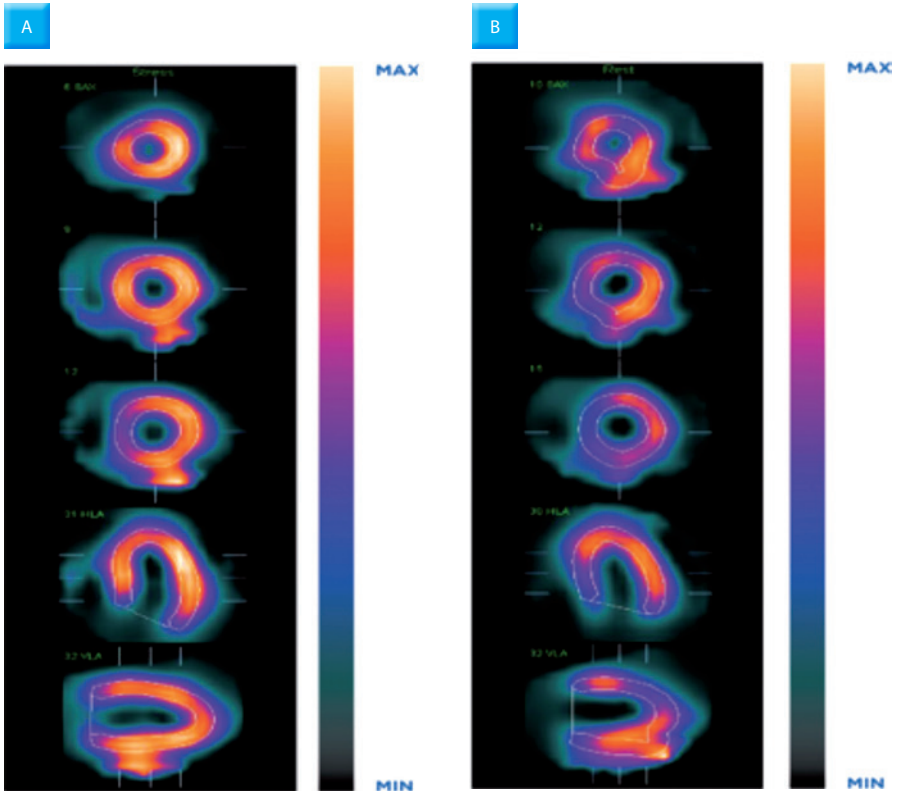
Courtesy of Atomedical, S.A., Nuclear Medicine Laboratory, Lisbon, Portugal

Figure 8 A, B: Correct LV contour detection (A) and influence of hot gastro-intestinal activity on the segmentation process (B).

Valve plane detection is responsible for determining the plane, which should enclose the chamber inner surface for the purpose of endocardial volume calculation, avoiding atrial uptake at the diastolic-gated intervals [26].

Regarding under-perfused tissue, in hypo-perfused regions of the tomograms the algorithm should be able to interpolate the correct myocardial edges according to the normal surrounding tissue [26]. The correct calculation of these hypoperfused areas may be hardly discernible. The example in Fig. 9 illustrates this drawback.
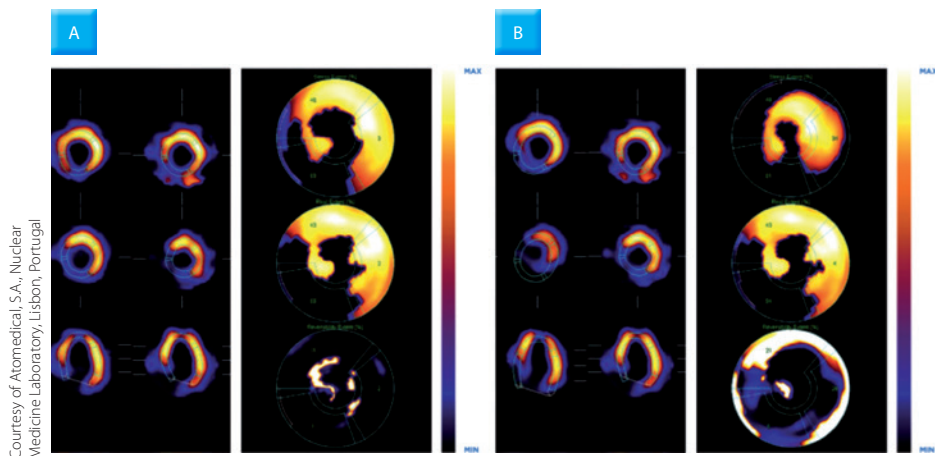
Figure 9 A, B: Under-perfused tissue criterion. A Correct estimation of the myocardial edges and corresponding polar maps. B Overestimation of the myocardial delimitation and subsequent incorrect lesion extension on polar map representation.

Concerning the examples showed above, the automatic detection of contours should be careful verified visually for both gated and ungated data because errors in LV segmentation may lead to significantly erroneous myocardial quantification [1]. To avoid these errors, most commercially available software packages will allow manual override of the automatic segmentation (Fig. 10). However, care should be taken because quantitative results will be associated with operator action.

Courtesy of Atomedical, S.A., Nuclear Medicine Laboratory, Lisbon, Portugal
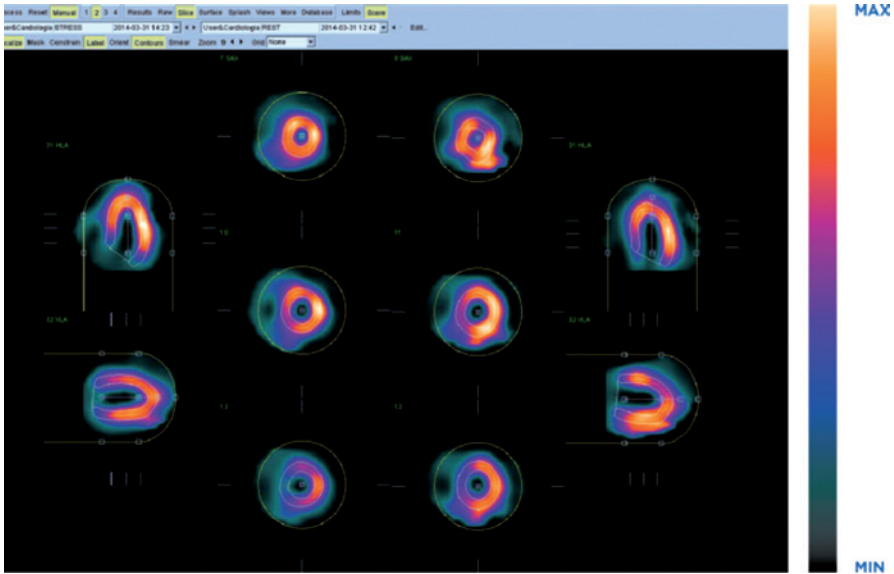
Figure 10: Example of manual override segmentation for adjustment and constraint of LV mask in QPS software. Same patient as in Fig. 8.

Polar maps

Polar maps are 2D representations of the 3D distribution of LV myocardium and are one of the most reliable and valuable tools for assessment of quantification parameters. They were developed in order to simplify the graphic display of the quantified data through presentation within a single picture. This kind of technique is used extensively in clinical practice [3, 11].

Polar maps, or bull's eye displays, are the standard for viewing circumferential profiles in order to extract a limited number of data samples

from the myocardium, allowing a comprehensive colour-coded image of the circumferential samples from all slices [21]. Depending on the "software", these samples are extracted using a base geometrical shape, for example, hybrid spherical–cylindrical (ECTb), or an ellipsoidal model (QPS) or an equidistant sampling model based on the length of the myocardium from base to apex (Corridor 4DM) [1].

As represented in Fig. 11, the most apical slice processed with circumferential profiles forms the centre of the polar map, and each successive profile from each successive

SA is displayed as a new ring surrounding the previous one. The outermost ring of the polar map comprises the basal slices of the LV [11, 21]. The polar maps can display the standardised classical nomenclature of 17 segments of the American Society of Nuclear Cardiology/American Heart Association (AHA)/American College of Cardiology or can be segmented by "vessels" [the left anterior descending coronary artery (LAD), right coronary artery (RCA) and left circumflex coronary artery (LCX)] or "walls" (anterior, inferior, lateral, septal and apical) (Fig. 11) [27]. The 20-segment model may be applied too, but the 17-segment model is usually recommended [3, 6].

Accordingly, based on a colour-coded method, different parameters may be "selected" on distinct maps – for example, the percentage of perfusion on rest and stress, the number of standard deviation (SDs) below normal, indicating the severity of any abnormality, and the blacked-out areas or extent of the defect region, thus creating a white-out reversibility polar map. Additionally, these polar maps can be an important tool in determining the LV functional parameters, such as regional wall motion, regional wall thickening, %ED perfusion, %ES perfusion and phase analysis. More recently, some 3D displays have been adopted in clinical practice.
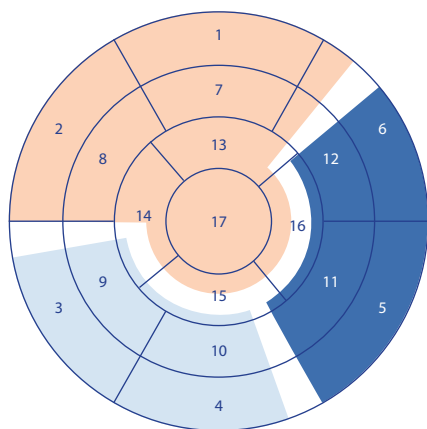
LEFT ANTERIOR DESCENDING CORONARY ARTERY	LAD
RIGHT CORONARY ARTERY	RCA
LEFT CIRCUMFLEX CORONARY ARTERY	LCX

Figure 11: Standard 17-segment polar map model with assigment of segments to the vascular territories of the left anterior descending coronary artery (LAD), right coronary artery (RCA) and left circumflex coronary artery (LCX)

Perfusion imaging quantification

Table 4: Quantitative perfusion measures of myocardial perfusion. Adapted from [11, 21]

Severity score		Defect extent			
Absent uptake	4	Small	Moderate	Large	
Severely reduced uptake	3	4–8	9–13	>13	SSS
Moderately reduced uptake	2	<10%	10–20%	>20%	Polar maps (% of LV)
Mildly reduced uptake	1				
Normal uptake	0	≤1	1–2	2 or 3	Vascular territories

As the potential of operator-independent automatic processing algorithms grows, the quantitative assessment of regional myocardial perfusion magnifies the competitive advantage of nuclear cardiology over other modalities [1, 11].

Despite the merits of conventional qualitative stress-rest display as illustrated in Fig. 7, all perfusion findings should be supported by semi-quantitative analysis with available software (Table 3), determining the extent and severity of hypoperfusion in addition to the summed scoring system and the total perfusion deficit [3, 28] (Table 4).

A typical model for scoring the myocardial perfusion defect is the 17-segment approach (Fig. 11), where each segment will represent 5.9% of the LV. By applying this score system to each segment, to both rest and stress images, a summed stress score (SSS), a summed rest score (SRS) and a summed difference score (SDS) can be derived [21].

The SSS represents the perfusion defect seen at stress (it equals the sum of the stress scores of all segments). The SRS is considered equal to the magnitude of a fixed defect (it equals the sum of the rest scores of all segments) and hence represents – in most cases – the size and severity of a myocardial infarction (although in some cases it may also represent hibernating myocardium with viability). Finally, the SDS is the difference between the SSS and the SRS and expresses the magnitude of ischaemia (reversibility), the most important parameter in terms of prognosis [21]. These semiquantitative scores have been shown to provide important prognostic information. The maximal abnormal score is 68.

For the calculation of the summed scores, the basic quantitative software approaches (shown in Table 3) are similar: regional radiotracer uptake is quantitatively compared with normal databases [1, 11] and can be expressed by:

$$SummedScores = (SeverityScore_{EachDefect}) \; x \; (TotalSegments_{WithDefect})$$

These normal databases are usually generated from patients with a low likelihood of CAD, i.e. usually less than 5% probability [11]. Consequently the automatic assignment score results should be carefully interpreted by experienced and authorised professionals.

It is also possible to combine defect severity and extent through calculation of the total perfusion deficit, using QPS software. This parameter reflects the extent and severity of the overall perfusion defect and can be an important tool for MPI quantification, having a strong correlation with a variety of widely used SSS displays [26].

Each of the programs is based on slightly different models that are used to generate the quantitative profiles, where the main difference is largely in the display data [11]. Examples of application of three commercial programs for quantification in the same patient are shown in Figs. 12–14. However, interpretation of summed scores should be consistent with the visual analysis of the images, since there are several possible pitfalls in the score calculation [21, 29].

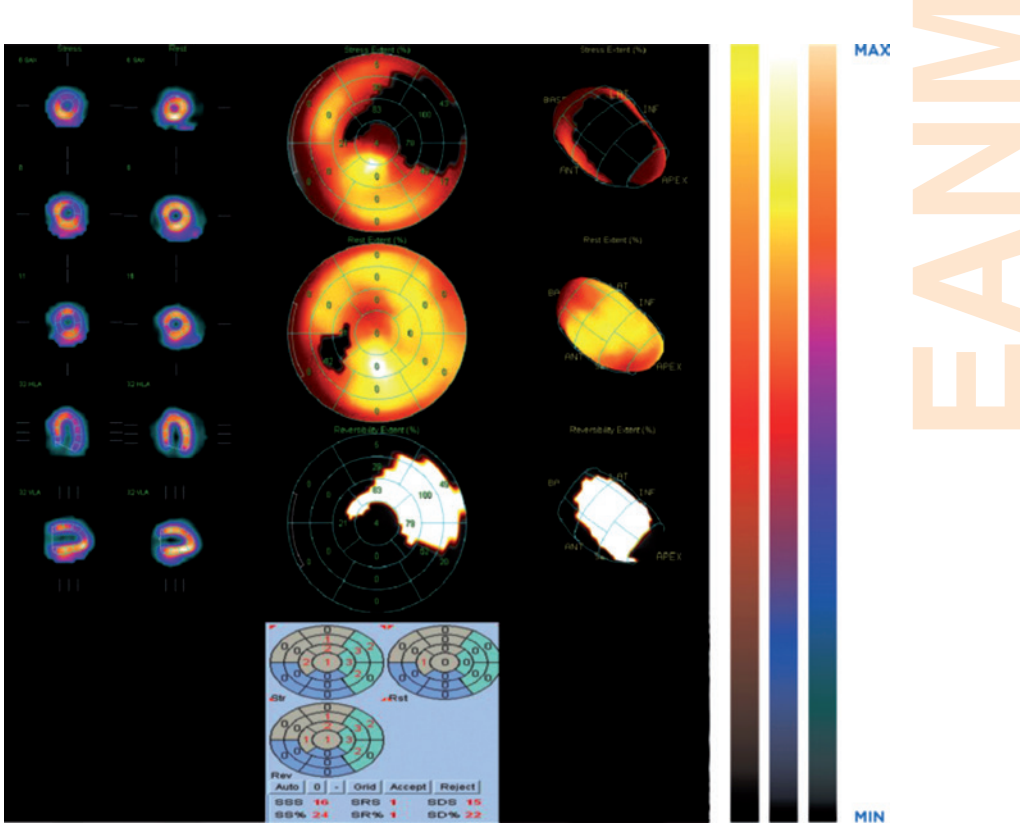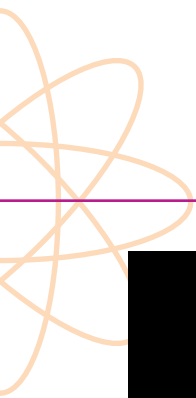Courtesy of Atomedical, S.A., Nuclear Medicine Laboratory, Lisbon, Portugal

Figure 12: Perfusion quantification results obtained with QPS processing, suggesting anterolateral ischaemia in a female patient. The ischaemia can be observed by analysis of the stress-rest slices, the polar map defect extension at stress and rest, and the whiteout reversibility map. The summed scores are displayed on the bottom of the image. Data reconstructed with WBR technology.
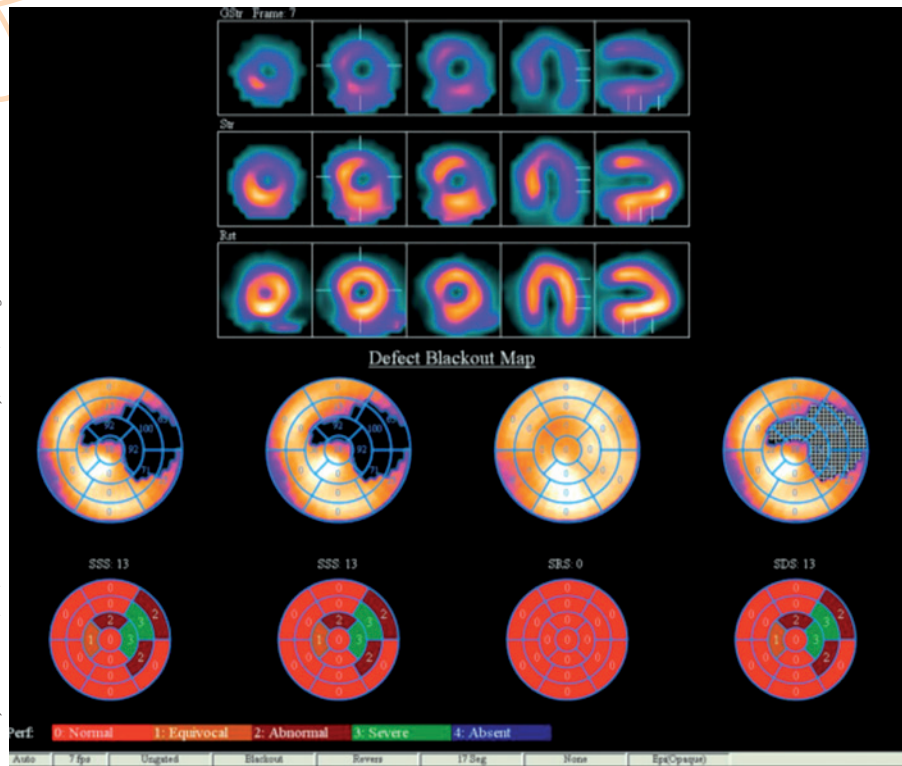
Figure 13: Perfusion quantification extension results obtained from processing with Corridor 4DM, in the same patient as in Fig. 12. Note the similarities of these results with those of Fig. 12.
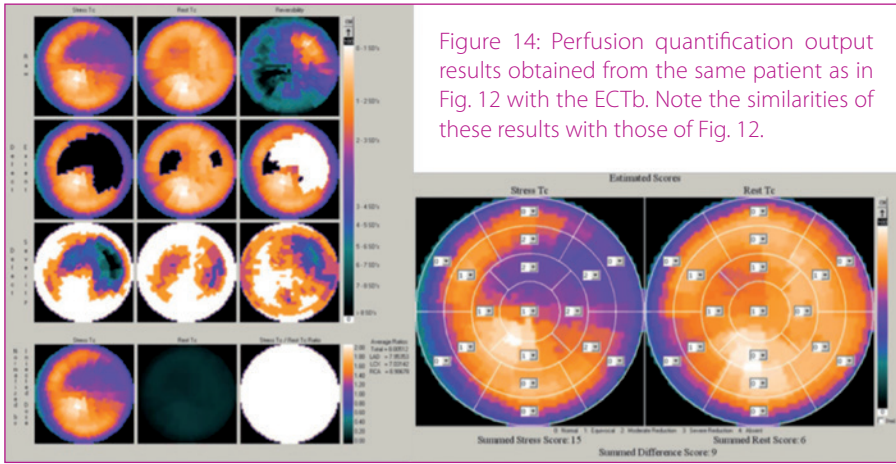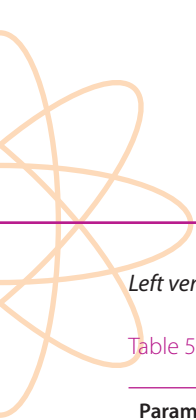
Figure 14: Perfusion quantification output results obtained from the same patient as in Fig. 12 with the ECTb. Note the similarities of these results with those of Fig. 12.

Importantly, quantitative interpretation should always be viewed as *complementary* to visual analysis of the images. Quantitative polar map display with the score system serves to *confirm* the visual qualitative impression [3, 6].

Left ventricular function imaging quantification

Table 5: Global and regional parameters of systolic and diastolic left ventricular function

Parameter	Systolic function	Diastolic function
Global	LVEF	PFR, TPFR
	EDV	PER, TPER
	ESV	MFR/3
	SWM	
	SWT	
	Phase	
Regional	WM	
	WT	
	Phase	

LVEF, left ventricular ejection fraction; EDV, end-diatolic volume; ESV, end-systolic volume; SWM, systolic wall motion; SWT, systolic wall thickening; WM, wall motion; WT, wall thickening; PFR, peak filling rate; TPFR, time to peak filling rate; PER, peak emptying rate; TPER, time to peak emptying rate; MFR/3, filling rate during first third of diastole

The *gated* technique is a widely used clinical tool that may improve the prognostic power of MPI through measurements of functional parameters [1, 11]. Gated perfusion images can be quantitatively analysed to assess a remarkable number of parameters of cardiac function: global, regional, systolic and diastolic (Table 5) [11].

Commonly a "canonical" shape of the time-volume curve for an 8- or 16-frame acquisition can also be obtained as a valuable tool for clinical interpretation. Quantitative phase analysis can also be performed either in a global manner (synchrony of contraction of the LV as a whole) or regionally, as the difference between the onset of contraction in different myocardial walls (see section "Ejection fraction and phase analysis").

Different software approaches for the analysis of ventricular function have been developed. The four most widely accepted commercial packages (Table 3), combining several algorithms, have been extensively studied and have been validated for the parameters they quantitate [1, 11, 30]. Figures 15 and 16 show typical examples of these commercial approaches.

When performing G-SPECT some technical considerations can be challenging as a consequence of the low spatial resolution of the images; this is particularly true with respect to wall thickening and wall motion, rather than global function [3]. It is indeed estimated that the overwhelming majority of institutions performing G-SPECT imaging today also employ quantification to some degree, as an enhancer tool for the reproducibility of the measured parameters [1, 11].

Courtesy of Atomedical, S.A., Nuclear Medicine Laboratory, Lisbon
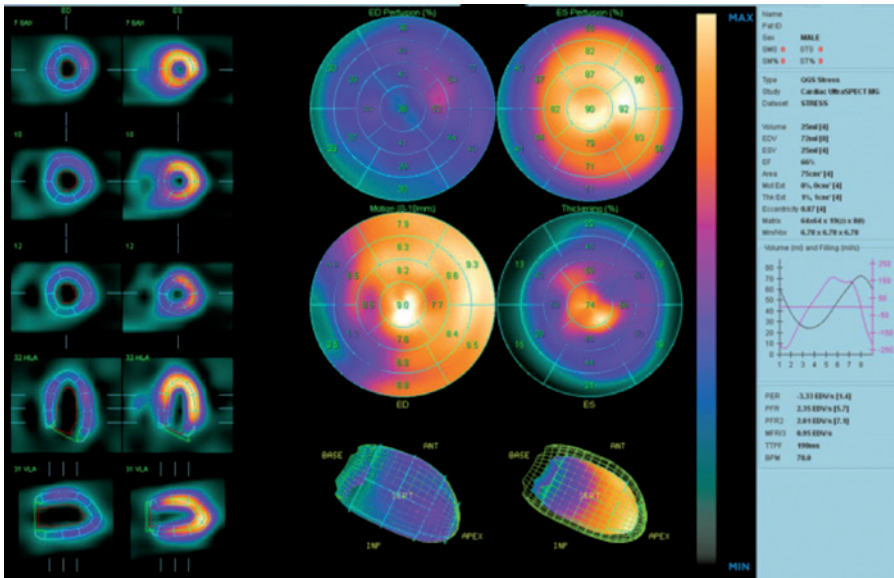
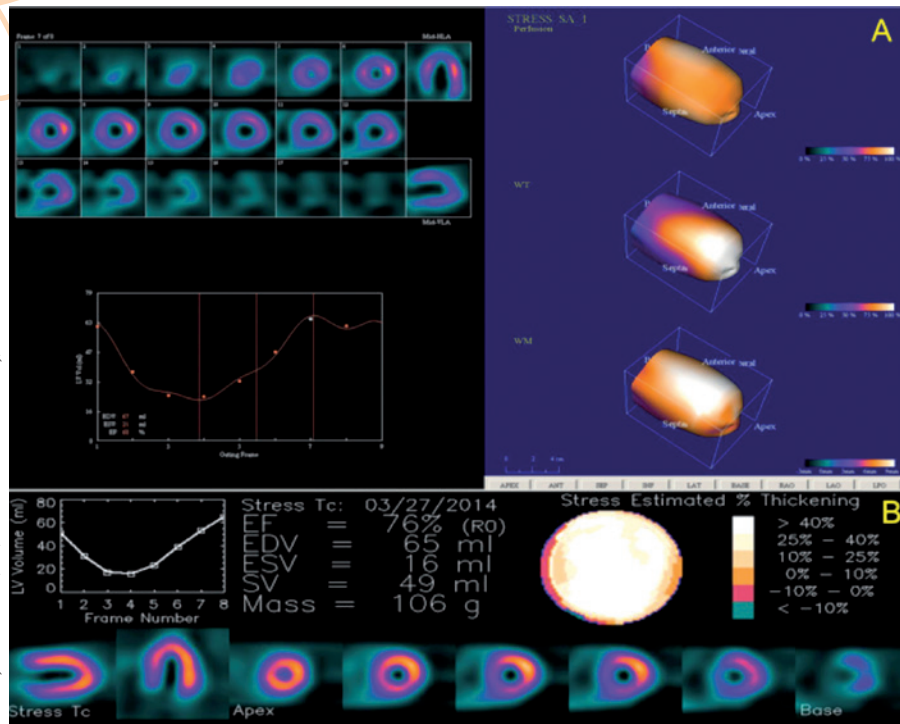Figure 15: Representative display for Cedars-Sinai Medical Center's QGS software.

Figure 16 A, B: A Representative display for the University of Michigan's Corridor 4DM software. B Representative display for Emory University's Cardiac Toolbox software.

Ejection fraction and phase analysis

LVEF is an important cardiac performance parameter and is typically measured using a volume-based rather than a count-based approach. Specifically, the location of the LV endocardium is estimated in the 2D or 3D space, and LV cavity volume is calculated as the territory bound by the endocardium and its valve plane. The process is repeated for every interval in the heart, after which the EDV and the ESV are identified as the largest and the smallest LV cavity volume, respectively [11], from which the ejection fraction is calculated:

$$\% LVEF = (EDV - ESV)EDV \times 100$$

The different commercially available algorithms output the LV function in distinct

displays, as represented in Figs. 15 and 16. However, all of them have been validated on studies showing the agreement between G-SPECT and reference standard measurements of quantitative LVEF, as described in detail by Germano et al. [1] and Zaret et al. [11].

Phase analysis, initially described with nuclear cardiology methods in the late 1970s, has recently re-emerged for the purposes of quantitative measurement of LV mechanical dyssynchrony from G-SPECT images, assessment of the likelihood of benefit from cardiac resynchronisation therapy and evaluation of internal cardiac defibrillators [11, 31]. The phase analysis technique is based on the mathematical technique of harmonic function decomposition developed by Jean-Baptiste Fourier (1768-1830), where a periodic function F of t, with frequency f, can be expressed as:

$$F(t) = \sum_{n=0}^{\infty} A_n \, cos(2\pi nft + P_n)$$

Each term in the equation is called a harmonic and for each harmonic, A represents its amplitude and P represents its phase. For example, A_0 is called the zero harmonic, $A_1 cos(2\pi ft + P_1)$ is called the first harmonic, $A_2 cos(4\pi ft + P_2)$ is called the second harmonic, and so on.

The phase analysis technique measures the first harmonic phase of regional LV count changes throughout the cardiac cycle. This phase information is related to the time intervals until different regions in the 3D LV myocardial wall start to contract, i.e. onset of mechanical contraction (OMC). It provides information on the homogeneity of these time intervals for the entire LV [11, 32, 33].

The basics of phase analysis are generally similar in most quantitative software packages, but practical implementations may vary significantly [11]. Figure 17 shows an example when using the Emory Synctool.
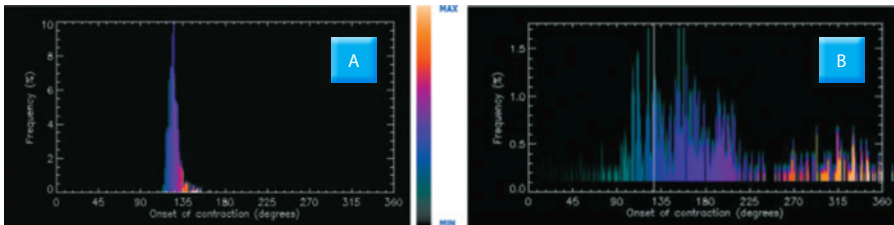

Figure 17 A, B: Phase histogram displaying normal pattern (A) and abnormal histogram (B) in a patient with left bundle branch block.

Courtesy of Atomedical, S.A., Nuclear Medicine Laboratory, Lisbon, Portugal

Attenuation correction

The attenuation phenomenon is a result of the interaction between the photons emitted by the radiopharmaceutical and the tissue or other materials as the photons pass through the body. The degree of attenuation increases with the atomic number of the atom, depends on the tissue density and decreases as the inverse of the photon energy. This interaction is predominant for heavy atoms like lead and for low energetic gamma rays, X-rays or bremsstrahlung [34].

Attenuation is particularly challenging for MPI because of the variability of the tissue density in the thoracic region (the attenuation values of lungs, myocardial tissue, breasts and diaphragm vary significantly). This normally produces attenuation-related artefacts, which vary in size and severity depending on the attenuator density and location. A typical breast artefact will be present in the lateral wall of the heart, given the overlay of the breast tissue and the anterolateral wall of the heart [35].

To achieve attenuation correction (AC), a detailed knowledge of the patient's anatomy is fundamental. This can be obtained either through direct measurements of the patient using an external radiation source or by computing an estimate using body contour delineation based on the acquired data set.

Transmission-based AC can be attained through a line source system, consisting of a collimated rod source of gadolinium-153 (^{153}Gd), cobalt-57 (^{57}Co), or cerium-139 (^{139}Ce), which can be fixed or rotating around the patient. The transmission acquisition provides an attenuation map for the specific radionuclide gamma ray, which is then derived for the imaging photon. This configuration presented drawbacks such as high cost for maintenance of long-lived radionuclide sources and unnecessary radiation exposure for staff and patients and did not produce diagnostic information other than AC [36]. Recent advances on imaging technology have led to hybrid imaging, in which a SPECT or PET scanner is coupled to a CT scanner. CT provides a regional map of attenuation coefficients, specific to each patient. This works in a similar fashion to the above-mentioned technique, with superior spatial resolution and the possibility of anatomical correlation. Since the patient's breathing or the constant myocardial motion can create discrepant co-registration between SPECT and CT images, it is mandatory to perform alignment quality control after image acquisition [34].

There has been much controversy on the subject of AC in MPI, mainly owing to the wide variety of available AC methods, which makes it difficult to achieve a consensus [37].

AC images must always be displayed complementary to non-corrected images (Fig. 18), and the decision on which AC method to use must take into account the patient's attributes.

No one approach has yet been identified as clearly definitive, but the interest in hybrid imaging and the recent RR/NS algorithms will likely result in greater reliance on AC.

An example of AC with the RR algorithms is shown in Fig. 19.

It would be easy to recommend that attenuation and scatter correction should be applied in all cases; however, things are not that simple: without a demonstrable change in the information that can be sustainably extracted from the data, conclusions must be carefully achieved [11].

Courtesy of Klinikum Passau – nuklearmedizinische Gemeinschaftspraxis
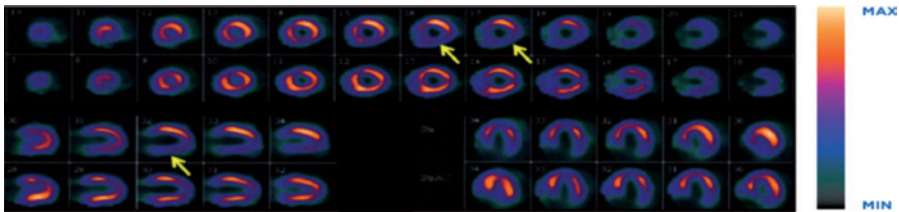
Figure 18. AC and non-AC images obtained with a SPECT/CT full-time acquisition.

Courtesy of Atomedical, S.A., Nuclear Medicine Laboratory, Lisbon, Portugal
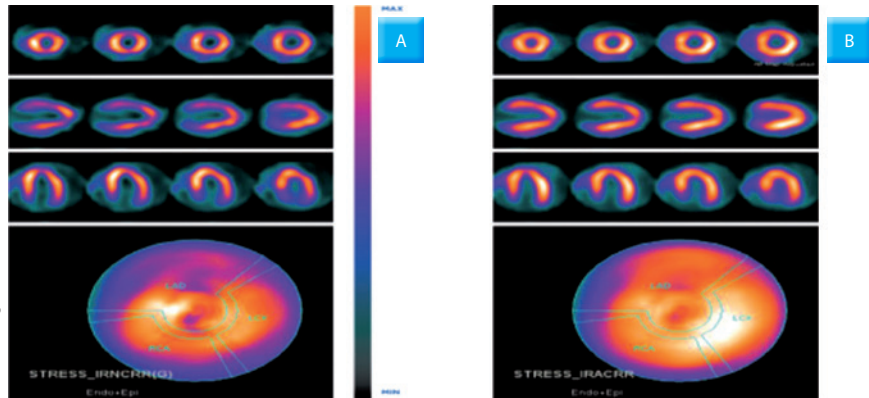
Figure 19: A , B: A OSEM-RR, non-AC. B OSEM-RR, with AC.

General image reconstruction and processing flow chart (tutorial)
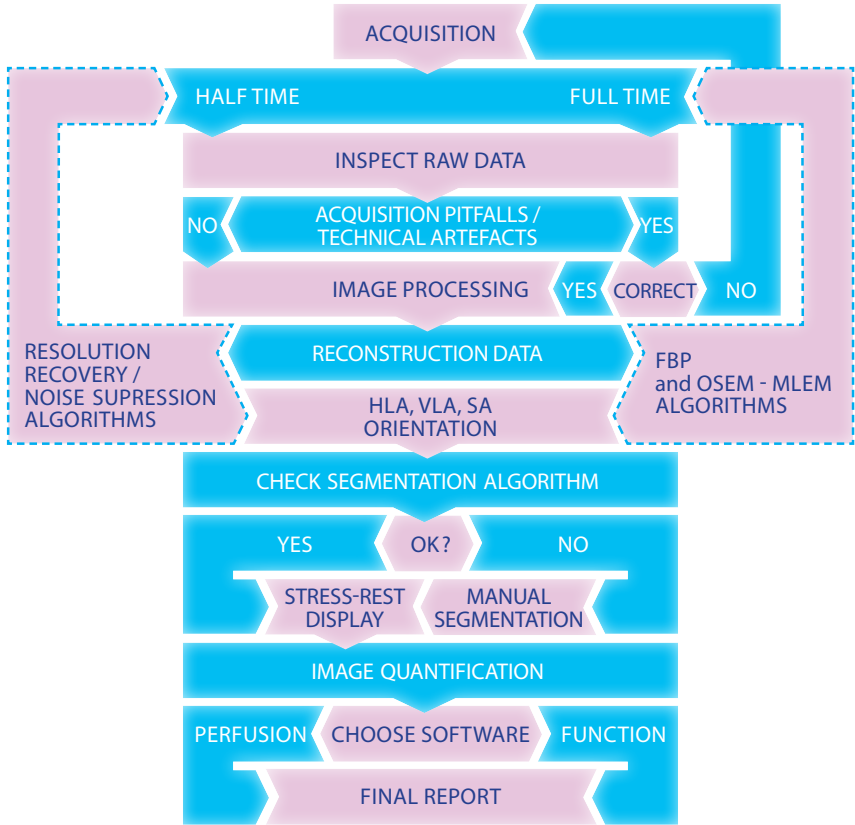
Figure 20: Generic image reconstruction and processing flow chart

# References Chapter 8

References

1. Germano G, Berman DS, eds. Clinical gated cardiac SPECT. Armonk, NY: Blackwell-Futura Publishing; 2006.

2. Garcia EV, Faber TL, Esteves FP. Cardiac dedicated ultra-fast SPECT cameras: new designs and clinical implications. J Nucl Med. 2011;52:210-7.

3. Holly TA, Abbott BG, Al-Mallah M, Calnon DA, Cohen MC, DiFilippo FP, et al. Single photon-emission computed tomography. J Nucl Cardiol. 2010;17:941-73.

4. Germano G. Technical aspects of myocardial SPECT imaging. J Nucl Med. 2001;42:1499-507.

5. DePuey EG. Advances in SPECT camera software and hardware: Currently available and new on the horizon. J Nucl Cardiol. 2012;19:551-81.

6. Hesse B, Tägil K, Cuocolo A, Anagnostopoulos C, Bardiés M, Bax J, et al. EANM/ESC procedural guidelines for myocardial perfusion imaging in nuclear cardiology. Eur J Nucl Med Mol Imaging. 2005;32:855-97.

7. Bruyant PP. Analytic and iterative reconstruction algorithms in SPECT. J Nucl Med. 2002;43:1343-58.

8. Lyra M, Ploussi A. Filtering in SPECT image reconstruction. Int J Biol Imaging. 2011;2011:1-14.

9. Vandenberghe S, D'Asseler Y, Van de Walle R, Kauppinen T, Koole M, Bouwens L, et al. Iterative reconstruction algorithms in nuclear medicine. Comput Med Imaging Graph. 2001;25:105-11.

10. Zeng GL. Image reconstruction – a tutorial. Comput Med Imaging Graph. 2001;25:97-103.

11. Zaret BL, Beller G. Clinical nuclear cardiology : state of the art and future directions, 4th ed. St. Louis, London: Elsevier Mosby; 2010.

12. GE, Healthcare. Evolution for Cardiac - White Paper. 2007.

13. DePuey EG, Gadiraju R, Clark J, Thompson L, Anstett F, Shwartz SC. Ordered subset expectation maximization and wide beam reconstruction "half-time" gated myocardial perfusion SPECT functional imaging: a comparison to "full-time" filtered backprojection. J Nucl Cardiol. 2008;15:547-63.

14. Pena H, Cantinho G, Shwartz SC, Figueiredo S, Marona D, Monteiro J, et al. Wide beam reconstruction technology: does it respect myocardial perfusion SPECT functional parameters? J Nucl Cardiol. 2007;14:S108.

15. Kadrmas DJ, Frey EC, Karimi SS, Tsui BM. Fast implementations of reconstruction-based scatter compensation in fully 3D SPECT image reconstruction. Phys Med Biol. 1998;43:857-73.

16. Yen J, Song X, Durbin M, Zhao M, Shao L, Garrard J. SPECT image quality improvement with Astonish software. White Paper - Philips Healthcare. 2010.

17. Hawman P, Ghosh P. IQ·SPECT: A technical and clinical overview. White Paper - Siemens AG. 2012.

18. Vija H. Introduction to xSPECT Technology: Evolving multi-modal SPECT to become context-based and quantitiative. White Paper - Siemens Medical Solutions USA, Inc Molecular Imaging. 2013.

19. Borges-Neto S, Pagnanelli RA, Shaw LK, Honeycutt E, Shwartz SC, Adams GL, et al. Clinical results of a novel wide beam reconstruction method for shortening scan time of Tc-99m cardiac SPECT perfusion studies. J Nucl Cardiol. 2007;14:555-65.

20. UltraSPECT. Wide beam reconstruction: Breaking the limitation of the line spread function. White Paper - UltraSPECT. 2007.

21. IAEA. Nuclear cardiology: Guidance and recommendations for implementation in developing countries. Vienna: IAEA; 2012.

22. Garcia EV, Faber TL, Cooke CD, Folks RD, Chen J, Santana C. The increasing role of quantification in clinical nuclear cardiology: the Emory approach. J Nucl Cardiol. 2007;14:420-32.

23. Sharir T, Germano G, Waechter PB, Kavanagh PB, Areeda JS, Gerlach J, et al. A new algorithm for the quantitation of myocardial perfusion SPECT. II: validation and diagnostic yield. J Nucl Med. 2000;41:720-7.

24. Germano G, Kiat H, Kavanagh PB, Moriel M, Mazzanti M, Su HT, et al. Automatic quantification of ejection fraction from gated myocardial perfusion SPECT. J Nucl Med. 1995;36:2138-47.
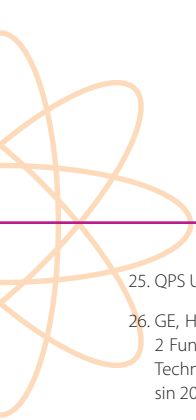
25. QPS User Manual. Cedars-Sinai Medical Center. 2007.

26. GE, Healthcare. Myovation PROTOCOL for XelerisTM 2 Functional Imaging P&R Systems - Operator Guide. Technical Publications - Revision 1. Milwaukee, Wisconsin 2006.

27. Cerqueira MD, Weissman NJ, Dilsisian V, Jacobs AK, Kaul S, Laskey WK, et al. Standardised myocardial segmentation and nomenclature for tomographic imaging of the heart. A statement for healthcare professionals from the Cardiac Imaging Committee of the Council on Clinical Cardiology of the American Heart Association. J Nucl Cardiol. 2002;9:240-5.

28. Slomka PJ, Nishina H, Berman DS, Akincioglu C, Abidov A, Friedman JD, et al. Automated quantification of myocardial perfusion SPECT using simplified normal limits. J Nucl Cardiol. 2005;12:66-77.

29. Burrell S, MacDonald A. Artefacts and pitfalls in myocardial perfusion imaging. J Nucl Med Technol. 2006;34:193-211.

30. Iskandrian AE, Garcia EV. Nuclear cardiac imaging: principles and applications. New York: Oxford University Press, 2008.

31. Chen J, Henneman MM, Trimble MA, Bax JJ, Borges-Neto S, Iskandrian AE, et al. Assessment of left ventricular mechanical dyssynchrony by phase analysis of ECG-gated SPECT myocardial perfusion imaging. J Nucl Cardiol. 2008;15:127-36.

32. Boogers MM, Van Kriekinge SD, Henneman MM, Ypenburg C, Van Bommel RJ, Boersma E, et al. Quantitative gated SPECT-derived phase analysis on gated myocardial perfusion SPECT detects left ventricular dyssynchrony and predicts response to cardiac resynchronisation therapy. J Nucl Med. 2009;50:718-25.

33. Chen J, Kalogeropoulos AP, Verdes L, Butler J, Garcia EV. Left-ventricular systolic and diastolic dyssynchrony as assessed by multi-harmonic phase analysis of gated SPECT myocardial perfusion imaging in patients with end-stage renal disease and normal LVEF. J Nucl Cardiol. 2011;18:299-308.

34. Patton JA, Turkington TG. SPECT/CT physical principles and attenuation correction. J Nucl Med Technol. 2008;36:1-10.

35. Bateman TM, Cullom SJ. Attenuation correction single-photon emission computed tomography myocardial perfusion imaging. Semin Nucl Med. 2005;35:37-51.

36. Cherry SR, Sorenson JA, Phelps ME. Physics in nuclear medicine, 4th ed. Philadelphia: Saunders; 2012.

37. Hendel RC, Corbett JR, Cullom SJ, DePuey EG, Garcia EV, Bateman TM. The value and practice of attenuation correction for myocardial perfusion SPECT imaging: a joint position statement from the American Society of Nuclear Cardiology and the Society of Nuclear Medicine. J Nucl Cardiol. 2002;9:135-43.

Chapter 9
Artefacts and Pitfalls in Myocardial Imaging (SPECT, SPECT/CT and PET/CT)
Ana Geão and Carla Abreu

Myocardial perfusion imaging (MPI) is a complex process, subject to a variety of artefacts and pitfalls related to image processing, the patient, and technical factors. The causes and effects of these potential artefacts and pitfalls need to be understood. Furthermore, it is important not only to implement means of preventing and/or limiting these factors and, when necessary, actions to correct them, but also to incorporate their influence into the interpretation of the study. Technologists play a key role in combating these artefacts and pitfalls, which may arise at any stage in the MPI process and can lead to misdiagnosis.

Artefacts in SPECT and SPECT/CT
Equipment-related artefacts
The interpretation of all diagnostic nuclear medicine procedures is based on the assumption that the performance of all systems used at any stage of the exams, including measurement of radiation and data acquisition, display and analysis, is reliable and accurate. To provide evidence that data of diagnostic quality are being obtained, a standardised programme of routine system performance assessment is essential. The quality control of nuclear instrumentation forms the basis for an effective overall nuclear medicine quality assurance programme.

It is recommended that *camera uniformity* is subject to daily quality control in units performing clinical studies. Small changes in uniformity in the detector may be misrepresented as different levels of activity or artefacts on the reconstructed images. These artefacts typically take the form of alternating concentric hot and cold rings and consequently give rise to defects such as streaks in the reconstructed MIP images (Fig. 1) [1]. Non-uniformities in multiple detector systems do not usually produce complete rings.

Satisfactory SPECT demands stringent quality assurance procedures. Field uniformity tolerances of 1% may be required instead of the 5% tolerance for planar imaging [2, 3].
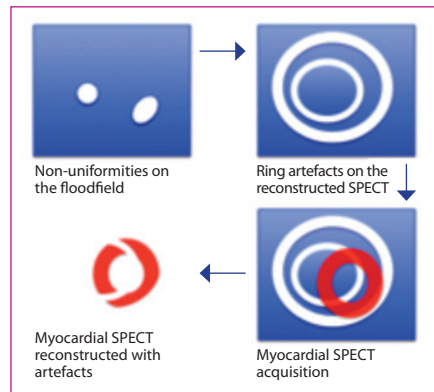

Non-uniformities on the floodfield

Ring artefacts on the reconstructed SPECT

Myocardial SPECT reconstructed with artefacts

Myocardial SPECT acquisition

Figure 1: Uniformity-related artefacts (adapted from the Nuclear Cardiology Technology Study Guide, p. 184, [3])

SPECT system alignment is also required. Proper (x, y) centering and gain adjustments are extremely important in SPECT imaging. The axis of rotation is an imaginary line that extends through the centre of the camera gantry. As the camera moves in a circular orbit,
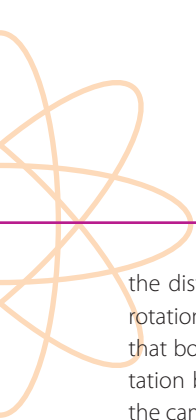
the distance of the detectors to this axis of rotation should not be variable. This requires that both the camera head and the yoke rotation be carefully set to place the plane of the camera crystal parallel to the axis of rotation. The computer image matrix must also be correctly aligned with the axis of rotation. Any misalignment in the acquired images, whatever the cause, will mean blurring and loss of resolution in the reconstructed images.

Centre of rotation (COR) is a calibration performed regularly to ensure that the frame of reference used by the computer in reconstructing images is aligned with the mechanical axis of rotation of the SPECT. If an offset error exists, spatial resolution and image contrast will be reduced and there will be increased blurring of the image with resultant significant image artefacts, especially in the apex of MPI images [1]. Such an error can also induce, in transverse images, characteristic "doughnut" (360° orbit) or "tuning fork" (180° orbit) artefacts. COR errors are easy to detect with radioactive point sources. However, they may be very difficult to detect with a clinical distribution of activity [4, 5].

Attenuation correction is an important tool to distinguish artefacts due to attenuation, but attenuation correction itself can cause artefacts. First of all, the emission scan and the transmission scan that are used to correct photon attenuation must be perfectly registered with each other. Improper quality control of an attenuation correction device can lead to a MIP artefact such as a truncation artefact due to a positioning error, a cross-talk artefact due to the off-peak or window set-up of the transmission source or a low-count density artefact due to decreased activity of the transmission source [1].

The use of *SPECT/CT* has improved the attenuation map quality that can be obtained with sealed transmission sources. However, the pixel values must be scaled to match attenuation coefficients appropriate for the radionuclide being imaged and the CT and SPECT images must be precisely aligned. This alignment should always be verified because any patient movement or even deep breathing can result in a spatial mismatch and consequently introduce artefacts into the attenuation correction map. Realignment can be done to correct some mismatches. It is also important to keep in mind that every artefact in the CT will reverberate into artefacts in the emission scan, such as metal objects, which will cause over-correction in the SPECT image.

Processing-related artefacts

A substantial numbers of artefacts are due to the processing phase of MPI. A proper *orientation of the heart* is vital to ensure that the entire myocardium is included and the axis angles are correct, otherwise significant errors in the perfusion imaging will occur (Fig. 2). In addition, unusual patient characteristics such as dextrocardia may cause pitfalls [1, 3].

A major source of error in SPECT reconstruction is data filtering. *Filters* that are too smooth or over-filtering due to the method of summation of gated files in gated SPECT may result in false negative studies for coronary artery disease and may have a particularly adverse impact on the detection of small or non-transmural defects. On the other hand, filters that are too coarse may result in false positive studies [6].

Incorrect matching of gender, tracer and protocol can lead to quantification errors since the quantitative software may misplace the contour incorrectly for perfusion as well as functional analysis.

Despite the best efforts of the technologist, artefacts may still arise in response to processing-related issues. It is therefore crucial for the physician to review the raw SPECT cine display before interpreting the MPI images.
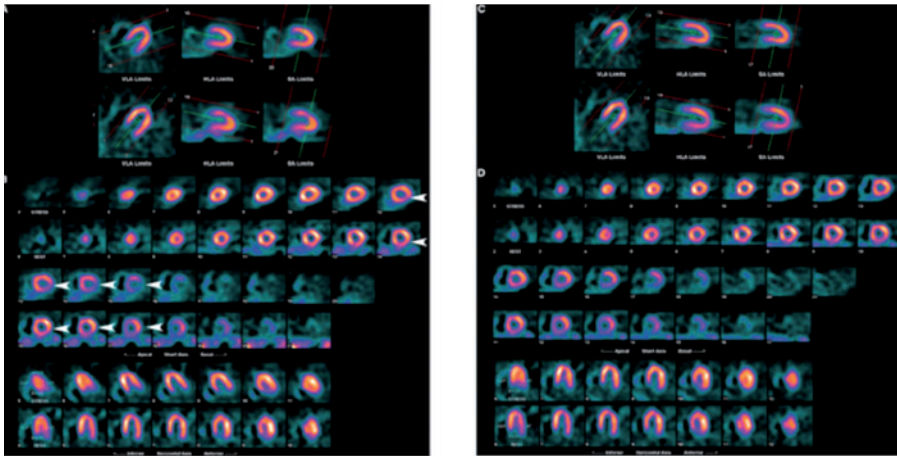

Figure 2: A: Processing images demonstrate incorrect axis alignment in the horizontal long-axis (HLA) plane on the stress study. Proper alignment is present on the rest study. B: Incorrect alignment results in an artefactual reversible defect in the lateral wall on perfusion images (arrowheads). C, D: Processing images (C) and perfusion images (D) from the same study, now with proper axis selection. Artefactual defect is no longer present. VLA, vertical long axis; SA, short axis. (From Burrell and MacDonald [3])

Patient-related artefacts

Good *patient preparation* is mandatory to ensure an optimal study and minimise the existence of artefacts and pitfalls. A maximal safe level of cardiac stressing (physical or pharmacological) optimises the sensitivity of MPI for ischaemia. In order to achieve that level of cardiac stressing, the patient should avoid some substances, such as chocolate and caffeine; in addition, when medically required, certain cardiac medications should be withheld [3].

Before imaging, radio-opaque material or another potential attenuator in the acquired region on the thorax must be removed. However, it is not only external material projecting over the heart during the SPECT acquisition that results in focal attenuation: the patient's body itself is responsible for one of the most frequent and discrete source of artefacts in MPI – *attenuation*. There are generally three sources of soft tissue attenuation artefacts (usually fixed defects in both stress and rest images): breast (anteroseptal, anterior and/or anterolateral wall), diaphragm and 'cold' bowel (inferior wall) and obese patients with lateral fat pads (lateral wall). One way of distinguishing attenuation artefacts from significant perfusion abnormalities, if attenuation correction is not available, is to perform a gated study (Table 1) [1, 6].

Proper patient positioning entails ensuring patient comfort during the scan, which will minimise or even avoid many artefacts caused by attenuation as well as patient motion. Typically, two positions can be used, supine (most commonly used) and prone, the latter having been shown to reduce patient motion and inferior wall attenuation when compared with supine imaging. Other positions may be considered according to the patient's needs [1].

When using 180° orbits for SPECT, the patient's left arm must be positioned outside the field of view. This is usually accomplished by placing the left or even both arms above the head using an arm support device to maximise comfort. When using 360° orbits, both arms need to be positioned away from the patient's side. Likewise, it is well known that the collimator surface should be as close to the patient's body as possible, to increase the image resolution. These requirements mean that the technician must be very aware of the danger that the patient's position will interfere with the gantry radius. It is important that patients be positioned similarly for both the rest and the stress study, with a consistent radius of rotation [2].

Inspection of cine display projection images or even the sinogram and linogram is one of the most useful means available to physicians to detect patient motion (Fig. 3). Most processing computers provide motion correction software; nevertheless, motion correction software does not always correct appropriately and must be used judiciously. Prevention of motion is the most effective way to avoid artefacts. Another type of motion is cardiac or upward creep, which can

result from the patient moving or from exaggerated diaphragmatic excursion related to heavy or erratic breathing. This phenomenon is more pronounced when post-exercise images are acquired too soon after exercise [1, 5].
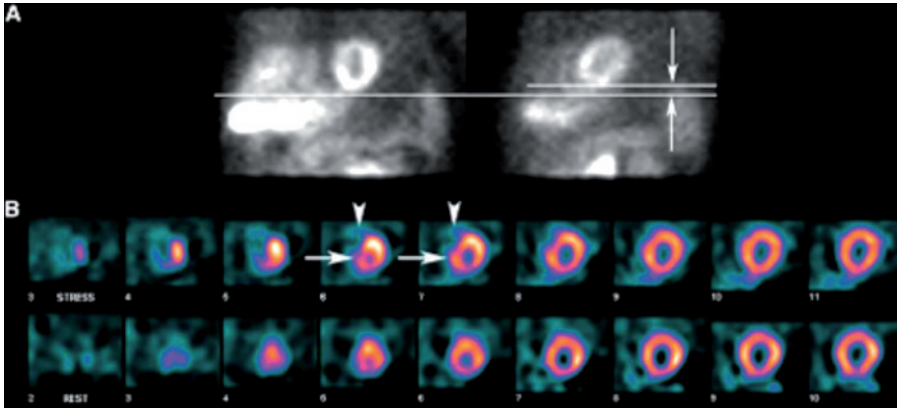

Figure 3: A Two frames from MPI raw data demonstrate offset of the left ventricle (LV) between frames, indicative of patient motion. B The resultant perfusion images demonstrate a defect in the apical septum and slight relative offset of lateral and septal aspects of the LV (arrows), along with a "tail" of activity extending from the LV (arrowheads) as a result of the patient motion. (From Burrell and MacDonald [3])

Other patient-related pitfalls and artefacts are due to physiological or extracardiac causes. Left bundle branch block can cause septal perfusion defects, and left ventricular hypertrophy can lead to underestimation of left ventricular ejection fraction due to an excessive blurring effect in the end-systolic phase; furthermore, markedly increased uptake in thickened myocardium can lead to the erroneous appearance of decreased perfusion to the remaining area of the myocardium. A mitral valve stenosis can lead to an increase in lung and right ventricular uptake of tracer as well as an increase in right ventricular volume, causing a D-shaped left ventricle. Pericardial effusion creates a halo effect around the myocardium on images and can cause inaccurate calculation of left ventricular ejection fraction. Another cause of pitfalls is non-cardiac incidental findings: for example, the MIP tracer can be concentrated in malignant tumours in the thorax (lung, breast tissue or lymph nodes), reducing the image quality [1, 4].

The validity of information gained from ECG-gated SPECT depends on a regular heart rate and appropriate synchronisation with the ECG, and in this context proper skin preparation and placement of electrodes are required to reduce the noise added to the ECG. The occurrence of an irregular heart rate results in missed data during image acquisition and may lead to errors in calculation of ejection fraction and display of cardiac function. These cause improper placement of counts into the individual temporal bins over the cardiac cycle and inconsistent image reconstructions for each temporal frame. Errors in the ECG-gated images can be propagated into the perfusion images when the temporal frames are summed to generate the perfusion images.

Theoretically, a gated SPECT study acquired with 8 frames per cardiac cycle is more likely to be corrupted by arrhythmias than a study acquired with 16 frames per cycle. ECG gating error may be suspected from the inspection of movie display of planar projection images or reconstructed slices but more easily from a sinogram (Fig. 4). To minimise the potential for artefacts, ECG-gated studies can be acquired with an acceptance window defining allowable variation between R-R peaks of the cardiac cycle [7, 8].
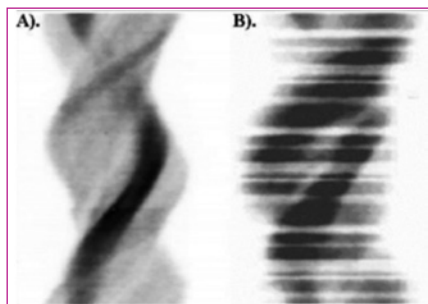

Figure 4 A, B: Comparison of a normal myocardial perfusion SPECT sinogram (A) and the striped appearance characteristic of count losses resulting from inadequate gating of the SPECT data (B). (From Wheat and Currie [6])

Prominent activity is frequently present in subdiaphragmatic organs adjacent to the heart. Activity is present in the liver and bowel as a result of hepatobiliary excretion of technetium-99m (^{99m}Tc)-labelled agents and can be present in the stomach due to reflux into the gastric lumen from the duodenum or because of uptake of free ^{99m}Tc-pertechnetate by the gastric mucosa. Typically this activity interferes with evaluation of the adjacent inferior wall; only rarely is the lateral wall affected, in the setting of a hiatal hernia (Fig. 5) [3].

Activity in subdiaphragmatic organs can interfere with evaluation of perfusion in two general ways. First, it can result in apparent increased activity in the adjacent inferior wall as a consequence of scatter and volume averaging. This can mask a true defect in the inferior wall or may lead to normalisation problems throughout the remainder of the myocardium. On the other hand, this adjacent "hot" activity can result in apparent decreased activity in the adjacent myocardium as a result of the reconstruction algorithm used in filtered back-projection [7].

Subdiaphragmatic activity can result in either increased or decreased activity in the adjacent myocardium and it is not possible in any given case to know what the effect of this activity has been. Furthermore, both influences may coexist; as they can exist on either the rest or the stress images, they may result in an artefactual fixed or reversible perfusion defect and the best solution is to avoid adjacent subdiaphragmatic activity altogether. However, this is not always an easy task and measures to reduce the amount of gastrointestinal activity are not consistently effective. A low level of exercise may decrease splanchnic uptake and drinking a large amount of fluid or even consumption of a small fat meal may help to move radioactivity through the gastrointestinal tract [3, 7].
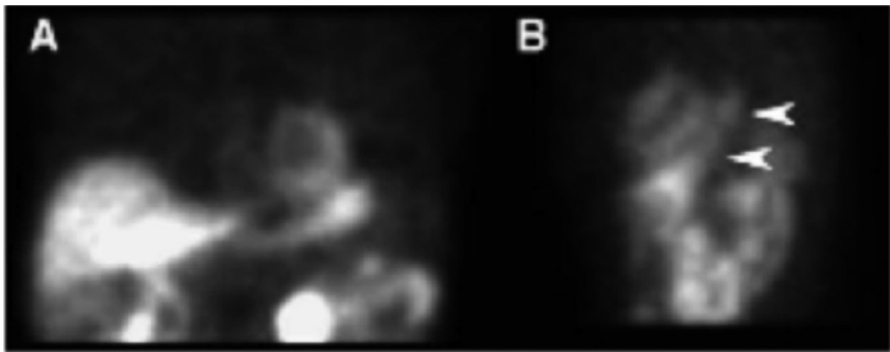

Figure 5: A Anterior raw data frame from a 99mTc-sestamibi study demonstrates activity in various subdiaphragmatic organs that can interfere with evaluation of perfusion of the inferior wall. B Left anterior oblique raw data frame from a patient with hiatal hernia and prominent gastric uptake (arrowheads), which can interfere with evaluation of the lateral wall. (From Burrell and MacDonald [3])

Technical-related artefacts

A very important technical issue that can compromise the quality of MPI is the administered patient dose in each stress and rest phase. Dose recommendations for MPI are provided in guidelines and should be adjusted according to patient weight to ensure the appropriate counting statistics and consequently a good quality study. The importance of the correct dose increases in the second phase of a same-day study, since the second scan will be dominated by activity from the first injection if insufficient dose is provided. Nevertheless, there are many reasons why a low-activity study may occur. Infiltration in the injection site and spilled dose in the patient's clothes not only provide low counting statistics but may also lead to an erroneous diagnosis of malignancy if "hot spots" are in the field of view. The insertion of an intravenous line reduces the possibility of an infiltrated dose, although it is imperative when administering the radiopharmaceutical to beware of potential contamination as well as to perform flushing with saline after the injection to reduce its retention in the intravenous line [1, 3].

The various pitfalls technical and equipment-, processing- and patient-related artefacts in SPECT MPI are summarized in Table 2.

Artefacts in PET/CT

Cardiac PET/CT has gained an important role in the evaluation of patients with either known or suspected cardiac disease. Adequate quality control of the imaging data is crucial to optimise clinical results. This section specifically outlines the most typical appearances of artefacts encountered in cardiac PET/CT, and describes some potential solutions to avoid and correct them. As with SPECT and SPECT/CT, the most commonly seen artefacts are due to the patient, processing and technical factors.

Patient motion- and patient-related artefacts

Metallic implants, including the metallic components of pacemaker and implantable cardioverter defibrillator leads near the myocardium, may give rise to artefacts on CT transmission images and pose an even more significant problem than in oncology. Such artefacts on PET images usually result in either over- or underestimation of the tracer uptake, so caution is required during the CT-based attenuation correction (CT-AC) procedures [9]. DiFillipo and Brunken [10] found that the presence of the aforementioned metal objects in the field of view of the heart can introduce artefacts in over 50% of patients.

Patient preparation is, as in SPECT MPI, a key component for successful cardiac PET/CT. Glucose metabolism in the heart is influenced by the availability of substrate, myocardial workload and adequacy of myocardial perfusion. Significant myocardial FDG uptake may impede detection of a lesion that is located either behind or closely attached to the heart border. Blood glucose level and fasting duration before the FDG PET scan are two well-known factors that influence the myocardial uptake [11]. FDG is decreased in normal myocardium, owing to the relatively low glucose and insulin levels and high free fatty acid levels, as well as in diabetics, owing to the low glucose levels. On the other hand, when a patient has a shorter period of fasting, the tracer uptake will be high [12].

Patient positioning is also important in avoiding artefacts. Patients are usually imaged supine with their arms raised above their head to prevent streak artefacts from beam hardening. Also, imaging of large patients with the arms down may result in a tight fit within the gantry and lead to truncation artefacts that appear as linear streaks through the reconstructed images. This issue is usually resolved by using full field of view reconstruction [13].

Image reconstruction and software
Several quantitative measures of myocardial perfusion can be derived automatically by software. The quantification of perfusion is relative in nature and therefore image counts in each study need to be normalised to a common level before comparison is made. The local samples of hypoperfusion can be aggregated into regional (per vascular territory) or global (per ventricle) measures in a polar map. The visual assessment of the amount of ischaemia may be challenging for the observer because there can be differences between rest and stress [14]. Lima et al. found that in patients with triple-vessel disease, combined perfusion/function analysis resulted in a significantly greater number of abnormal segments per patient compared with perfusion analysis alone [15]. The fact that PET can be acquired dynamically allows, through the use of kinetic models, absolute measures of *myocardial blood flow* or *myocardial metabolism*. These techniques rely on a dynamic acquisition of the tracer and a model for tracer transport from the blood into the cell. Use of a two-compartment model offers a way of modelling the transport from the blood pool into the myocardium. Ideally, the first dynamic frame is free of any counts from the radiotracer, so beginning the acquisition late can lead to an underestimation of the blood pool and thereby an overestimation of the myocardial blood flow [3].

As in SPECT MPI, excessive subdiaphragmatic activity from high counts in the liver or bowel may result in decreased counts in the adjacent inferior left ventricular wall when filtered back-projection is used for image reconstruction. This kind of artefact is not common with PET as iterative methods are generally used for image reconstruction [13].

Attenuation correction
Accurate attenuation correction is critical for cardiac PET images. The transmission images and attenuation map should be checked for quality.

Artefacts may also be introduced when *contrast-enhanced CT* data are used for PET attenuation correction due to overestimation of absorption values for PET attenuation correction. Nevertheless, these artefacts can be minimised by use of post-processing algorithms [16]. Misalignment of transmission and emission images can produce an erroneous attenuation map that projects lung attenuation parameters onto the heart wall, thereby causing underestimation of the attenuation and creating artefactual areas of hypoperfusion that can be misinterpreted as myocardial ischaemia or infarction and consequently produce false-positive results. The extent and direction of this misalignment will determine whether artefacts will be apparent in the attenuation-corrected images. Over-correction of the inferior wall is a possi-

ble artefact that results from the difference in scanning times between PET and CT images.

Respiratory, gross physical motion of the patient and cardiac motion are the major causes of misalignment leading to inconsistencies and hence artefacts when CT-AC is used. By far the most common technique for misalignment correction is a rigid shift of the emission dataset over the attenuation image to achieve optimal superimposition and co-registration of the cardiac free wall and re-reconstruction of the images using the shifted emission data [3]. The cardiac motion due to heart contraction and respiration can cause artefacts that are difficult to compensate. Whilst diagnostic CT is acquired during breath-holding and corrected for cardiac motion by prospective ECG triggering, the PET data have to be acquired during free breathing and are normally acquired without gating [13, 16].

A potential solution to the effects of possible respiratory motion when using CT-AC for PET studies is the use of *cine CT*, in which the idea is to acquire multiple phases of the breathing cycle and average all of the phases together. Another solution to correct the motion effects is gating both the CT and the PET. Four-dimensional (4D) PET and CT imaging (*respiratory gating*) is technically feasible and is realised during free normal breathing. Each gate contains a small portion of the respiratory cycle and correspondingly reduces the

motion present in that gate. It is noteworthy that this method assumes that 4D PET and 4D CT match well despite the sequential nature of PET and CT acquisitions, thereby providing an artefact-free image.

In the absence of gating, the PET acquisition, as a consequence of the lengthy scan duration, unavoidably averages over many cardiac and respiratory cycles. Thus, in combination with 4D CT that maps cardiac and respiratory motion, each gated PET image could be properly attenuation corrected using the appropriate set of time-dependent CT images (Fig. 6). However, the signal-to-noise ratio of the resulting image is poor since most of the acquired PET information and all other respiratory PET gates are discarded [13, 17, 18].
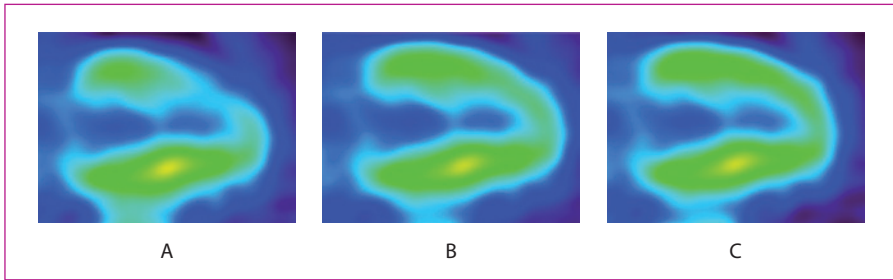
Figure 6 A–C: Attenuation correction using helical CT (A), average cine-CT (B) and gated PET and cine CT (C). Note the difference in the anterior wall between the first image and the last two.

References Chapter 9

References

1. Alessi AM, Farrell MB, Grabher BJ, Hyun MC, Johnson SG, Squires P. Nuclear cardiology technology study guide. Reston, VA: Society of Nuclear Medicine; 2010:37–46; 99–108; 137– 143.

2. Christian PE, Waterstram-Rich KM. Nuclear medicine and PET/CT technology and techniques. 6th ed. Missouri: Mosby Elsevier; 2007:85–98; 267–313; 487–495.

3. Burrell S, MacDonald A. Artifacts and pitfalls in myocardial perfusion imaging; J Nucl Med Technol. 2006;34:193–211.

4. Dilsizian V, Narula J. Atlas of nuclear cardiology. 4 ed. New York: Springer; 2013:1–54;

5. DePuey EG. Imaging Guidelines for Nuclear Cardiology Procedures. A Report of The American Society of Nuclear Cardiology Quality Assurance Committee. American Society of Nuclear Cardiology; 2006.

6. Wheat J, Currie G. Recognising and dealing with artifact in myocardial perfusion SPECT. The Internet Journal of Cardiovascular Research. 2006; 4(1). Available from: http://ispub.com/IJCVR/4/1/10112#

7. Wackers FJ, Bruni W, Zaret BL. Nuclear cardiology: The basics. How to set up and maintain a laboratory. New Jersey: Humana Press Inc.; 2004:143–225.

8. Heller GV, Mann A, Hendel RC. Nuclear cardiology. Technical applications. New York: McGraw–Hill; 2009:187–210.

9. Case JA, Baterman TM. Taking the perfect nuclear image: Quality control, acquisition, and processing techniques for cardiac SPECT, PET, and hybrid imaging. J Nucl Cardiol. 2013;20:891–907.

10. DiFilippo FP, Brunken RC. Do implanted pacemaker leads and ICD leads cause metal-related artifact in cardiac PET/CT? J Nucl Med 2005;46:436–43.

11. Ding HJ, Shiau YC, Wang JJ, Ho ST, Kao A. The influences of blood glucose and duration of fasting on myocardial glucose uptake [18F]fluoro-2-deoxy-D-glucose. Nucl Med Commun. 2002;23:961–5.

12. Lobert P, Brown RK, Dvorak RA, Corbett JR, Kazerooni EA, Wong KK. Spectrum of physiological and pathological cardiac and pericardial uptake of FDG in oncology PET-CT. Clin Radiol. 2013;68:e59–e71.

13. Di Carli MF, Lipton MJ. Cardiac PET and PET/CT imaging. New York: Springer; 2007.

14. Slomka P, Xu Y, Berman D, Germano G. Quantitative analysis of perfusion studies: Strengths and pitfalls. J Nucl Cardiol. 2013;19:338–46.

15. Lima RS, Watson DD, Goode AR, Siadaty MS, Ragosta M, Beller GA, Samady H. Incremental value of combined perfusion and perfusion over perfusion alone by gated SPECT myocardial perfusion imaging for detection of severe three-vessel coronary artery disease. J Am Coll Cardiol. 2003;42:64–70.

16. Schafers KP, Stegger L. Combined imaging of molecular function and morphology with PET/CT and SPECT/CT: image fusion and motion correction. Basic Res Cardiol. 2008;103:191–9.

17. Daou D. Respiratory motion handling is mandatory to accomplish the high-resolution PET destiny. Eur J Nucl Med Mol Imaging. 2008;35:1961–70.

18. Nehmeh SA, Erdi YE. Respiratory motion in positron emission tomography/computed tomography: A review. Semin Nucl Med. 2008;38:167–76.

Table 1: Biological and physiological artefacts: their causes, scan appearances and techniques for eliminating or minimising them (from Wheat and Currie [6])

Cause of artefacts	Scan appearance	Solution/comments
Breast attenuation	Fixed anterior, anteroseptal or anterolateral defects	Examine gated cine for wall motion and wall thickening; perform 360° reconstruction
Diaphragm attenuation	Fixed inferior defect	Perform a prone SPECT (this may, however, create an anterior artefact); examine gated cine for wall motion and wall thickening
Fat chest (not breast) – obese patient	Fixed lateral defect	Examine gated cine for wall motion and wall thickening; perform 360° reconstruction
Splenic flexure (cold) – post barium, ascites	Inferolateral defect	Perform a prone SPECT and/or examine gated cine for wall motion and wall thickening
Liver attenuation	Inferior defect	Examine gated cine for wall motion and wall thickening; 180° reconstruction
Left bundle branch block	Reversible septal or anteroseptal defect sparing apex and anterior wall	Dipyridamole stress; examine gated cine for wall motion and wall thickening
Upward creep	Reversible inferior and basal inferolateral defects and possibly reversible anterior defects	Delay scanning until 15 min post exercise and repeat any study with upward creep
Hot spot	Anterolateral hyperperfusion with or without anterolateral hypoperfusion	Examine gated cine for wall motion and wall thickening
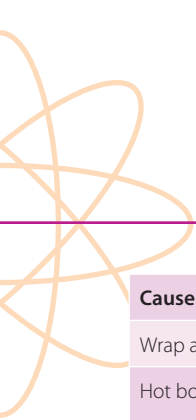
Cause of artefacts	Scan appearance	Solution/comments
Wrap around lung	Hyperperfusion of lateral wall	360° reconstruction
Hot bowel	Hyper- or hypoperfusion of inferior wall; may be more significant on rest or pharmacological stress images	Prone imaging; examine gated cine for wall motion and wall thickening; cholecystokinin to evaluate gallbladder; metoclopramide to stimulate gastric and intestinal activity
Liver activity	Inferior or inferolateral defect (worse on rest studies and pharmacological stress studies)	Examine gated cine for wall motion and wall thickening; delay scanning time post injection; 360° reconstruction
Apical thinning	Fixed apical effect	Examine gated cine for wall motion and wall thickening
Papillary muscles	Anterolateral and/or posterolateral defects	

Table 2: Summary of the various pitfalls and artefacts in SPECT MPI

Artefact/pitfall related to:		Type of artefact/pitfall
Equipment	Uniformity	Ring artefacts
	Centre of rotation	"Doughnut" or "tuning fork" artefact
	Attenuation correction	Truncation; cross-talk; low-count density artefacts
	CT mismatch	Attenuation artefacts
	Detector alignment	Myocardial perfusion defects
	Radius of rotation	Myocardial perfusion defects
Processing	Reconstruction filters	Low sensitivity for identifying ischaemia
	Incorrect axis alignment	Reorientation artefacts
Patient	Patient morphotypes	Attenuation artefacts
	Dextrocardia	Reorientation artefacts
	Movement	Myocardial perfusion defects
	Extracardiac activity	Myocardial perfusion defects
	Attenuating materials	Attenuation artefacts
	Different position stress/rest	Myocardial perfusion defects
	Arrhythmia	Gated artefacts
	Patient preparation	Low sensitivity for identifying ischaemia
	Insufficient/inadequate stress test	Low sensitivity for identifying ischaemia
Technical	Postexercise images acquired too soon	Cardiac creep
	Low dose	Lower counting statistics
	Contamination	Non-diagnostic MIP images
	Infiltration of the RF	Lower counting statistics; non-diagnostic MIP images

Notes

Notes

Imprint

Publisher:
European Association of Nuclear Medicine
c/o verein*t*: Association & Conference Management Ltd.
Hollandstrasse 14, 1020 Vienna, Austria
Phone: +43-(0)1-212 80 30 | Fax: +43-(0)1-212 80 30-9
Email: info@eanm.org | URL: www.eanm.org

Editors:
Ryder, Helen (Dublin)
Testanera, Giorgio (Rozzano, Milan)
Veloso Jerónimo, Vanessa (Almada)
Vidovič, Borut (Munich)

English Language Editing:
Rick Mills

Project Management:
Katharina Leissing

Content:
No responsibility is taken for the correctness of this information.
Information as per date of printing September 2014.

Association & Conference Management:
verein*t*: Association & Conference Management Ltd.
Hollandstrasse 14, 1020 Vienna, Austria
Phone: +43-(0)1-533 35 42 | Fax: +43-(0)1-533 35 42-19
Email: office@vereint.com | URL: www.vereint.com

Layout & Design:
kreativ · Mag. Evelyne Sacher-Toporek
Linzer Strasse 358a/1/7, 1140 Vienna, Austria
Phone: +43-(0)1-416 52 27 | Fax: +43-(0)1-416 85 26
Email: office@kreativ-sacher.at | URL: www.kreativ-sacher.at

Printing:
Colordruck GmbH
Kalkofenweg 6, 5400 Hallein, Austria
Phone: +43 (0)6245 90 111 26 | Fax: +43 (0)6245 90 111 22
Email: info@colordruck.at | URL: www.colordruck.at

*vereint Ltd. is licensee of the
Austrian Eco-label for
„Green Meetings and Green Events"*

Mag. Evelyne Sacher-Toporek